UNIVERSITY OF NAIROBI

MODELING AND SYNTHESIS OF ANTIPLASMODIAL BENZOXAZINES FROM NATURAL PRODUCTS OF KENYA

BY

ROGO MICHAEL OPATA

I56/79390/2012

A Thesis submitted in Partial Fulfillment of the Requirements for Award of the Degree of Master of Science in Chemistry of the University of Nairobi

2016

DECLARATION

I declare that this thesis is my original work and has not been submitted elsewhere for examination, award of a degree or publication. Where other people's work or my own work has been used, this has been acknowledged and referenced in accordance with the University of Nairobi's requirements.

Signature .... Date ...06/05/2015...

Name: Rogo Michael Opata

I56/79390/2012

Department of Chemistry

School of Physical Science

University of Nairobi

This thesis is submitted for examination with our approval as research supervisors:

Dr. Solomon Derese,
University of Nairobi,
Department of Chemistry,
P.O. Box 30197-00100,
Nairobi, Kenya.

Signature   Date

....   06/05/2016
....

Dr. Albert Ndakala,
University of Nairobi,
Department of Chemistry,
P.O. Box 30197-00100,
Nairobi, Kenya.

Signature   Date

....   09/05/2016
....

ii

DEDICATION

I dedicate this work to Opata and family

ACKNOWLEDGEMENT

ABSTRACT

Natural products research has taken place in Kenya for decades. This has led to the explosion of data about natural products which largely remains scattered in theses, published articles and books of abstracts and proceedings. As a result, natural products of Kenya are not accessible for drug design studies. Therefore the objective of this study was to create a web-based database of natural products of Kenya and use it in molecular modeling studies for the design of antiplasmodial compounds.

Currently the database contains 1112 compounds. It has been named *Mitishamba*, a Kiswahili word referring to herbal medicine and is hosted online at (http://mitishamba.uonbi.ac.ke). The compounds in the database were utilized in the generation of suitable fragments for molecular modeling studies using the *OpenyEye* scientific software suite. Benzoxazine scaffold was identified as a suitable molecular framework, due to its similarity to Primaquine (an existing antimalarial drug). Analogs of the scaffold were generated and subjected to docking against the target, 3D shape comparison and electrostatics studies with promising molecules synthesized and assayed.

A validated *Plasmodium falciparum* enzyme target, *Plasmodium falciparum* dihydroorotate dehydrogenase *(Pf*DHODH), was used in the docking studies. Three benzoxazines, 7-Methoxy-4H-1, 4-benzoxazin-3-one (**25**), (7-methoxy-3-oxo-1,4-benzoxazine-4-carbaldehyde (**54**) and 4-acetyl-7-methoxy-1,4-benzoxazin-3-one (**56**) were synthesized and then subjected to *in vitro* antiplasmodial assay against chloroquine resistant K1 and chloroquine sensitive 3D7 strains of *P. falciparum*. The results showed 7-methoxy-3-oxo-1,4-benzoxazine-4-carbaldehyde had an activity of 11.05 µg/mL against chloroquine resistant K1 isolate while 4-acetyl-7-methoxy-1,4-benzoxazin-3-one had an activity of 8.32µg/mL. The latter has activity classified by the WHO as active and should be pursued further through optimization to investigate its antimalarial potency.

The results above demonstrate the potential use of the database in the identification of lead antiplasmodial compounds. Therefore more benzoxazine derivatives should be identified through virtual screening and synthesized to optimize their antiplasmodial activity.

TABLE OF CONTENTS

LIST OF TABLES

LIST OF FIGURES

LIST OF SCHEMES

LIST OF APPENDICES

LIST OF ABBREVIATIONS

µg/ml – microgram per milliliter

ACTs – Artemisinin Combination Therapy

ADMET – Absorption, Distribution, Metabolism, Excretion and Toxicity

AUC – Area under the curve

CADD – Computer Aided Drug Design

CSD – Cambridge Structural Database

D6 – Chloroquine sensitive strain of *Plasmodium falciparum*

3D7 – Chloroquine sensitive strain of *Plasmodium falciparum*

DHODH – Dihydroorotate Dehydrogenase

DMAP – Dimethylaminopyridine

DNA – Deoxyribonucleic acid

DUD – Directory of Useful Decoys

DUD-E – Directory of Useful Decoys Enhanced

ED – Effective Dose

E-window – energy window

FDA – Food and Drug Administration

FMN – Flavin mononucleotide

GB – Giga Bytes

GHz – Giga Hertz

GPCRs – G-Protein Coupled Receptors

GUI – Graphical User Interface

IC$_{50}$ – Inhibitory concentration at half concentration

IUPAC – International Union of Pure and Applied Chemistry

K1- Chloroquine resistant strain of *Plasmodium falciparum*

LogP – Partition coefficient

MlogP – Moriguchi Partition coefficient

mM – Millimolar

MM – Molecular Mechanics

MMFF94 – Merck molecular force fields

NMR – Nuclear Magnetic Resonance

PDB – Protein Data Bank

***Pf*DHODH** – *Plasmodium falciparum* dihydroorotate dehydrogenase

PIC$_{50}$ – Negative Antilogarithm of IC$_{50}$

PSA – Polar Surface Area

QM – Quantum Mechanics

RMS – Root mean square

RNA – Ribonucleic acid

RO5 – Rule of five

ROC – Receiver operator curve

Rocs – Rapid Overlay Characteristics

TEA – Triethylamine

TCM – Traditional Chinese Medicine

TCMD – Traditional Chinese Medicine Database

TLC – Thin layer chromatography

VS – Virtual Screening

W$_2$ – Chloroquine resistant strain of *Plasmodium falciparum*

WHO – World Health Organization

CHAPTER ONE

INTRODUCTION

1.1   Background

Malaria is a disease caused by (eukaryotic) protozoan parasite of red blood cells transmitted by the female mosquito of the genus *Anopheles* that may reach burdens as high as 10^{13} in the blood of the host, although most symptomatic infections are caused by between 10^7 and 10^{12} parasites (World Health Organization, 2014). Five species of protozoan parasites of the genus *Plasmodium* known to affect humans are: *P. malarie* and *P. knowlesi*. *P. falciparum, P. ovale* and *P. vivax*, with *P. falciparum* being the most predominant and deadly in Africa (World Health Organization, 2014).

The disease is entirely preventable and treatable provided there is proper implementation of the following recommended interventions by WHO (World Health Organization & Global Malaria Programme, 2012):

i.   Vector control through the use of insecticide-treated nets (ITNs), indoor residual spraying (IRS) and larval control.

ii. Chemoprevention for the most vulnerable populations, particularly pregnant women and infants.

iii. Timely treatment with appropriate antimalarial medicines (according to the parasite species and any documented drug resistance).

Among the above methods, antimalarial drugs have been one of the most powerful tools in

malarial control (Cui & Su, 2009). There exists a group of both naturally occurring drugs and synthetic drugs that are used for treating malaria. Quinine (**1**) and artemisinin (**2**) are naturally-occurring antimalarial drugs, while chloroquine (**3**), amodiaquine (**4**), sulphadoxine (**5**), pyrimethamine (**6**) among others are examples of synthetic drugs.
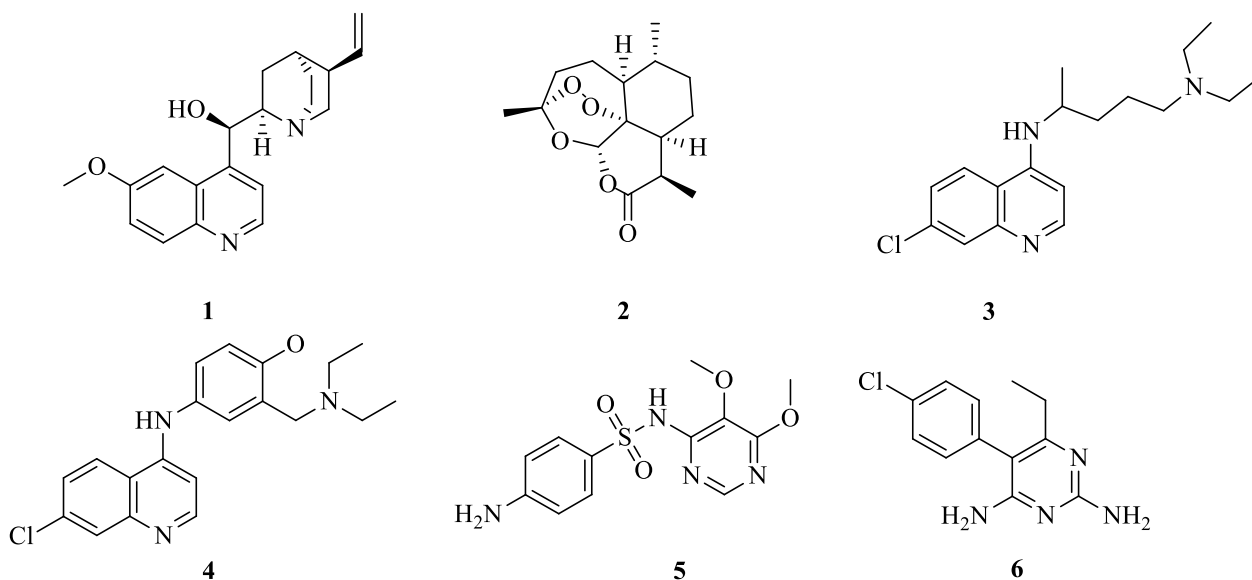
Quinine **(1)** and its derivatives and antifolate-combination drugs have been the most widely used for decades (Bloland & Organization, 2001). However the resistance of the *Plasmodium* parasite to available drugs has seen the adoption of artemisinin **(2)** combinations in the efforts to curb the malaria epidemic. This has led to more combination therapies taking center stage in malaria management.

1.2 *Plasmodium falciparum* **Dihydroorotate Dehydrogenase (*Pf*DHODH)**

Generally, cells synthesize their genetic material, DNA and RNA, through either the *de novo* or salvage pathways (Phillips & Rathod, 2010). Whereas human beings synthesize

their DNA and RNA through both pathways, *Plasmodium* species can only synthesize their genetic material through the *de novo* pathway (Booker *et al.*, 2010). Pyrimidines are essential precursors for DNA and RNA biosynthesis.

In the *de novo* biosynthesis, dihydroorotate dehydrogenase (DHODH), a flavin mononucleotide (FMN)-dependent mitochondrial enzyme catalyzes the oxidation of dihydroorotate (DHO) to produce orotate in the fourth step of *de novo* pyrimidine biosynthesis shown Scheme 1.1 below (Patel *et al.*, 2008).
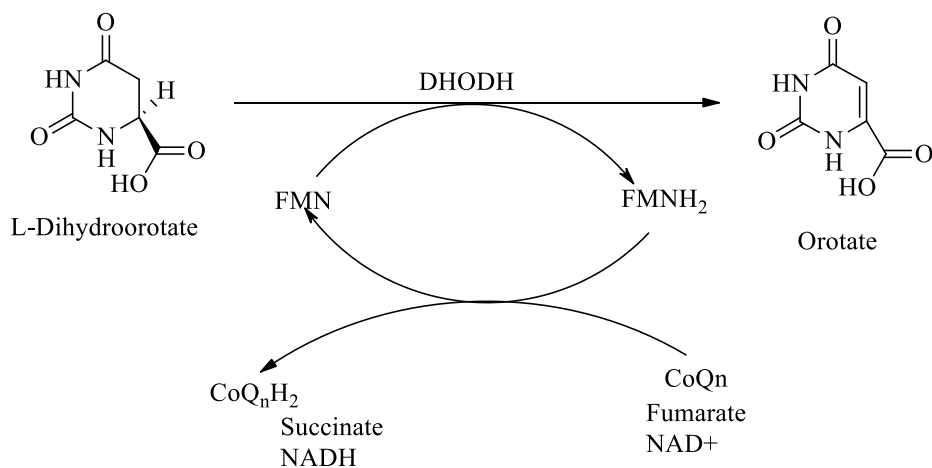
Scheme 1.1: Reactions catalyzed by DHODH

Inhibiting *Pf*DHODH, will block the synthesis of pyrimidine bases and therefore the synthesis of its DNA and RNA leading to its eventual death. *Pf*DHODH has been validated as a target (Hurt, Widom, & Clardy, 2006). The researchers have measured its inhibition using A77 1726 inhibitor (**7**). It is therefore important to target the enzyme (*Pf*DHODH) within the biosynthetic process to suppress the growth and multiplication of the parasite which can be done by developing an inhibitory drug. This is the back-bone of this research; identifying inhibitors that can be used as lead compounds in the discovery of antimalarial drugs for treatment of *Plasmodium* type malaria.

7
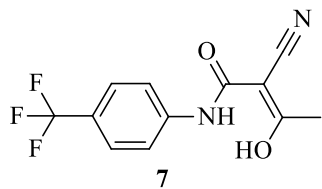
1.3 Structural Databases

A database is a structured collection of information that consists of data and metadata, with metadata being the structured part. In a database, data is the actual stored descriptive information, while the metadata defines the data (O'Donnell, 2008). Several structural databases exist online that serve different roles.

Among the experimentally determined 3D structural databases, Cambridge Structural Database (CSD) is a depository of small molecules while Protein Data Bank (PDB) is a depository of macro molecules. CSD contains information on small-molecule crystal structures with approximately 717,876 entries whose structures have been determined either by X-ray crystallography or neutron diffraction (Allen, 2002), while PDB is a public repository for the coordinates of 3D models of biological macromolecules which have been determined by X-ray crystallography, NMR and electron-microscopy (Berman *et al.,* 2013).

There are several databases available for natural products isolated from nature (Chen, 2011; Ntie-Kang *et al*., 2013; Valli *et al*., 2013). One of these is the Traditional Chinese Medicine (TCM) database @ Taiwan (tcm.cmu.edu.tw), a free 3D small molecular structure database based on natural products isolated from Chinese medicinal plants available for virtual screening (Chen, 2011). The database of Natural products built in this study is akin to the TCM. It is meant to be open for use by other research groups to conduct research in the

field of drug design based on Computer Aided Drug Design and medicinal chemistry. It is also available for download for molecular modeling.

In addition to structure databases, docking decoy databases which are important for benchmarking virtual screening studies also exist online and are freely accessible. An important source of such databases is the Directory of Useful Decoys (DUD) http://blaster.docking.org/dud (Huang *et al*., 2006). As at 2006, the database contained a total of 98,266 decoy compounds to help in ligand enrichment during molecular docking. These decoys help to obtain a relationship between them and the ligands under study to help in assessing enrichment factors during docking screens. An improved benchmarking set, the directory of useful decoys, enhanced (DUD-E) http://dude.docking.org (Mysinger *et al,* 2012) includes more diverse targets such as GPCRs and ion channels. This leads to improved quantitative assessment of the performance of molecular docking screens in terms of enrichment in docking hit lists.

1.4   Modeling

A model is a rule that typically involves the deliberate introduction of simplifying approximations into a more general theory so as to extend its practical utility (Cramer, 2004). These approximations sometimes go to the extreme of rendering the model deliberately qualitative. Chemists use models to predict molecular geometry, simulate temperature and study solvent effects in complex reactions and other properties that would be difficult to measure experimentally (Hinchliffe, 2003).

Advances in computer hardware and software have brought high-performance computing and graphics within the reach of most academic and industrial laboratories. This has led to

several studies of various aspects of science, in general, and chemistry, in particular, with content spanning all major branches of chemistry as noted by Cohen *et al*. (1990). The sub-branch of theoretical chemistry involving molecule simulation is called *molecular modeling*.

Various operations carried out in molecular modeling involve the use of computer programs or algorithms which calculate the structure and property data for the molecule in question. The computational methods used can be classified into two categories: molecular mechanics (MM) and quantum mechanics (QM). In MM, equations used are those that follow the laws of classical physics and apply them to the nuclei of an atom without consideration of the electrons, i.e. the molecule is treated as a series of spheres (atoms) connected by springs (bonds) (Patrick & Spencer, 2009). Equations derived are used to calculate the different interactions and energies (force fields) resulting from bond stretching, angle bending, non-bonded interactions and torsional energies (Patrick & Spencer, 2009).

On the other hand, QM uses quantum physics to calculate the properties of a molecule by considering the interactions between the electrons and nuclei of the molecule. Here, two major assumptions are made: (a) that the nuclei are motionless and (b) that the electrons move independently of each other, so the influence of other electrons and nuclei is taken as an average (Patrick & Spencer, 2009). This research deploys principles of molecular mechanics. It involves modeling of small organic molecules that can be used as lead compounds with the hope of modifying them into an antimalarial drug.

1.5   Problem Statement

Despite the efforts to 'roll back malaria', statistics still show that there are 97 countries and territories with ongoing malaria transmission, and 7 countries in the prevention or relapse phase, making a total of 104 countries and territories in which malaria is presently considered endemic (World Health Organization, 2014). Globally, an estimated 3.4 billion people are at risk of malaria. WHO estimates that 197 million cases of malaria occurred globally in 2013 and 584,000 deaths were registered; of the cases (70%) occurred in Africa (World Health Organization, 2014).

Widespread multi-drug resistance of malarial parasites to the recommended and provided drug treatments (i.e., chloroquine and sulphadoxine/pyrimethamine) across Asia, South America and Africa has prompted the use of artemisinin-based combination treatments (ACTs) (Breman *et al, 2007)*. The derivatives of artemisinin are some of the most efficacious drugs available in the treatment of serious antimalarial cases. However, the evolving resistance to artemisinin-based compounds threatens to derail the gains that had been made to control malaria (Cheeseman *et al*., 2012).

This necessitates profiling of new antimalarial drugs that are effective against the deadly *P. falciparum*. Strategic plans need to be put in place to discover and develop novel antimalarial compounds that are not encumbered by pre-existing mechanisms of drug resistance (Fidock *et al*, 2004). This can be done by discovering noble lead compounds that can be further optimized to serve as drugs.

However, it takes time (10-15) years and resources ($800 million to $1 billion) to develop a lead compound which can be further optimized to come up with a drug exhibiting

7

appropriate pharmacodynamics and pharmacokinetics (ADMET) properties. The various processes involved in the development cycle ultimately contribute to the shelf price of drugs. In addition, major drugs fail at later stages resulting in wasted resources. Therefore, appropriate methods should be used in the process of discovery. In this research, a database of natural products of Kenya is developed from which appropriate scaffolds are identified and modeled *in silico* against *Pf*DHODH enzyme to generate the best hit list. The promising compounds are then synthesized and subjected to *in vitro* antiplasmodial assay to evaluate their potency.

1.6   Objectives

1.6.1   Overall Objective

The overall objective of this study was to develop a web-based *in-silico* database of natural products of Kenya for antimalarial drug discovery.

1.6.2   Specific Objectives

The specific objectives of the study were to:

1. Develop a searchable database of natural products of Kenya.

2. Identify benzoxazines with desirable binding properties against the *Plasmodium falciparum* dihydroorate dehydrogenase (*Pf*DHODH) enzyme through various computational techniques.

3. Synthesize promising benzoxazines for *in-vitro* assay against *Plasmodium falciparum*.

1.7   Justification and Significance

A lasting solution has not been found to the malaria burden despite the fact that it has been around for centuries. This is due to the multi-drug resistance found in existing mono and combination therapies. Therefore further investigation of small organic compounds that can be used as new treatment agents to cure the disease needs to be undertaken.

On the other hand, the random drug discovery process is time consuming and expensive. Therefore, there is need to design drugs using convenient techniques. This can be achieved using computational methodologies. In this study, a database of natural products of Kenya has been virtually screened against *Pf*DHODH for the design of antiplasmodial lead compounds. This is a relatively cheaper method of tackling the disease which could go a long way in reducing the burden.

CHAPTER TWO

LITERATURE REVIEW

2.1 Drug Discovery and Development

Patrick and Spencer. (2009) notes that it takes a lot of time (10 to 15 years) and resources (roughly $800 million) to discover a drug, with numerous complex and risky processes carried out in the developmental stages (Ghose *et al*, 2006). The seven steps in the drug discovery process involve: disease selection, target hypothesis, lead compound identification (screening), lead optimization, preclinical trial, clinical trial and pharmacogenomic optimization (Xu & Hagler, 2002). The scheme of this process is summarized in Scheme 2.1.
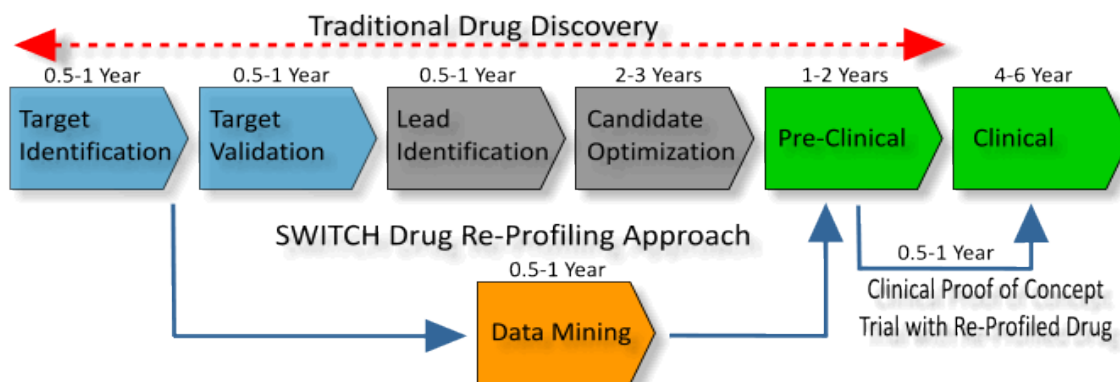
Scheme 2.1: A schematic diagram of drug development process (adopted from http://newdrugapprovals.org/)

The numerous methods that have been used to develop compounds for drug discovery include; isolation from plants and other natural sources, combinatorial chemistry, molecular modeling and synthetic chemistry (Cragg & Newman, 2013). Some drugs such as the mustard-like analogs used to treat leukemia have been historically discovered through serendipity (Patrick & Spencer, 2009).

Early processes of drug development rely on hit finding procedures followed by extensive experimental confirmation in order to select high priority hit series which then undergo further scrutiny in hit-to-lead studies (Duffy *et al*, 2012). Despite the promising methods of natural products and combinatorial chemistry, chemoinformatics defined as the use of computer technologies to process chemical data has become the choice of pharmaceutical companies (Xu & Hagler, 2002). Data driven methods and rules that almost serve as industry standards have been developed by different researchers from different pharmaceutical companies (Egan, *et al*. 2000; Lipinski, *et al*., 2012; Veber *et al*., 2002).

The Lipinski rule of five describes in details the experimental and computational approaches to estimate solubility and permeability in drug discovery that predicts poor absorption or permeation of a drug (Lipinski *et al*., 2012). This involves the use of physicochemical parameters like molecular weight, calculated LogP (MlogP) (partition coefficient), hydrogen donors and hydrogen acceptors to approximate the permeability of a given compound. The rule predicts that poor absorption or permeation is more likely when there are more than 5 H-bond donors, 10 H-bond acceptors, molecular weight greater than 500 and calculated LogP (CLogP) greater than 5 (or MlogP>4.15) (Lipinski, *et al.*, 1997) (Lipinski *et al*., 2012) .

Veber *et al*, 2002 found that reduced molecular flexibility as measured by the number of rotatable bonds, and low polar surface area or total hydrogen bond count (sum of donors and acceptors) are important for good oral bioavailability with molecular weight being an independent factor. In another study by Egan *et al*. (2000), the use of multivariate statistics is applied to predict drug absorption. The study involved building a statistical pattern recognition model of passive intestinal absorption using PSA and AlogP98 as descriptors.

The method was validated extensively using hundreds of known orally delivered drugs which demonstrated successful predictions (72-92%), (Egan *et al.*, 2000) .The trend in the use of advanced computer hardware and software adopted in the industry is seen as a better way of developing novel drugs that can be used to treat diseases.

2.2   Treatment of Malaria

One of the measures put in place to ensure that the burden of malaria disease is reduced is the administration of chemotherapeutic drugs to the affected parties. A number of these drugs have different mechanisms of action depending on the chemical formulation (Schlitzer, 2008). Major sources of these therapeutic agents include natural products and semi-synthetic routes. In our effort to develop potential lead compounds, natural sources were identified as a starting point.

2.2.1   Natural Products as Therapeutic Drugs for Treatment of Malaria

Several plant extracts have been used to treat malaria for years. Quinine (**1**), an alkaloid component of the bark of cinchona tree, was used to treat malaria as early as the 1600s. It is an arylaminoalcohol which is used to treat severe malaria complications (Schlitzer, 2008). Other cinchona alkaloids including quinidine (**8**), cinchonine (**9**) and cinchonidine (**10**) are also effective against malaria, however, the malaria parasite has developed resistance against these compounds due to their heavy use (Achan *et al.*, 2011).

Artemisinin (**2**), isolated from *Artemisia annua* L. (Asteraceae) is another plant derived antimalarial agent. It is a sesquiterpene lactone with an endoperoxide linkage which is responsible for the antimalarial activity, (Abdi, 2003). It provides a scaffold which is of

utmost importance in the current antimalarial campaign (Balint, 2001).
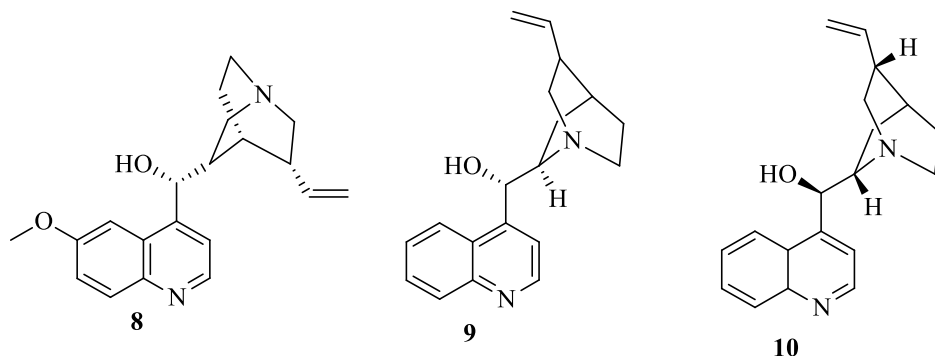
By 2007, WHO issued a recommendation that almost all malaria endemic countries should implement policies endorsing the use of Artemisinin-based combination therapy (ACT) as the primary treatment regimen for uncomplicated malaria (Frosch *et al.*, 2011). Despite the promising nature of its combination therapies, artemisinin resistance has been detected in the Greater Mekong sub region (World Health Organization & Global Malaria Programme, 2012). WHO (World Health Organization, 2014) takes it a matter of great concern considering that the resistance might eventually spread to other regions. It has also been reported that if resistance to artemisinin and its analogs exist, it is more likely that resistance to the partner drugs lumefantrine (**11**) will also develop and vice versa. Consequently, resistance to ACT partner drugs is also an important concern and must be monitored carefully.
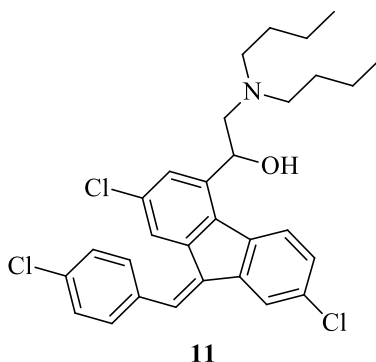
2.2.2 From Natural Products to Synthetic Drugs

In the search for a lasting treatment of the endemic malaria disease, a number of synthetic drugs have been developed from the scaffolds of existing natural products. Over time, natural products have served as attractive starting points inspiring the development of more efficacious synthetic drugs. Quinine (**1**) remained the mainstay of malaria treatment until the 1920s, when more effective synthetic antimalarials became available (Achan *et al*., 2011). The most important of these synthetic drugs was chloroquine, CQ (**3**) which was extensively used, especially in the 1940s (Abdi, 2003). CQ was developed based on the quinine scaffold as shown in Figure 2.1, the major difference being their side chains.
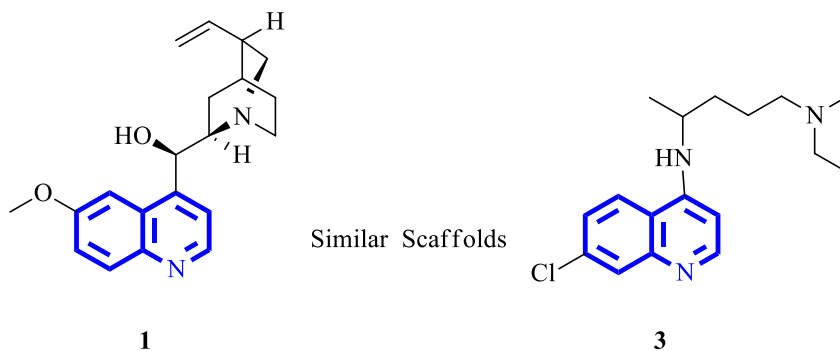
Figure 2.1: Quinine and Chloroquine Scaffolds

The efficacy of chloroquine against chloroquine sensitive D6 and chloroquine resistant W2 of *Plasmodium falciparum* of 0.008±0.002 and 0.075±0.002 ng/mL, respectively, is higher as compared to that of quinine with an efficacy against chloroquine sensitive D6 and chloroquine resistant W2 0.050±0.02 and 0.28±0.02 ng/mL, respectively (Andayi *et al*., 2006).

The natural product lapachol (**12**) (a naphthoquinone) the active ingredient in the stem bark

of Lapacho tree (*Handroanthus impetiginosus)* led to the discovery of lapinone (**13**), which in turn provided the foundation for the discovery of atovaquone (**14**), Figure 2.2, a component of *Malarone* ®, a combination of atovaquone and proguanil used to treat or prevent malaria (Wells, 2011).
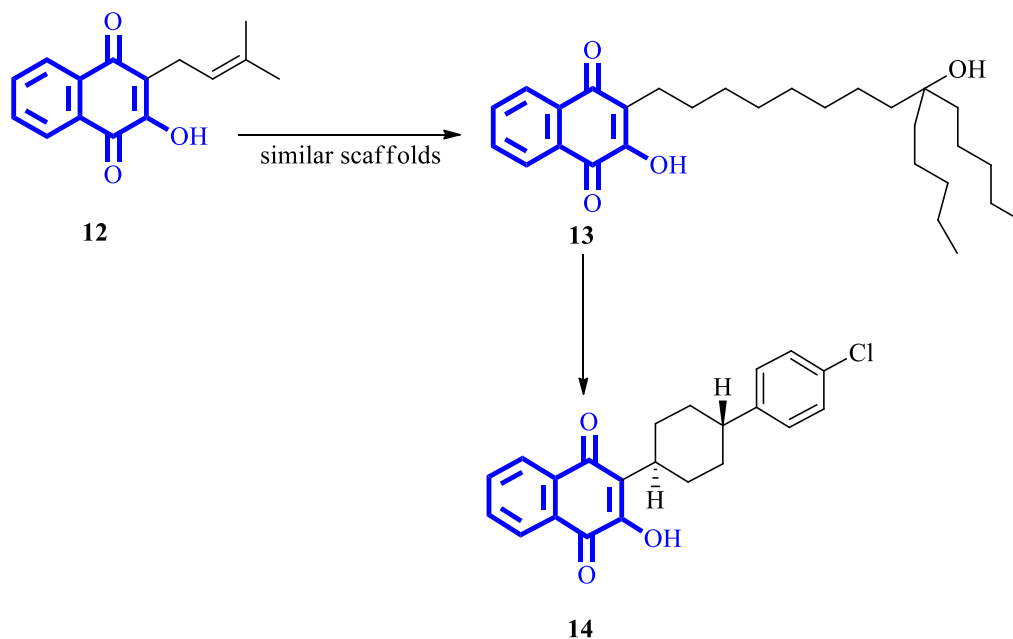
Figure 2.2: Scaffolds of Lapachol and its derivatives

Artemisinin (**2**) contains a trioxane lactone that can be easily reduced with diisobutyl aluminium hydride resulting in the formation of dihydroartemisinin (**15**) (van *et al*., 1999). Derivatives of artemisinin; artesunate (**16**), artemether (**17**) and arteether (**18**) can therefore be synthesized from dihydroartemisinin as shown in **Error! Reference source not found.**. These derivatives, produce more profound reductions in parasitaemia and more rapid symptom relief than agents from any other antimalarial class, (Morris *et al*., 2011).
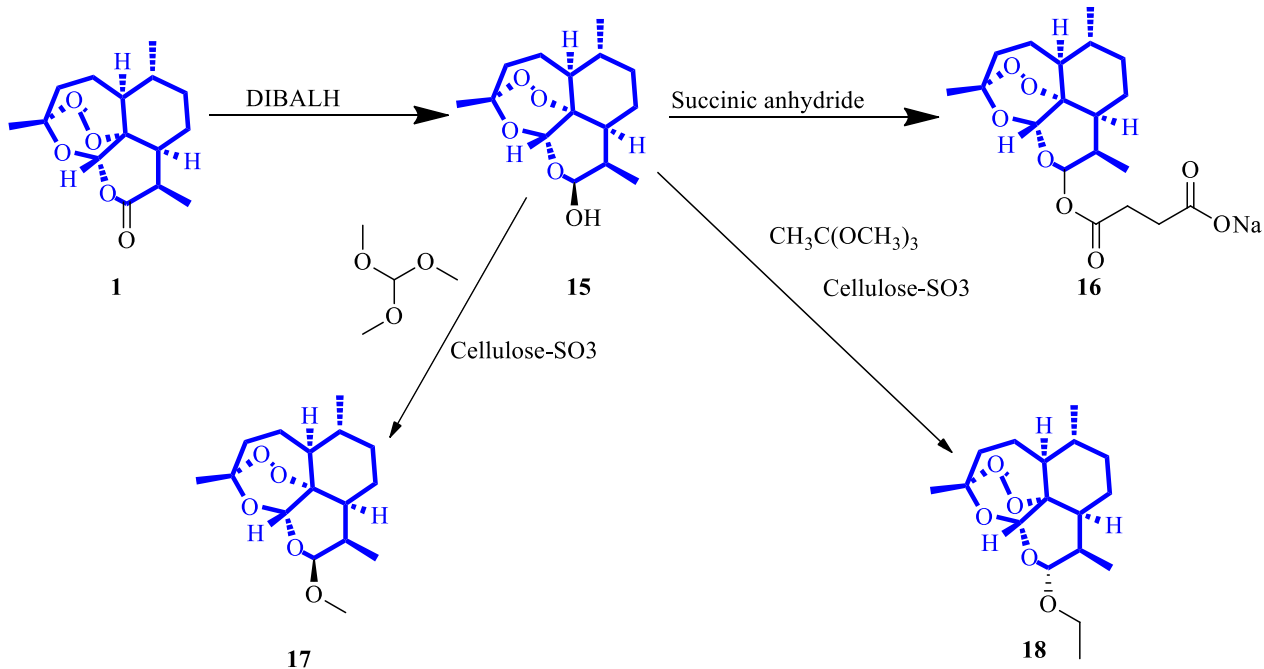
Figure 2.3: Synthesis of artmesinin derivatives

This shows that the efficacy of naturally occurring drugs can be improved by using their scaffolds to produce more potent synthetic drugs through side chain modification. Their scaffolds are important lead starting points that can be further modified to improve the ADMET properties and other physicochemical parameters that qualify a compound to be approved as a drug. Modifications are done with an overall goal of developing synthetically accessible side chains while improving on the activity of the existing known scaffold.

2.2.3   Natural Products of Kenya

An extensive body research on natural products of Kenya has shown that traditional medicinal plants remain the greatest potential source of medicine in the fight against malaria. *Erythrina abyssinica* (Yenesew *et al*., 2004), *Erythrina sacleuxii* (Andayi *et al*., 2006), *Albizia gummifera* (Rukunga *et al*., 2007), *Tephrosia elata* (Muiva *et al*., 2009),

Derris trifoliata (Yenesew *et al*., 2009) and *Cyperus articulatus* (Rukunga *et al*., 2008) are some of the plants in Kenya that have exhibited antiplasmodial activities. Current estimates suggest that, in many developing countries, a large proportion of the population relies heavily on traditional practitioners and medicinal plants to meet its primary healthcare needs (Kokwaro, 2009). However, Nguta *et al.* (2012) notes that concerns have been raised regarding their safety.

Although quinine (**1**), lapachol (**12**) and artemisinin (**2**) have been used widely, a number of plants obtained from Kenya have exhibited promising antimalarial efficacy which if modified or used in combination therapies, could provide cheap alternatives to current antimalarial drugs. The diverse scaffolds of the compounds isolated from these plants can be used as starting points for generating more potent drugs. Research done by Andayi *et al*. (2006), showed that the acetone extracts of the root bark and stem bark of *Erythrina sacleuxii* has antiplasmodial activities against the chloroquine sensitive D6 ($IC_{50} = 3.8 \pm 0.9$ µg/mL for stem bark) and chloroquine resistant W2 ($IC_{50} = 6.3 \pm 1.4$ µg/mL for root bark) strains of *Plasmodium falciparum*. In the research, abyssinone V (**19**) had IC_{50} values of 4.9 ± 0.8 (D6) and 6.1 ± 1.3 µg/mL (W2).

The data obtained in the findings supports the traditional use of the plant to manage malaria in East Africa (Kokwaro, 2009). Another study done by Yenesew *et al*., 2004 showed that the ethyl acetate extract of the stem bark of *Erythrina abyssinica* exhibited antiplasmodial activity against the chloroquine sensitive D6 ($IC_{50} = 7.9 \pm 1.1$ µg/mL) and chloroquine-resistant W2 ($IC_{50} = 5.3 \pm 0.7$ µg/mL) strains of *Plasmodium falciparum*. A flavanone Abyssinin III (**20**) was found to have antiplasmodial activity against the Chloroquine-sensitive D6 ($IC_{50} = 5.8 \pm 1.1$ µg/mL) and Chloroquine-resistant W2 ($IC_{50} = 5.2 \pm 1.7$ µg/mL)

strains of *Plasmodium falciparum.* Sigmoidin A (**21**) was also found to exhibit activity towards the strains with values of 5.8±1.7 µg/mL (D6) and 5.9±1.1 µg/mL (W2).
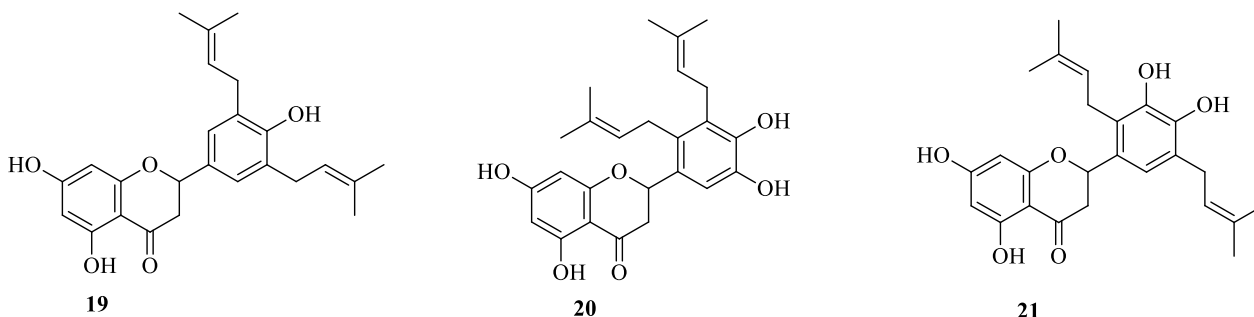
Figure 2.4: Abyssinone V, Abyssinin III and Sigmoidin A

In the recent past, efforts have been directed by Kenyan scientists towards studying plants usage in curing other diseases such as antimicrobial infections (Yenesew *et al*., 2005), antinociceptive (Ochieng' *et al.,* 2012) and a significant amount of phytochemistry on plants of Kenya have been studied by Midiwo *et al*. (2001). This has led to significant explosion of data about the medicinal potential of natural products of Kenya.

2.3 Databases of Natural Products in Kenya

The large amount of data from natural products of Kenya has not been organized in a useful manner to aid current and future researchers in carrying out meaningful research. In other parts of the world, where similar research has been undertaken, databases of the same exist to ease access of information about the native natural products (Chen, 2011; Ntie-Kang *et al*., 2013; Valli *et al*., 2013). An example in case is the TCM database which provides comprehensive information about all aspects of Chinese medicine including prescriptions, constituent herbs, herbal ingredients, molecular structure and functional groups of active ingredients among other useful information that may help scientists carry out further

research on the Chinese plants.

In Kenya, such a database doesn't exist. The information remains largely scattered in published articles, theses and books of abstracts and conference proceedings. This research aims at creating a database that exclusively contains natural products of Kenya. It will be used as an invaluable source of knowledge and information about the rich diversity of Kenyan flora that may be used in drug discovery. The information is intended to be web-based so that it can be accessible to scientists and the general public.

As Wells. (2011) suggests, the continual emergence of drug resistance calls for new classes of molecules to combat malaria. Novel sources that represent new pharmacophores which can be warheads are needed for killing the malaria parasite. Careful identification of natural product scaffolds, followed by their modification for clinical use by a combination of medicinal chemistry, formulation development and combination therapy can help in coming up with noble drugs. Such a database can be used in molecular modeling to come up with small molecules that will eventually treat infectious diseases.

2.4   Benzoxazines

Benzoxazines are composed of an oxazine ring (a heterocyclic aromatic six-membered ring with oxygen and nitrogen), attached to a benzene ring. There are several benzoxazine derivatives depending on the position of the oxygen and nitrogen in the ring. Among them, 1,4-benzoxazines, Figure 2.5, are the most important scaffolds present in various agrochemicals (Ramesh *et al*, 2011) and in synthetic and medicinal organic chemistry (Sharifi *et al*, 2010).
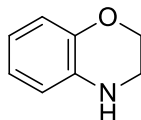
Figure 2.5: 1,4-Benzoxazine Scaffold

Specifically, the 2*H*-1,4-benzoxazin-3-(4*H*)-one and 3,4-dihydro-2*H*-1,4-benzoxazine scaffolds, Figure 2.6, have been studied intensively as important heterocyclic systems for building natural and designed synthetic compounds as reviewed by Ilaš *et al*. (2005). They note that these skeletons have been used to design biologically active compounds, ranging from herbicides and fungicides to therapeutically usable drugs.
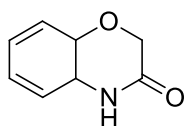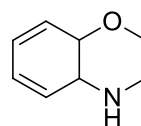
A   **B**

Figure 2.6: Structures of 2H-1,4-benzoxazin-3-(4H)-one (**A**) and 3,4-dihydro-2H-1,4-benzoxazine (**B**)

A number of benzoxazines have been used as chemotherapeutic agents for several ailments. Benzoxazinone, Figure 2.7, patented by Bird. (2004) is used in the treatment of angiogenesis and vascular damaging agents. Frechette & Beach. (1997) have also reported related benzoxazines, Figure 2.8, and pyrido-oxazine compounds for treating bacterial infections. Similar derivatives prepared by Manabu *et al*. (1996), Figure 2.9, have also been used as a medicament for preventing or treating disorders induced by intracellular acidosis during myocardial ischemia, such as cardiac dysfunction, myocardial necrosis, arrhythmia, reperfusion injury, and other diseases observed in ischemic heart diseases (e.g. myocardial infarction, angina pectoris, etc.).
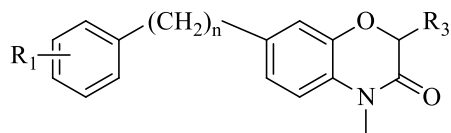
R1 = R2 = R3 = H or C_{1-4}Alkyl

Figure 2.7: Benzoxazinone used in the treatment of angiogenesis
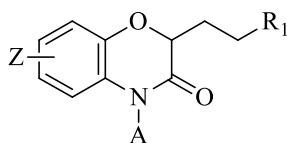
R1 = NHR1R2   Z = H   A = C1-C6 Alkyl, C1-C6 Akylaryl, C1-C6 heterocyclyl

Figure 2.8: Benzoxazinone used in the treatment of bacteria
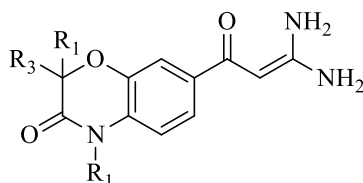
$R_1 = R_2 = R_3 = H$ or C_{1-6} Alkyl

Figure 2.9: Benzoxazines for preventing or treating disorders induced by intracellular acidosis

French investigators, Fleury *et al.* (1999) have also previously reported a number of compounds with benzoxazine skeleton, Figure 2.10, used as neuroprotectants. In their patent, they acknowledge that the benzoxazine moiety plays a critical role in the activity of the derivatives developed.
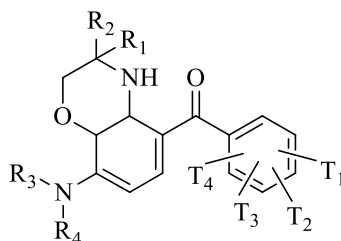
$R_1 = R_2 = R_3 = H$, Alkyl, Cycloalkyl, Cyloalkylalkyl, aryl or a $(CH_2)p$-O-$(CH_2)p$-R_5
T1 = T2 = T3 = T4 = H, Halogen, Alkyl, Hydroxy, Alkoxy, cyano, amino, acyl group

Figure 2.10: Benzoxazines used as neuroprotectants

In the search for new natural product scaffolds, cappamensin A (**22**), isolated and characterized from *Capparis sikkimensis* subsp. *formosana* (Capparaceae) by Wu *et al.* (2003) has been identified as containing a unique benzoxazine scaffold which with the exception of the oxygen atom is similar to Primaquine (**23**), an 8-aminoquinoline that has been approved for treatment of malaria since 1952. Primaquine is unique in that it remains the only FDA licensed drug capable of clearing the intra-hepatic schizonts and hypnozoites of *Plasmodium vivax* (Fernando *et al.*, 2011). The scaffold of cappamensin A, Figure 2.11, is therefore worth exploring as a starting point for antimalarial lead compound development.
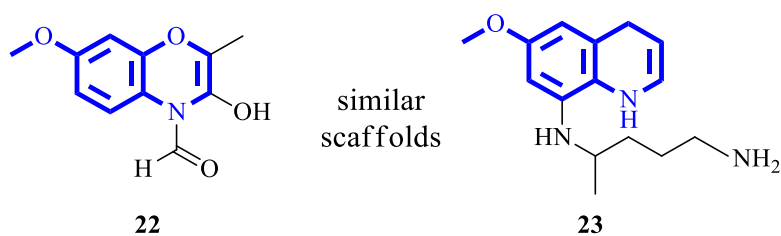
Figure 2.11: Structures of cappamensin A (**22**) and primaquine (**23**)

Cappamensin A (3-hydroxy-7-methoxy-2-methyl-1,4-benzoxazine-4-carbaldehyde) has an *in vitro* anticancer activity against ovarian (1A9) [2.4 µg/mL], lung (A549) [3.6 µg/mL], ileocecal (HCT-8) [3.6 µg/mL], breast (MCF-7) [4.0 µg/mL], nasopharyngeal (KB) [4.0 µg/mL], vincristine resistant (KB-VIN) [3.5 µg/mL] and human tumor cell lines with ED_{50} values of 4.0 µg/mL (mean GI_{50} value of 15.1 µM) (Wu *et al.*, 2003).

The antimalarial activity of cappamensin A (**22**) has not been investigated. Furthermore, there exists no literature on computational work done on the scaffold of benzoxazine, making its structural similarity to Primaquine (**23**) a rich candidate for exploration through modeling and modification. It can be used to develop novel synthetic antiplasmodial lead

compounds which can be optimized to be used as antimalarial drugs.

2.5 Strategies for Synthesis of Benzoxazines

Common approaches for construction of the 2*H*-1,4-benzoxazin-3-(4*H*)-one have been extensively reviewed by Ilaš *et al*. (2005). Generally, synthesis of these compounds is achieved by reacting suitable 2-aminophenols of interest and a favorable alkyl group followed by ring closure. The resulting skeleton can then be modified using a number of synthetic methods.

Huang *et al*. (2003) designed and synthesized a series of benzoxazine derivatives. In their work, 5-methoxy-2-nitrophenol (**24**) is used as a starting material. The nitro group is first reduced to an amine through catalytic hydrogenation using palladium on charcoal in methanol as reducing agent, followed by *O*-alkylation using chloroacetyl chloride. Spontaneous cyclization takes place to achieve 1,4-benzoxazine (**25**) skeleton shown in Scheme 2.2.

(a) Pd/C (10%), H_2 (1 atm), MeOH
(b) Chloroacetyl chloride, satd. $NaHCO_3$
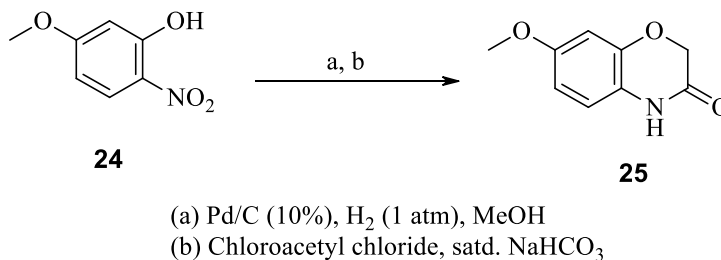
Scheme 2.2: Cyclization of nitrophenol (**24**) to 1,4-benzoxazine (**25**) using chloroacetyl chloride

The reduction of the nitro group can alternatively be achieved using sodium dithionite dissolved in warm water followed by consequent addition of the nitro phenol (**26**) dissolved

in ethanol and the mixture is heated on a steam bath (Maag., *et al* 2004), Scheme 2.3. The resulting aminophenol (**27**) is alkylated with chloroacetyl chloride in a one pot synthesis using saturated $NaHCO_3$ as a base.
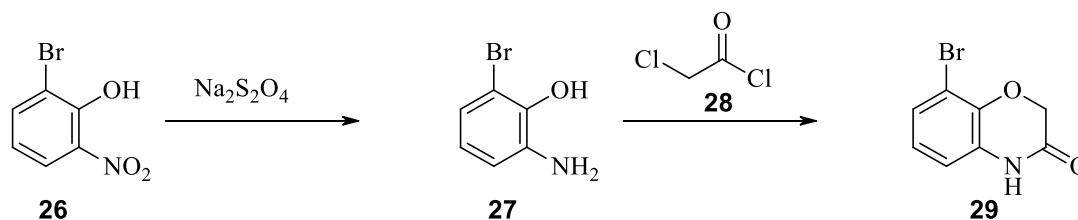
Scheme 2.3*: Reduction of nitrophenol using sodium dithionite followed by cyclization*

In the work of Vianello & Bandiera. (2004), a methodological difference is employed while still using chloroacetyl chloride (**28**) as an alkylating agent, Scheme 2.4. An appropriate aminophenol (**24**), trimethylamine (TEA) and dimethylaminopyridine (DMAP) in anhydrous dichloromethane at 0 ^{0}C and under nitrogen atmosphere, chloroacetyl chloride is refluxed for 10 h to achieve a benzoxazine (**25**).

Scheme 2.4: Synthesis of benzoxazines using chloroacetyl chloride

Similar products can be achieved by using different alkylating agents. Maag *et al*. (2004) highlights the use of 2-bromo-2-methyl-propionylbromide as an alkylating agent. Contrast to the *O*-alkylation procedure above, this method occurs via *N*-alkylation, Scheme 2.5, using pyridine as a base and followed by cyclization using DMF solution in K_2CO_3 as a

base. The same result can be achieved by replacing the 2-bromo-2-methylpropionyl (**30**) with 2-chloro-propionyl chloride.
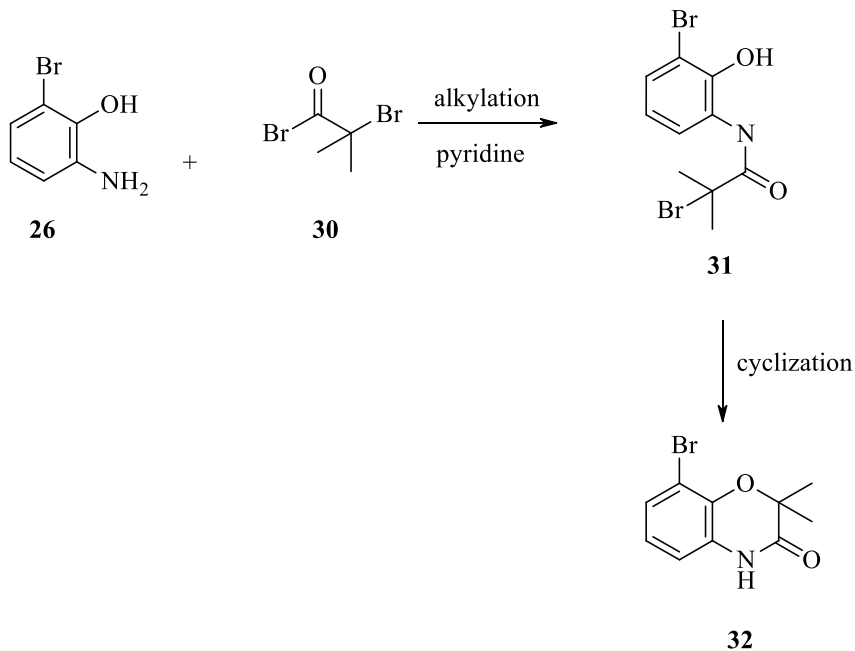
Scheme 2.5: *N*-alkylation of aminophenols as a method of synthesizing 1,4-benzoxazines

A divergent approach was taken by Caliendo *et al*. (2004). Their method involves synthesis of benzoxazines under microwave irradiation which they document to be efficient in terms of yield and reaction time when compared to the conventional methods. The reaction involves *N*-alkylation of an appropriate aminophenol using bromoacetyl bromide (**34**) or 2-bromoisobutryl bromide (**35**), in the presence of $NaHCO_3$ as a base in $CHCl_3$. Irradiation is done at 40 ^{0}C. The resulting *N*-alkylated product is cyclized using anhydrous K_2CO_3 and DMF under μv at 80 ^{0}C.

Scheme 2.6: Cyclization on *N*-alkylated aminophenols using bromoacetyl bromide

Modification of the 1,4-oxazine rings has been done by several investigators. The manipulation of the amide moiety substituent at position four has been of particular interest and has been done in two ways: (a) introduction of a substituent as a precursor and (b) *N*-alkylation of the 1,4-oxazine rings. The later has been a frequently used method involving activation of the amide nitrogen using sodium hydride (Caliendo *et al*., 2004), Scheme 2.7, potassium carbonate (Lohray *et al*., 2000), Scheme 2.8, or potassium fluoride-mediation (Anderluh *et al*., 2005) Scheme 2.9. The method by Caliendo *et al*. (2004) reduces reaction time and increase yields significantly.

Scheme 2.7: *N*-alkylation of 1,4-oxazine ring using NaH

Scheme 2.8: *N*-alkylation of 1,4-oxazine ring using K₂CO₃
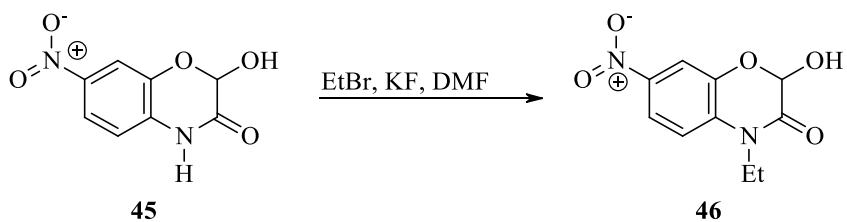
Scheme 2.9: *N*-alkylation of 1,4-oxazine ring using KF

A similar type of approach has been achieved by Rutar & Kikelj. (1998) using the alkylating agents; iodomethane, ethyl bromide and benzyl bromide in acetonitrile under phase-transfer conditions with benzyltriethylammonium chloride (BTEAC) as a catalyst, Scheme 2.10. This reaction is documented as selective.
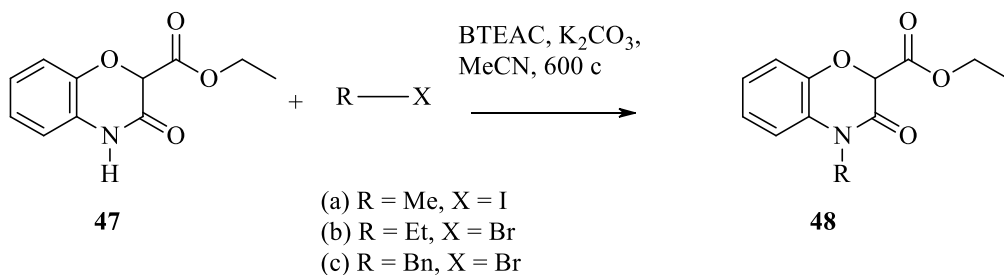
Scheme 2.10: *N*-alkylation of 1,4-oxazine ring under phase-transfer

2.6   Computer Aided Drug Design (CADD)

The previous section discussed ways of identifying a scaffold through comparisons of natural products with known drugs. Since screening and identifying molecules that may have drug-like properties is an important process, appropriate methods are needed for the success of a drug discovery project. Computer aided drug design (CADD) is one such promising methodologies that can be employed in this process.

CADD involves the use of computational tools i.e. both hardware and software to conduct complex chemical processes and theories. Strategies used to develop drugs in CADD include; structure based drug design (Amzel, 1998; Anderson, 2003; H.-J. Huang *et al*., 2010), ligand based design (Lee, Huang, & Juan, 2011), and a combination of structure and ligand based design methods (Merz, 2010).

Structure based design generally involves binding of potential ligands into an active site of known protein (Huang *et al*., 2010) through a technique referred to as docking or structure based virtual screening (VS) (Jones & Willett, 1995). VS usually ranks the ligands by some score (Hawkins *et al*, 2008). Successful VS relies on methods that assign good scores to interesting molecules (usually active against a target protein of interest) and worse scores to uninteresting (inactive) molecules (Hawkins *et al*., 2008).

The availability of a large number of protein crystal structures online such as the PDB (Berman *et al*., 2013) and small molecules in CSD (Allen, 2002) has strengthened the use of structure based designs in drug discovery efforts. During docking, a database of decoys is usually necessary to provide ligand enrichment among top ranking molecules (Huang *et al*., 2006). Ligand enrichment is a metric to assess the capacity to place true ligands at the

top-rank of the screen list among a database of decoys presumed to be inactive and are not likely to bind to the target (Mysinger *et al*., 2012).

Databases such as DUD (Huang *et al*., 2006) and DUD-E (Mysinger *et al*., 2012) contains decoy molecules that can be used to improve docking enrichments. In DUD, decoys and ligands are matched by their physical chemistry parameters (molecular weight, ClogP, number of rotatable bonds, and hydrogen bond donors and acceptors) using 2-D similarity fingerprints to minimize topological similarity. However, weaknesses in DUD such as target diversity of proteins and analogue bias led to the development of an enhanced version, DUD-E. Chemotype diversity has also been ensured in DUD-E by clustering each target's ligands by their Bemis-Murcko atomic framework leading to improved quantitative assessment of the performance of molecular docking screens in terms of enrichment in docking hit lists.

Furthermore, data from bindingdb.org contains binding information of known inhibitors that can be used to study the binding of unknown molecules (Liu *et al*, 2007). It focuses chiefly on the interactions of protein considered to be drug-targets with small, drug-like molecules. The database has 1,142,124 binding data, for 7,032 protein targets and 495,498 small molecules.

On the other hand, ligand based design involve studies where 3D structural information of the protein under study is unknown (Lee *et al*., 2011). Instead known ligands to the target are used as starting points in investigating new and potent molecules. Quantitative structure activity relationship (QSAR), molecular similarity and pharmacophore models are methods employed in ligand based design (Lee *et al*., 2011).

Dependent variables e.g. activity values (K_i, IC_{50}) and a set of calculated molecular properties or independent variables called descriptors are usually used to generate QSAR models for compounds of interest (Merz, 2010). The overall goal of QSAR is to relate the physical properties of a ligand with its biological activity. Pharmacophore refers to the molecular framework that carry essential features responsible for a drugs biological activity (Cereto-Massagué *et al*., 2015). It complements the data used in QSAR studies.

Molecular similarity on the other hand, involves the use of a set of dissimilar active molecules to extract similar features between them and using the information to design novel dissimilar molecules with biological activities (Dean, 2012). These similarities comprises of bonding patterns, atomic positions, conformation, shape and spatial disposition of molecular properties.

A popular technique used in molecular similarity is finger printing. In this method, the molecular abstractions are used by converting the molecule into a sequence of bits that can be easily compared between the molecules (Cereto-Massagué *et al*., 2015). The *tanimoto* coefficient is used as the industry standard where the number of common bits is set to 1 in both fingerprints divided by the total number of bits set to 1 between both fingerprints (Cereto-Massagué *et al*., 2015). This means that the *tanimoto* coefficient will always have a value between 0 and 1 regardless of the fingerprint length. Therefore, two molecules are judged as being similar if they have a large number of bits in common (OpenEye Scientific, 2015). The information from both structure based and ligand based strategies in drug discovery can help in quick and accurate identification of molecules that are likely to be active.

To develop a drug trade-offs among desired drug features is necessary, but for the treatment of malaria in the developing world, the provision of affordable, orally active treatments that are safe for children is, for practical purposes, mandatory. This therefore calls for affordable methods in developing potential antimalarial drugs that can be beneficial to the African community. A computational approach adopted in this research would significantly reduce the expenses and time used to identify lead compounds that can be further optimized to develop drugs.

CHAPTER THREE

MATERIALS AND METHODS

3.1   Overall Workflow

This project involved computer modeling techniques, synthesis and bioassay. Scheme 3.1

shows an overview of the methodological approach employed in this study.

Database of Natural Products of Kenya

[a] Creation of the database
[b] Conversion of 2D to 3D
[c] Generation of analogs
[d] Virtual Screening (docking)
[e] 3D shape comparison (ROCS)
[f] Synthesis of analogs
[g] Biological evaluation
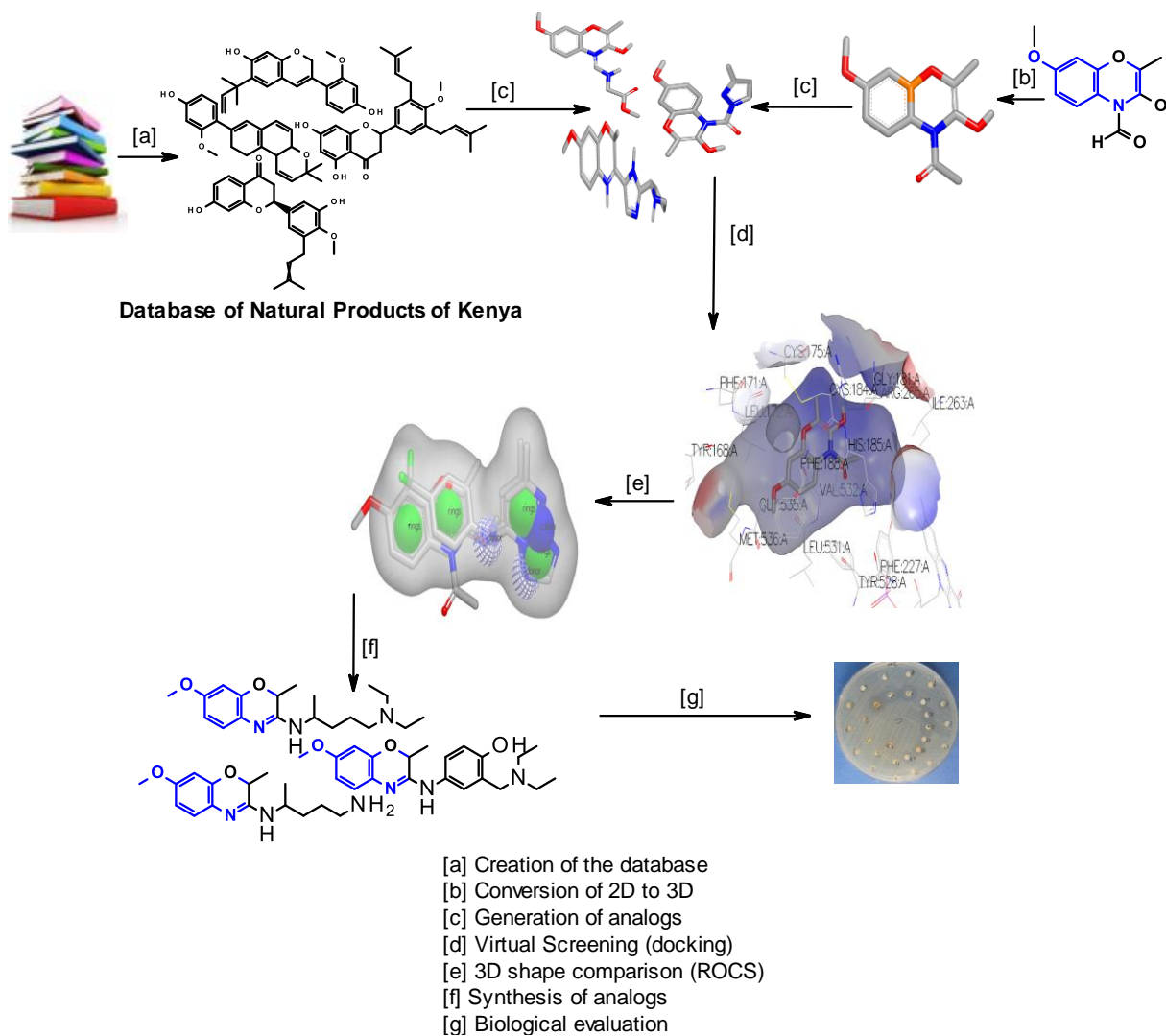
Scheme 3.1: Overview of the methodological approach of the study

3.2   Creation of the Database of Natural Products of Kenya

The computational aspects of the study were conducted on a computer running Linux operating system with an Intel corei3 processor (1.5 GHz), 4 GB of physical memory, and 500GB Hard disk space. Structure based and ligand based virtual screening was done exclusively using OpenEyes' Scientific software suite (OpenEye, Santa Fe, NM, USA, 1997) containing main applications and their subsidiary utility programs). Result analysis was done using Microsoft office Excel (Microsoft Corporation Inc. Redmond, WA, USA).

Information on the natural products was collated from theses, journal articles, published books of abstracts and conference proceedings. The data was then used to prepare a database of Natural products of Kenya. In addition to the structures of the compounds, the database contains information on the types of compounds, physicochemical properties, biological activity as well as the botanical source, plant part, place of collection and the authors.

The 2D structures were drawn using the *Accelrys* structure editor (BIOVIA, San Diego, USA). Consequently, the 1D and 3D structural formats of the compounds were generated using *lexichem* and *omega* programs of the OpenEye software suite, respectively. The data was then organized using the *Discovery studio* software (BIOVIA, San Diego, USA) and uploaded to MySQL relational database (Oracle Corporation, USA).

Creation of the database search engine was adapted from Nobert Haider's open source software MOLDBR6 (Haider, 2010). The architecture of the implementation is shown in Figure 3.1 and involves the client accessing the data in the server through the internet using a web browser.
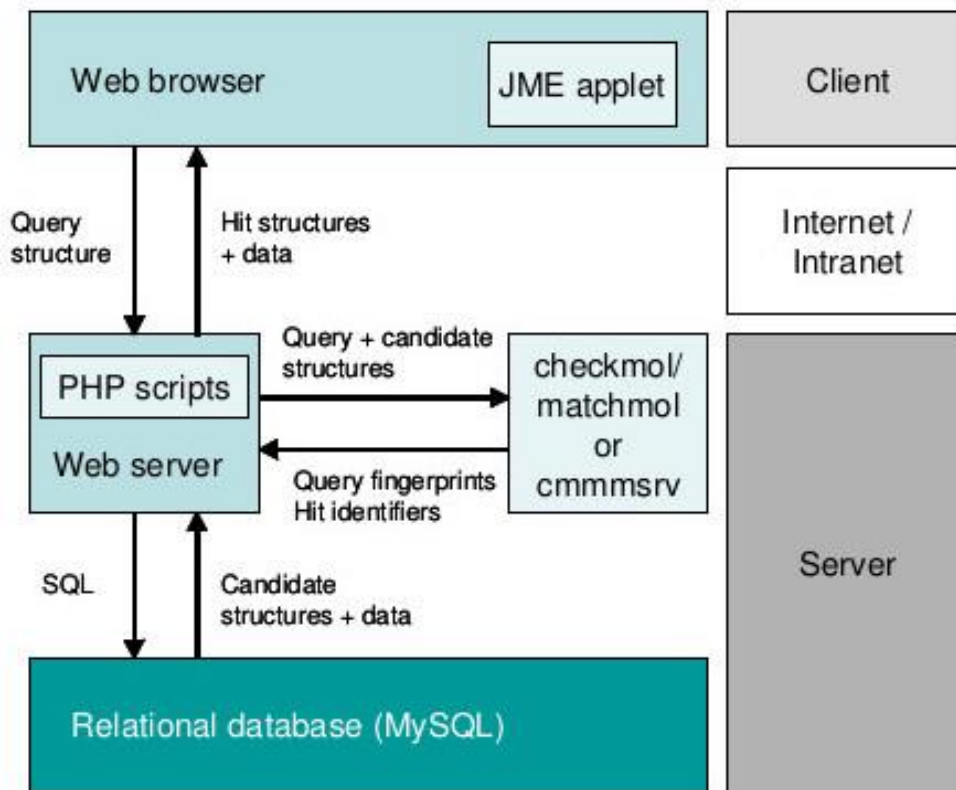
Figure 3.1: Architecture of *mitishamba* database search engine adapted from MOLDBR6
(Haider, 2010)

The search engine utilizes hypertext preprocessor (PHP) scripts and MySQL database architecture to achieve its basic utility. Information is stored in the MySQL database in normalized tables where each compound has been given a unique identification code.

A command-line program called *checkmol* (Haider, 2010) is used to read chemical structures from the database when text or 2D molecular input is executed. Its *matchmol* (Haider, 2010) counterpart matches the input with the database molecules and gives a structure hit feedback. To display the output in a web browser, PHP scripts are used. The database can be accessed from http://mitishamba.uonbi.ac.ke.

3.3 Scaffold Identification and Database Preparation (Side Chain Generation)

The next step after creation of the database involved generation and preparation of benzoxazine analogs to be used in structure based and ligand based virtual screening studies. The primary position on the benzoxazine scaffold (**49**) for generation of analogs was position 3 which was extended by replacing it with side chains of known antimalarial drugs. An alternative position that was substituted in benzoxazine was position 4 which was acylated.

49
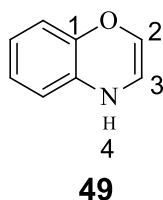
Analogs of the substituted benzoxazines were then prepared by generating bioisosteres of the side chain fragments. This was done by entering a single query fragment of each molecule in ***brood*** program to search two databases of known molecular fragments. Each database fragment was compared to the query in 3D with regard to shape, chemistry, electrostatics and geometrical presentation of the attached group.

The two databases used were;

a) Default OpenEye Brood database: A database containing a collection of roughly 12 million commercially available compounds downloaded from OpenEye's main website (www.eyesopen.com).

b) Mitishamba Database: This database was prepared using the *chomp* program which allows fragmentation of molecules, filtration of the fragments, generation of 3D conformations, organizing and indexing of the fragments for rapid searching.

The obtained molecules were then prepared for structure-based and ligand-based studies by generating their tautomers, assigning partial atomic charges and generating their 3D conformers.

3.4 Assignment of Charges and Generation of Tautomers

Appropriate atomic partial charges (floating-point values assigned to each atomic center intended to model the distribution of electrons over a molecule) were assigned to the molecules before conversion to 3D format. These partial charges provide a much better model that describes the electric field, dipole moment and other observable properties of the molecules. The *molcharge* program in the *quapac* application in the *OpenEye* suite was used to assign the appropriate atomic charges. The type of charges used were those utilized by MMFF94s force fields. The *tautomer* program was used to generate the required tautomers of the database.

3.5 Generation of 3D Conformers

The compounds were then converted into 3D format using *OpenEye's Omega* program. The default parameters were used, but with the following adjustments: e-window (50.00), maximum conformers (10), rms (0.50), and strict stereo (true). The file output format used to generate the 3D conformers of the molecules was the zipped *OpenEye* binary (oeb.gz). The 3D file containing the conformers was used in binding studies against the *Pf*DHODH receptor.

3.6   Preparation of *Pf*DHODH Receptor

A 3D protein-ligand complex structure of *Pf*DHODH *(*1tv5.pdb*)* with a bound ligand ((2Z)-2-cyano-3-hydroxy-*N*-[4-(trifluoromethyl) phenyl] but-2-enamide, A77 17726) was obtained   from   the   protein   data   bank   (PDB) http://rcsb.org/pdb/explore/explore.do?structureId=1tv5.
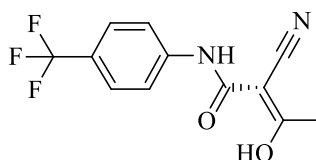
Figure 3.2: Structure of A77 17726 inhibitor

This protein-ligand complex was then converted into a receptor using *pdb2receptor* utility program found in *oedocking* application. After preparing the database and the receptor, virtual screening i.e. (structure-based and ligand-based) studies were carried out.

3.7   Structure Based Virtual Screening

The study database was docked against the active site of the receptor to generate Chemgauss scores in Kcal/mol. As a model to investigate the relationship between IC_{50} and docking scores, known inhibitors of *Pf*DHODH obtained from http://bindingdb.org were docked against the prepared receptor.

3.7.1   Docking of the 3D Conformers

The conformationally expanded 3D molecules were subjected to virtual screening in order to investigate their binding interactions with the prepared *Pf*DHODH receptor. This gave an insight on how the compounds interacted with protein fingerprints thereby sieving the molecules of interest. The process involved the use of *Fred and Hybrid* docking programs

found in the *oedocking* application. *Hybrid* docking (ligand-guided docking) utilizes the bound ligand information and performs a systematic, exhaustive, nonstochastic examination of all possible poses within the protein active sites. It filters poses based on their shape and chemical complementarity to a known bound ligand. These poses are scored using the Chemgauss4 scoring function. It is worth noting that *Hybrid* can accept more than one receptor and determines the best receptor for the ligands in the database.

Fred docking (Fast exhaustive docking) performs a systematic, exhaustive, nonstochastic examination of all possible poses within the protein active site, filters for shape complementarity and pharmacophoric features before selecting and optimizing poses using the Chemgauss4 scoring function. The keynote is that unlike *Hybrid*, it doesn't take into consideration the bound ligand in the active site while docking and it only docks using one receptor per process.

Consequently a docking report of the docked molecules together with their binding scores was generated in pdf format using the *docking_report* program. The report gives extra details including residue fingerprint, shape interactions, hydrogen bonding, ligand desolvation and protein desolvation.

3.7.2   Docking of Known Inhibitors of *Pf*DHODH

As a model, a total of 172 inhibitors out of 632 known *Pf*DHODH inhibitors and their IC_{50} values were obtained from http://bindingdb.org for use in the docking process. These molecules were then converted to 3D format and docked against the prepared *Pf*DHODH using the *Fred* program**.** The model was used to investigate whether there is any relationship between IC_{50} values and docking scores and/or z-score values. To establish a

direct relationship, the IC_{50} values of the inhibitors were converted to PIC_{50} values. After docking, a graph of the PIC_{50} against the z-scores was constructed to determine the correlation.

3.7.3 Converting Docking Scores to Z-Scores

As docking score is unrelated to activity and tends to be more of a function of the protein target under study (Swann *et al*., 2011), the absolute scores of the database molecules and those of the known inhibitors were converted to z-scores using the formula in (eq1). This was done in order to filter and quantitatively represent the data (Ebalunode *et al.*, 2008).

$$Z=\frac{x-\mu}{\sigma} \qquad \text{Equation 1}$$

Where; Z is the Z-score, x is the docking score value, μ is the mean of the docking score and σ is the standard deviation of the docking score. Swann *et al*. (2011) suggests that a z-score of 3 corresponds to 1% probability of being active, while a z-score of 4 corresponds to 5% or greater chance of being active. As a result, compounds with a z-score of 3 and above were chosen for further ligand based studies. Compounds with a z-score of 2 were also considered to widen the scope of chemistry and take into consideration synthetic accessibility factors.

3.8 Ligand Based Virtual Screening

Compounds from structure-based methods meeting the set threshold with a z-score of at least 2 were chosen for further ligand-based screening. The data was prepared by assigning charges and converting the molecules into 3D format. A 3D rapid shape overlay characteristics method was used to compare the study database molecules with a model

representative query of 10 known *Pf*DHODH inhibitors. Both shape-alignment and color (chemical alignment) metrics were used in the superposition and similarity process to identify compounds in the study database that are similar to the query model.

The query was first prepared by taking known inhibitors from 10 *Pf*DHODH crystal structures (1TV5.pdb, 3I6R.pdb, 3I65.pdb, 3I68.pdb, 3O8A.pdb, 3SFK.pdb, 4CQ8.pdb, 4CQ9.pdb, 4CQA.pdb, 4ORM.pdb) from PDB (http://rcsb.org). These known inhibitors were used to build a new query model using *vrocs* program. The dataset was prepared by aligning the 10 protein crystal structures and then extracting the ligands in the protein binding pocket. The ligands were then saved in one file and run in a graphical user interface (GUI) query wizard to get the most representative model of the 10 ligands. Default parameters in *vrocs* program were used to generate the query. The model query was validated for its ability to discriminate between a true active molecule from an inactive molecule in a given database set of decoys and active molecules and used in shape similarity studies. . However, in the electrostatics similarity studies, inhibitor A177 1726 was used as a query.

3.8.1   Validating of the Query

Before the query could be used, a set of active and decoy molecules were used to validate it to ascertain whether it was selective i.e. if it could discriminate between an active and decoy molecule from a given database. A set of active and decoys of PYRD enzyme (Dihydroorotate   Dehydrogenase)   were   downloaded   from   DUD-E (http://dude.docking.org) database (Mysinger *et al*., 2012), an enhanced version of DUD http://dud.docking.org/ (Huang *et al*., 2006).

The protein structure used is of human dihydroorotate dehydrogenase complexed with antiproliferative agents. Both datasets were used to generate statistical evaluations that showed how well the query discriminated between true active molecules from decoy molecules. From the run, the following metrics were reported to analyze whether a query was indeed selective:

i. Receiver operation curve (ROC) together with its Area Under the Curve (AUC) ± 95% confidence limits.

ii. Score histogram to examine the distribution of the scores obtained for the active and decoys dataset.

iii. Early enrichment at 0.5%, 1% and 2% of decoys retrieved ± 95% confidence limits.

iv. P-values for each enrichment level & AUC.

3.8.2 Performing Shape Similarity Studies

Once the query was ascertained to be selective, it was used for 3D comparison with the study database in a ***rocs*** run. Shape and Color (i.e. chemical similarity) were used as favorable metrics in the run. A parameter to specify the number of random starting configurations was additionally set. A value of Random starts of 50 was chosen instead of the default inertial start as adopted by Sykes *et al*. (2008). All the other default parameters were used during the run.

A score (*Tanimoto score*) datasheet was generated after the run which was used to select the molecules that were to be pursued further for electrostatics studies. Similar to the docking scores, the overlay scores were converted to z-scores to quantitatively represent

the data.

3.8.3 Performing Electrostatic Potential Studies

A dataset prepared from *rocs* overlay hits was used to carry out electrostatic potential comparison studies. It was not possible to use the model ligand built for use in the 3D shape comparison as it could only be saved as a shape query. A177 1726 inhibitor extracted from the *Pf*DHODH receptor (1tv5) was used for this purpose using *eon* program. Molecules were ranked based on the sum of full Poisson-Boltzmann (PB) electrostatics (ET_pb) and the shape *tanimoto* (ET_shape_tani) between the given molecule and the query to give ET_combo overall score. Z-scores were consequently generated from the ET_combo scores in order to quantitatively represent the data.

3.8.4 Combining the Data from Shape and Electrostatics

The data from the *rocs* and *eon* calculations were combined in order to rank the molecules in terms of their average shape and electrostatics. This process was used to rank molecules in terms of their overall metric scores for synthesis consideration.

3.8.5 Synthesis of Modeled Benzoxazines

The methodological approach that was used in the synthesis of the benzoxazines of interest identified from molecular modeling studies is as highlighted in Scheme *3.2*.
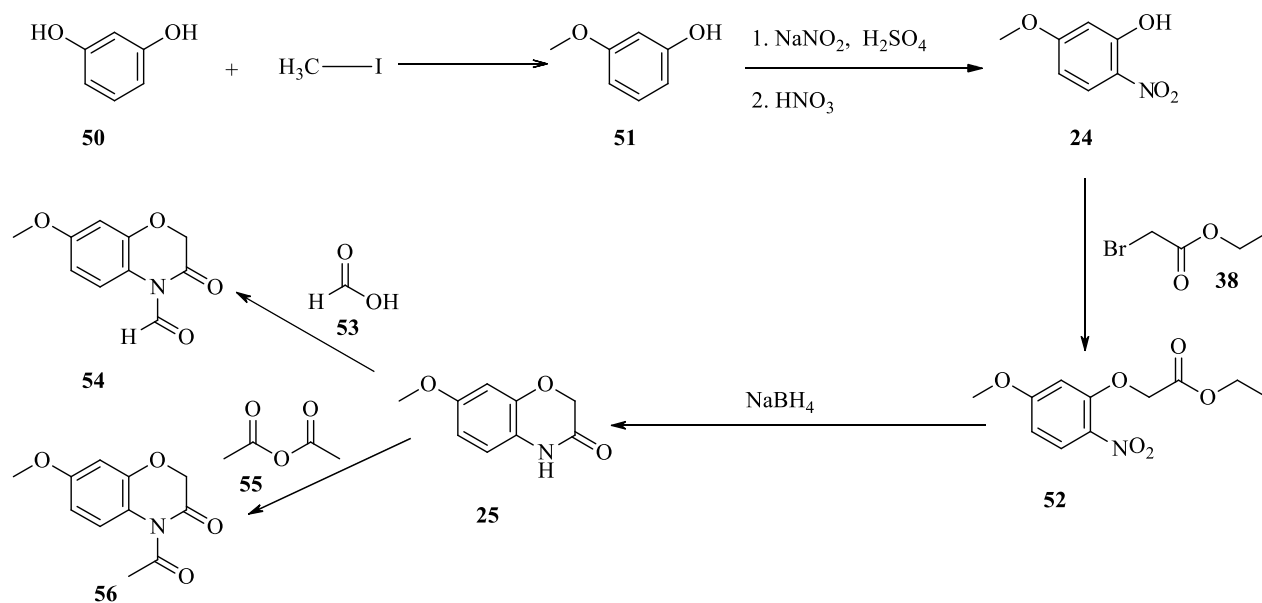
Scheme 3.2: Overall Scheme for synthesizing target benzoxazine product

The procedures that were used to synthesize the intermediates in the synthesis of the target benzoxazines are specified below.

3.8.6 Synthesis of 3-Methoxyphenol (51)
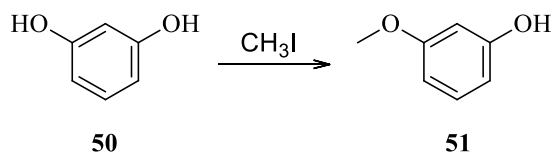
Resorcinol (**50**) (15.00 g, 136 mmol) was added to a suspension of potassium carbonate (19.00 g, 138 mmol) in acetone (60.0 mL). The mixture was stirred for 3 hours and then

methyl iodide (10.2 mL, 163 mmol) was added and the reaction mixture heated under reflux overnight at 55ºC. The reaction was filtered and concentrated under reduced pressure. The residue was diluted with methylene chloride (90.0 mL) and washed with 10% aqueous sodium hydroxide (120.0 mL). The mixture was then acidified using 1M hydrochloric acid and the methoxyphenol extracted using methylene chloride (3×45.0 mL). The resulting extract was dried over sodium sulphate, filtered and concentrated under reduced pressure to yield a reddish pink liquid. The resulting residue was purified through column chromatography (ethyl acetate/hexane 1:9) to afford of 3-methoxyphenol (**51**) (5.00 g, 30% yield) as a reddish-brown or yellowish liquid.

^{1}H NMR (600 MHz, CD$_2$Cl$_2$) δ 7.17 (*t*, *J* = 8.1 Hz, 1H), 6.53 (*ddd*, *J* = 8.2, 2.4, 0.9 Hz, 1H), 6.46 (*ddd*, *J* = 8.1, 2.4, 0.9 Hz, 1H), 6.44 (*t*, *J* = 2.4 Hz, 1H), 3.81 (*s*, 3H); ^{13}C NMR (151 MHz, CD$_2$Cl$_2$) δ 161.0, 156.9, 130.1, 107.6, 106.2, 101.3, 55.2.

3.8.7 Synthesis of 5-Methoxy-2-nitrophenol (24)
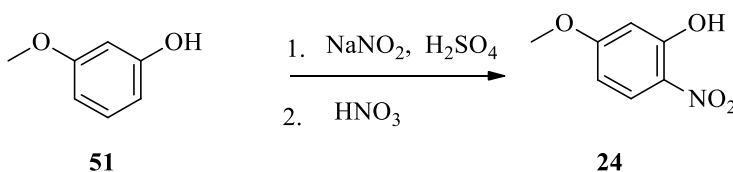
Methoxyphenol (**51**) (5.00 g, 40 mmol) was added to a solution of sodium nitrite (4.20 g, 61 mmol) in water (200.0 mL) at RT and then stirred in an ice bath for 30 minutes. 2M Sulphuric acid (16.8 mL) was then added drop wise. The reddish-brown solid that formed was filtered off and suspended in a dark flask of water (100.0 mL) at 20ºC. 50% Nitric acid (100.0 mL) was added dropwise for 90 minutes while keeping the internal temperature between 20 and 25ºC. The crude product was filtered off, washed with ice water (100.0 mL) and re-crystallized from methanol to afford yellow needle-like crystals of 5-methoxy-

2-nitrophenol (**24**) (2.5000 g, 37% yield). The NMR characterization and the melting point

(94-95°C) are in agreement with previously obtained data (Hartenstein & Sicker, 2010).

^{1}H NMR (600 MHz, CD$_2$Cl$_2$) δ 11.04 (*s*, 1H), 8.07 (*d*, *J* = 9.05 Hz, 1H), 6.59 (*m*, 2H), 3.92

(*s*, 3H); ^{13}C NMR (151 MHz, CD$_2$Cl$_2$) δ 167.2, 157.9, 127.7, 126.9, 109.4, 101.4, 56.3.

3.8.8 Synthesis of Ethyl-2-bromoacetate (38)

52   **38**
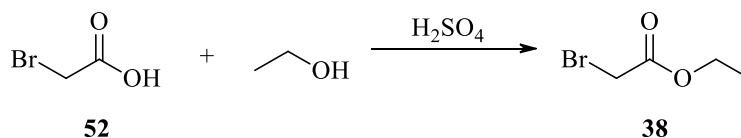
Bromoacetic acid (**52**) (5.00 g, 36 mmol) was dissolved in ethanol (23.0 mL). 30 drops of

sulphuric acid was then added and the reaction stirred at 60°C for 6 hours. The reaction

was cooled to room temperature and quenched with water (150.0 mL). The mixture was

extracted with methylene chloride (3×230.0 mL). The combined organic layers were dried

over sodium sulphate and the solvent removed under vacuum to afford ethyl-2-

bromoacetate (**38**) (Han, Alexander, & Tochtrop, 2008) (5.8 g, 97% yield) as a yellow

liquid.

3.8.9 Synthesis of Ethyl 2-(5-Methoxy-2-nitro-phenoxy)acetate (53)

24   **38**   **53**
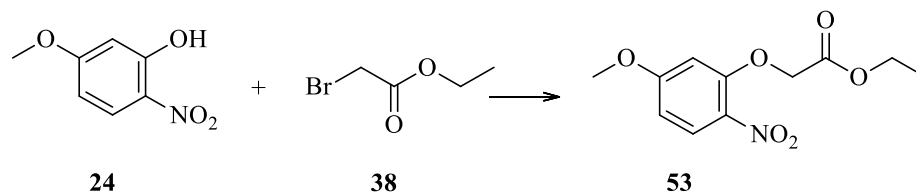
A solution of 5-methoxy-2-nitrophenol (**23**) (2.3700 g, 14 mmol) in acetone (25.0 mL) was

treated with potassium carbonate (23.3 g, 169 mmol) and heated, while stirring, at 35°C for

2 hours. A solution of ethyl bromoacetate (**38**) (3.34 g, 20 mmol) in acetone (12 mL) was

added dropwise and heated at 50ºC for 4 hours. The mixture was filtered to remove potassium carbonate and the filtrate concentrated. The residue was taken up in ethyl acetate (25.0 mL), washed with distilled water (5×100.0 mL) and dried over sodium sulphate. The mixture was filtered and the filtrate concentrated under vacuum. The residue was purified through column chromatography (ethyl acetate/hexane 2:8) to provide ethyl 2-(5-methoxy-2-nitro-phenoxy)acetate (**53**) (1.0000 g, 28% yield) as a yellow liquid which forms yellow crystals on cooling.

^{1}H NMR (600 MHz, CD$_2$Cl$_2$) δ 7.90 (*d*, *J* = 9.13 Hz, 1H), 6.51 (*dd*, *J* = 9.14, 2.47 Hz, 1H), 6.37 (*d*, *J* = 2.50 Hz, 1H), 4.67 (*s*, 2H), 4.17 (*q*, *J* = 7.14 Hz, 2H), 3.78 (*s*, 3H), 1.20 (*t*, *J* = 7.16 Hz, 3H); ^{13}C NMR (151 MHz, CD$_2$Cl$_2$) δ 167.4, 164.5, 153.6, 133.3, 128.2, 105.9, 101.1, 66.3, 61.6, 55.9, 13.8.

3.8.10 Synthesis of 7-Methoxy-4H-1, 4-benzoxazin-3-one (25)
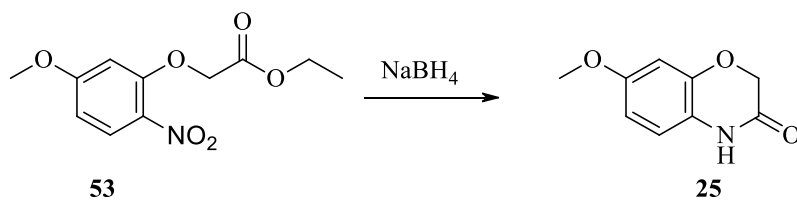
5% Pd/C (100.0000 mg,) was suspended in an aqueous solution of 1,4-dioxane (50.0 mL, 1:1). Sodium borohydride (650.0000 mg, 17 mmol) was added to the mixture and the solution vigorously stirred. A solution of ethyl 2-(5-methoxy-2-nitro-phenoxy) acetate (**53**) (0.5 g, 2 mmol) in 1,4-dioxane (1 mL) was added dropwise to the suspension and the reaction monitored by TLC. The suspension was filtered off and the filtrate acidified with 10% HCl to pH 2. The mixture was then extracted with ethyl acetate (50.0 mL) and dried over sodium sulphate. The solvent was removed under vacuum and the residue purified

through column chromatography (ethyl acetate/hexane 1:9) to obtain 7-methoxy-4H-1, 4-benzoxazin-3-one (**25**) (100.0000 mg, 29% yield) as a brownish crystalline compound.

^{1}H NMR (600 MHz, Acetone-d_6) δ 7.25 (*d*, *J* = 8.80 Hz, 1H), 6.67 (*dd*, *J* = 8.78, 2.66 Hz, 1H), 6.59 (*d*, *J* = 2.64 Hz, 1H), 4.71 (*s*, 2H), 3.79 (*s*, 3H); ^{13}C NMR (151 MHz, Acetone-d_6) δ 158.9, 156.6, 144.9, 123.0, 113.6, 107.4, 102.5, 68.1, 55.1.

3.8.11 Synthesis of 7-Methoxy-3-oxo-1,4-benzoxazine-4-carbaldehyde (54)
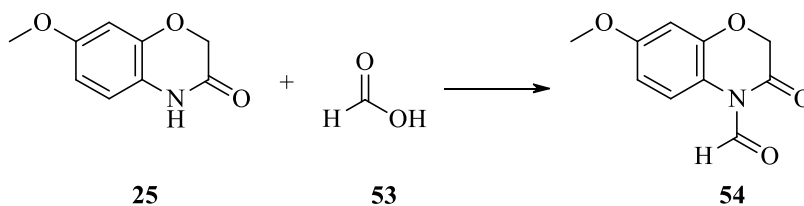
7-Methoxy-4H-1,4-benzoxazin-3-one (**25**) (0.08 g, 0.45 mmol) and formic acid (**53**) (2.0 mL) was stirred at 60°C and the reaction was monitored by TLC. After completion of the reaction, the mixture was diluted with ethyl acetate (3×20.0 mL) and washed with a saturated solution of NaHCO$_3$ (20.0 mL). The solution was then dried under Na$_2$SO$_4$ and filtered. The filtrate was concentrated and the residue recrystallized using ethyl acetate to obtain 7-methoxy-3-oxo-1,4-benzoxazine-4-carbaldehyde (**54**) (18.0000 mg, 19% yield) as a dark-brown solid.

^{1}H NMR (500 MHz, CD$_2$Cl$_2$) δ 8.74 (*s*, 1H), 6.78 (*d*, *J* = 8.6 Hz, 1H), 6.60 (*d*, *J* = 2.6 Hz, 1H), 6.56 (*dd*, *J* = 8.6, 2.7 Hz, 1H), 4.61 (*s*, 2H), 3.78 (*s*, 3H); ^{13}C NMR (101 MHz, CDCl$_3$) δ 219.5, 165.2, 156.6, 144.5, 119.4, 116.2, 108.1, 103.0, 67.2, 55.6.

3.8.12 Synthesis of 4-Acetyl-7-methoxy-1,4-benzoxazin-3-one (56)
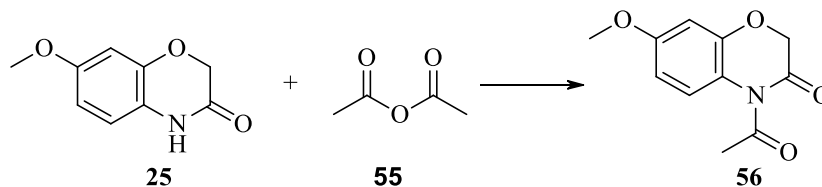
Acetic anhydride (0.1 ml) was added to a solution of 7-methoxy-1,4-benzoxazin-3-one (**25**) (0.1670 g, 0.1 mmol) in a mixture of toluene and triethylamine (6 ml, 1:1). The mixture was heated at 60°C for 4hrs. After cooling to RT, the mixture was then washed with water (3×20.0 ml) and the organic phase concentrated under vacuum. The residue obtained was purified by column chromatography (ethyl acetate/hexane 1:20) to obtain 4-acetyl-7-methoxy-1,4-benzoxazin-3-one (**56**) (80.0000 mg, 36% yield) as a yellow solid.

^{1}H NMR (500 MHz, CD$_2$Cl$_2$) δ 7.59 (*m*, 1H), 6.67 (*m*, 2H), 4.60 (*s*, 2H), 3.82 (*s*, 3H), 2.68 (*s*, 3H); ^{13}C NMR (101 MHz, CDCl$_3$) δ 170.8, 169.4, 158.0, 148.9, 124.4, 119.0, 108.6, 102.8, 70.2, 55.6, 28.2.

3.9   *In Vitro* Antiplasmodial Assay

Antiplasmodial assay of the target compounds was carried out against chloroquine sensitive 3D7 and chloroquine resistant K1 isolate strains of *P. falciparum* using a non-radioactive assay technique. This procedure was adopted from the work of Heydenreich *et al*. (2011) with modifications. The method uses the flourochrome called "SYBR Green I", a non-radioactive DNA dye that accurately depicts *in vitro* parasite replication. Concurrently, twofold serial dilutions of the drugs chloroquine (1.953 - 1000 ng/mL), mefloquine (0.488-250 ng/mL) and test sample (97.7 - 50,000 ng/mL) were prepared on a 96 well plate. The culture-adapted *P. falciparum* were reconstituted to 1% parasitemia and

added on to the plate containing dose range of the reference drugs and test samples. They were incubated in gas mixture (5% CO_2, 5% O_2, and 90% N_2) at 37 °C. The assay was terminated after 72h by freezing at -80 °C for 24h. After thawing, lysis buffer containing SYBR Green I ($1 \times$ final concentration) was added directly to the plates and gently mixed by using the Beckman Coulter Biomek 2000 automated laboratory workstation (Beckman Coulter, Inc., Fullerton, CA). The plates were incubated for 5 -15 min at room temperature in the dark. Parasite growth inhibition was quantified by measuring the per-well relative fluorescence units (RFU) of SYBR Green 1 dye using the Tecan Genios Plus (Tecan US, Inc., Durham, NC) with excitation and emission wavelengths of 485 nm and 535 nm, respectively, and with the gain set at 60. Differential counts of relative fluorescence units (RFUs) were used in calculating 50% inhibition concentration (IC_{50}'s) for each drug using Prism 4.0 windows software (Microsoft Corporation Inc, Redmond, WA, USA). A minimum of three separate determinations was carried out for each sample.

CHAPTER FOUR

RESULTS AND DISCUSSION

4.1   Outline of the Study

In this study, a web based *in silico* database of natural products of Kenya was created. It was utilized in virtual screening studies to model antiplasmodial benzoxazine analogs. Benzoxazines with promising binding affinities were then synthesized and assayed against chloroquine sensitive and resistant strains of *Plasmodium falciparum.*

4.2   Features of the Database of Natural Products of Kenya (*Mitishamba* Database)

A total of 1112 natural products were collated from theses, published articles, books of abstracts and conference proceedings to create an interactive web based database of natural products of Kenya. The database was named *Mitishamba,* a Kiswahili word referring to herbal medicine. In addition to chemical structures of the natural products, the database contains information on their IUPAC names, trivial names, physicochemical properties and botanical information on their source plants. More detailed information on these compounds is captured in the *Mitishamba* database and hosted at http://mitishamba.uonbi.ac.ke. Figure 4.1 highlights the architecture of the database.
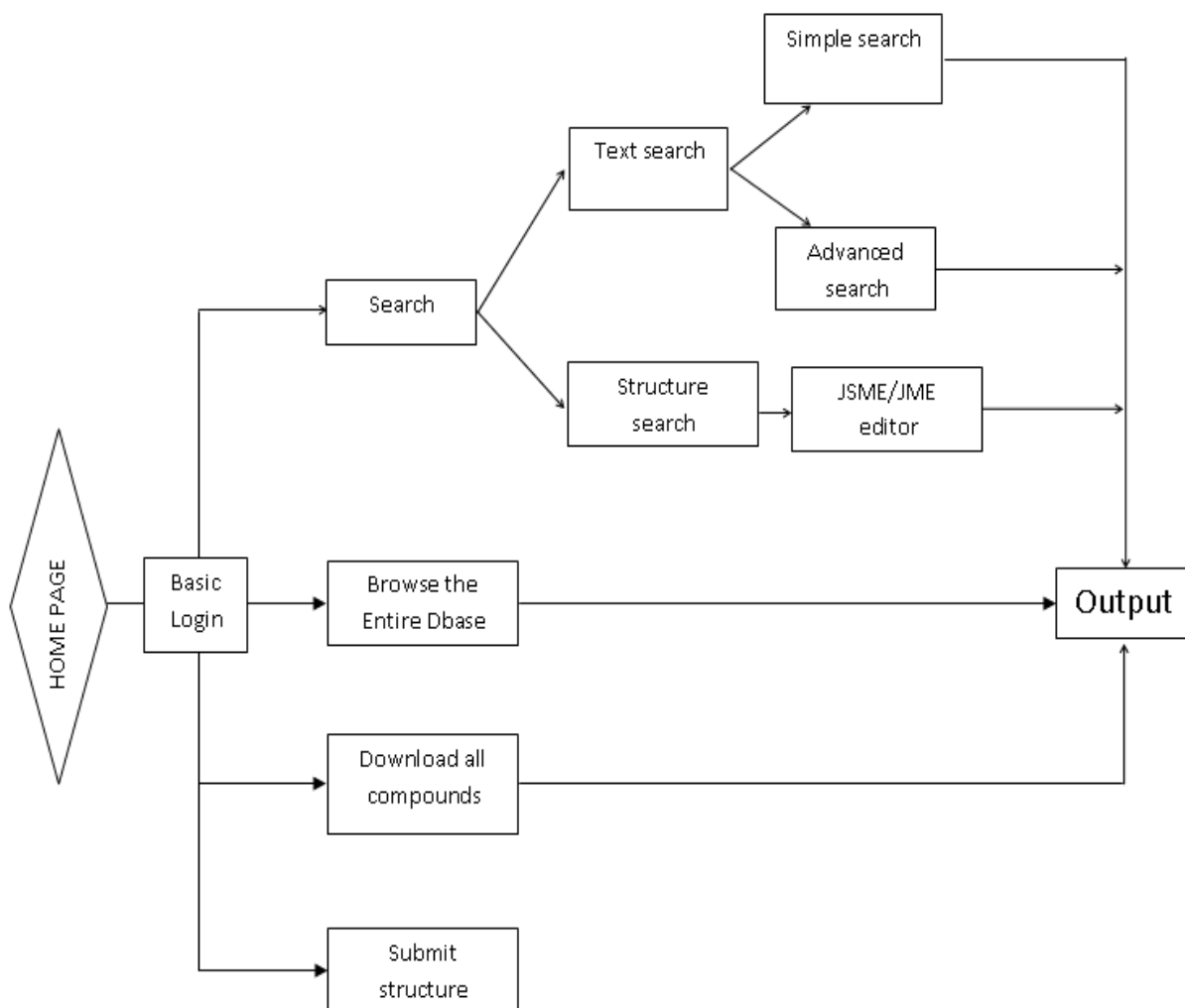
Figure 4.1: *Mitishamba* Database flowchart

The interactive nature of the database and its rich features allow users to search, download, browse and submit structures. Users must first register for free in the system and login in order to access all the above features.

4.2.1 Searching the Database

It has two search options: (a) Text search and (b) Structure search. Users can search for structures in the text search option using either IUPAC or trivial names. An advanced search feature also allow users to search for compounds based on plant family and species.

For structure search, 2D structure input is entered in a JavaScript editor (JSME) or Java molecule editor (JME) adopted from Peter Etrl of Novartis (Bienfait & Ertl, 2013);. The options are detected automatically on the users' browser and one is used as a fallback incase either JavaScript or Java feature is turned off. Optional parameters available for structure search include exact match, substructure search and similarity search on the scale of zero to hundred ratio. Once an output is obtained, structures can be downloaded in sdf format.

A functional group search option is also available where users can search compounds based on the functional group present on the structure of interest. Pressing control key while clicking the specific functional groups of interest allows for selection of a combination of functional groups.

4.2.2   Browse and Download Structures

Users can browse through the entire database structure by structure. Each structure has a "view full details" link that allows for checking additional information about a specific compound. A download link is provided next to the name of the compound that can be used to download the structure of interest in mol format. Alternatively users can download the entire database in the following file formats: SDF, MOL, OEB and SMILES.

4.2.3   Submitting Structures

In this project, the framework of organizing information on Natural Products from plants of Kenya has been created. Recognizing that natural products research is continuous and there are many groups studying natural products of Kenya, a structure submission feature has been included in the database system to enable researchers submit their work.

4.3 Scaffold Identification and Database Preparation

The benzoxazine scaffold was chosen as the favorable scaffold due to its similarity to the quinoline scaffold in the antimalarial drug, primaquine (**19**). The benzoxazine scaffold also occurs in cappamensin A (**18**) isolated from the root and seeds of *Capparis sikkimensis* (Wu *et al*., 2003). Cappamensin A (**18**) is reported to exhibit cytotoxicity against various cancer cell lines.
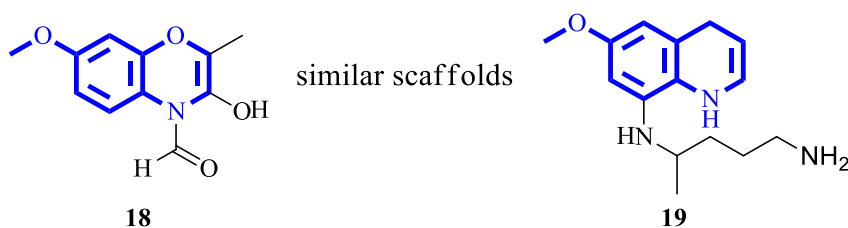
Despite the similarity of Cappamensin A scaffold with the quinoline scaffold in primaquine, its antiplasmodial activity has not been investigated. In order to investigate the antiplasmodial potential of the benzoxazine scaffold, a datab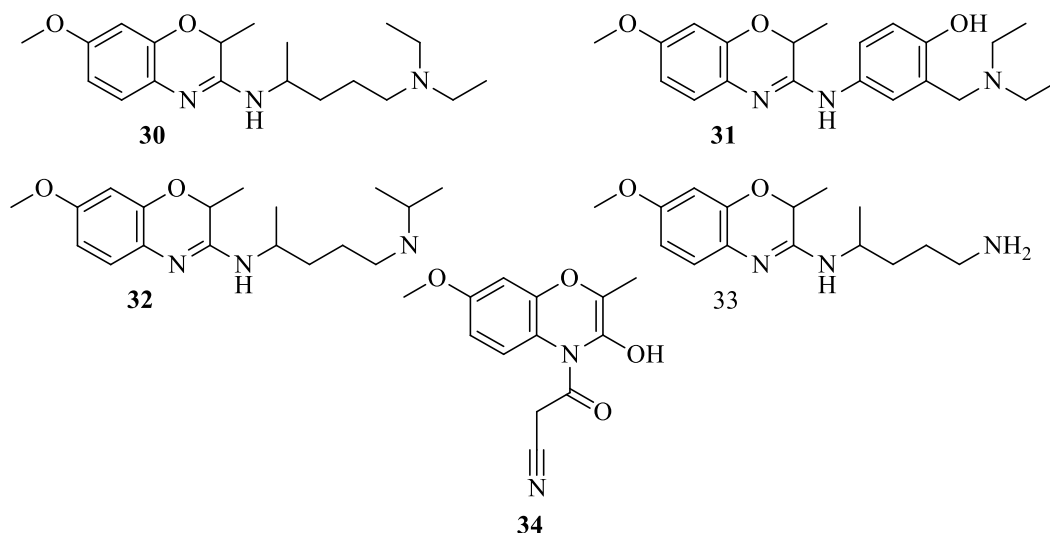ase of benzoxazine derivatives was generated by replacing the hydroxyl side chain in cappamensin A with side chains of known antimalarials chloroquine, amodiaquine, isopentaquine, and primaquine. The side chains of known antimalarial drugs were used because the diversity that side chains provide to drug molecules is quite low. It is suggested that only about 20 side chains account for over 70% of the side chains of marketed drugs (Bemis and Murcko, 1999). In addition, *N*-acylation with a cyano acetyl moiety was done at position four because the 1tv5 enzyme inhibitor (A77 17726) has a cyano group which is attached to an amide group. This attachment was to mimic the binding mode of the inhibitor. This resulted in the initial database of cappamensin A analogs shown in Figure 4.2.

Figure 4.2: A database of benzoxazine derivatives of cappamensin A

The five molecules in Figure 4.2 were used to computationally derive 790 bioisosteres using **vbrood** program. Emphasis was given to electrostatics and shape metrics during the bioisostere generation process. The *molcharge* program used to assign atomic partial charges to these molecules provides for a better model or approximation of the wave function describing the distribution of electron density around them. Additionally, the *tautomer* program was used to generate "canonical" representations (unique representations) of the molecules so as to identify the physiologically preferred form(s) as illustrated in Figure 4.3 for molecule (**35**).
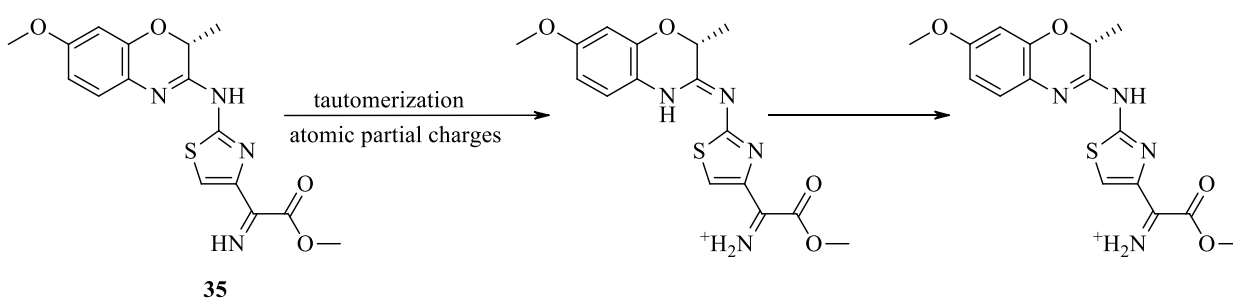
Figure 4.3: Assignment of charges and generation of tautomers of **35**

54

Consequently 3D formats of the molecules were generated. This involves converting the molecules to three dimensional coordinates that is essential for the interaction of the molecule with the receptor. Molecules of the lowest conformational energy are preferred as they are stable.

4.4   Identification of the Active Site of the *Pf*DHODH Receptor

The 1tv5 *Pf*DHODH enzyme from PDB was converted into a receptor using *pdb2receptor* program. The prepared receptor had an active site with amino acid residues (**His185, Arg 265A, Tyr 528**) and a bound inhibitor (**6**) as shown in Figure 4.4.
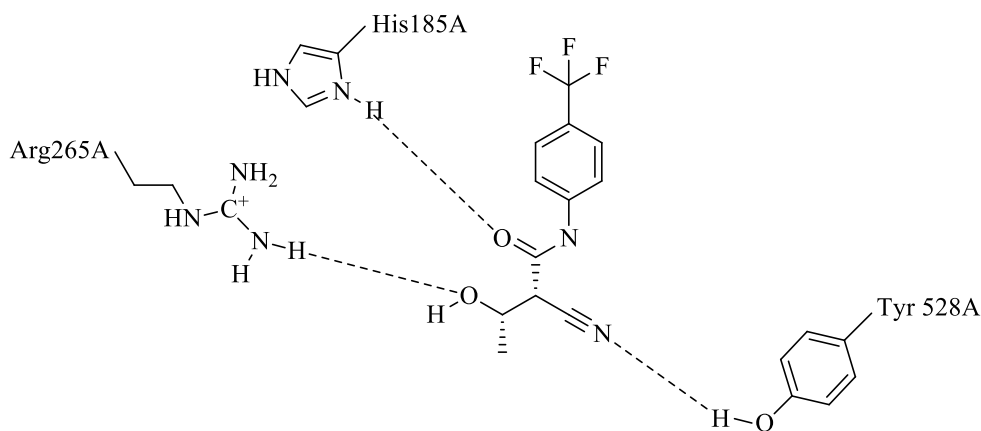
Figure 4.4: Binding mode of the prepared 1tv5 receptor

The inhibitor (**6**) is an active metabolite of leflunomide (Arava), a disease modifying anti-rheumatic drug (Rückemann *et al*., 1998). The site was the pocket to which the database molecules were docked. Generally, the binding pocket is usually identified prior to the docking process (Azam & Abbasi, 2013).

4.5   Structure Based Virtual Screening

The 790 molecules were docked against the prepared *Pf*DHODH receptor using *fred*

program to give binding scores**.** The scores are normally a function of the protein target rather than activity of the molecules. Therefore they have to be converted into their respective z-score in order to filter and quantitatively represent the data (Ebalunode *et al.*, 2008). Compounds with z-score equating to 3 have 1% probability of being active while compounds with z-score equating to 4 or greater corresponds to 5% or higher chances of being active (Swann *et al.*, 2011). The top 10 molecules with z-score of 3 and above are shown in **Table** *4.1*.

Table 4.1: Normalized scores for 790 analogs docked against 1tv5 enzyme

No.	Smiles	Score (Kcal/mole)	Z-score
1	CC1=C(N(c2ccc(cc2O1)OC)C(=O)Nc3ccon3)O	-15.74	4
2	COc1ccc2N(C(=O)N(C)C=O)C(=C(C)Oc2c1)O	-14.54	4
3	COc1ccc2N(C(=O)N(C)CC#N)C(=C(C)Oc2c1)O	-13.55	4
4	CC1=C([N+](=CNCC(=O)OC)c2ccc(cc2O1)OC)O	-13.32	3
5	Cc1ccn(n1)C(=O)N2c3ccc(cc3OC(=C2O)C)OC	-13.04	3
6	CC1=C([N+](=CNCC(=O)OC)c2ccc(cc2O1)OC)O	-13.02	3
7	CC1=C(N(c2ccc(cc2O1)OC)C(=O)CC3CCCO3)O	-13.01	3
8	CC1=C(N(c2ccc(cc2O1)OC)C(=[NH2+])c3ccccn3)O	-12.98	3
9	CC1=C(N(c2ccc(cc2O1)OC)C(=O)Nc3ccon3)O	-12.84	3
10	CC1=C(N(c2ccc(cc2O1)OC)C(=O)CC3CCCO3)O	-12.79	3

In order to widen the chemical space of obtaining active compounds from the database and taking into consideration of synthetic accessibility factors, molecules with z-score of 2 were also considered giving rise to a total of 108 compounds.

As an illustration of the interaction of these 108 compounds with the receptor, the binding mechanism of the top molecule, 3-hydroxy-*N*-isoxazol-3-yl-7-methoxy-2-methyl-1,4-benzoxazine-4-carboxamide, in **Table *4.1*** is discussed below. Generally the inhibition mechanism of the inhibitor (**6**) to the Quinone-binding tunnels of the *Pf*DHODH is as shown in Figure 4.4 in Section 4.4.

Greater binding of inhibitors to the 1tv5 *Pf*DHODH enzyme would occur for compounds that maintain the correct configuration for hydrogen bonding to the conserved trio residues of **His185**, **Arg265** and **Tyr528** which are donor atoms (Hurt *et al*., 2006). It is these three conserved residues that guided the virtual screening studies on a database of benzoxazine molecules. Indeed the results from the binding studies showed that the best binding molecule has hydrogen bonding with the conserved trio residues as shown in Figure 4.5 and Figure 4.6.
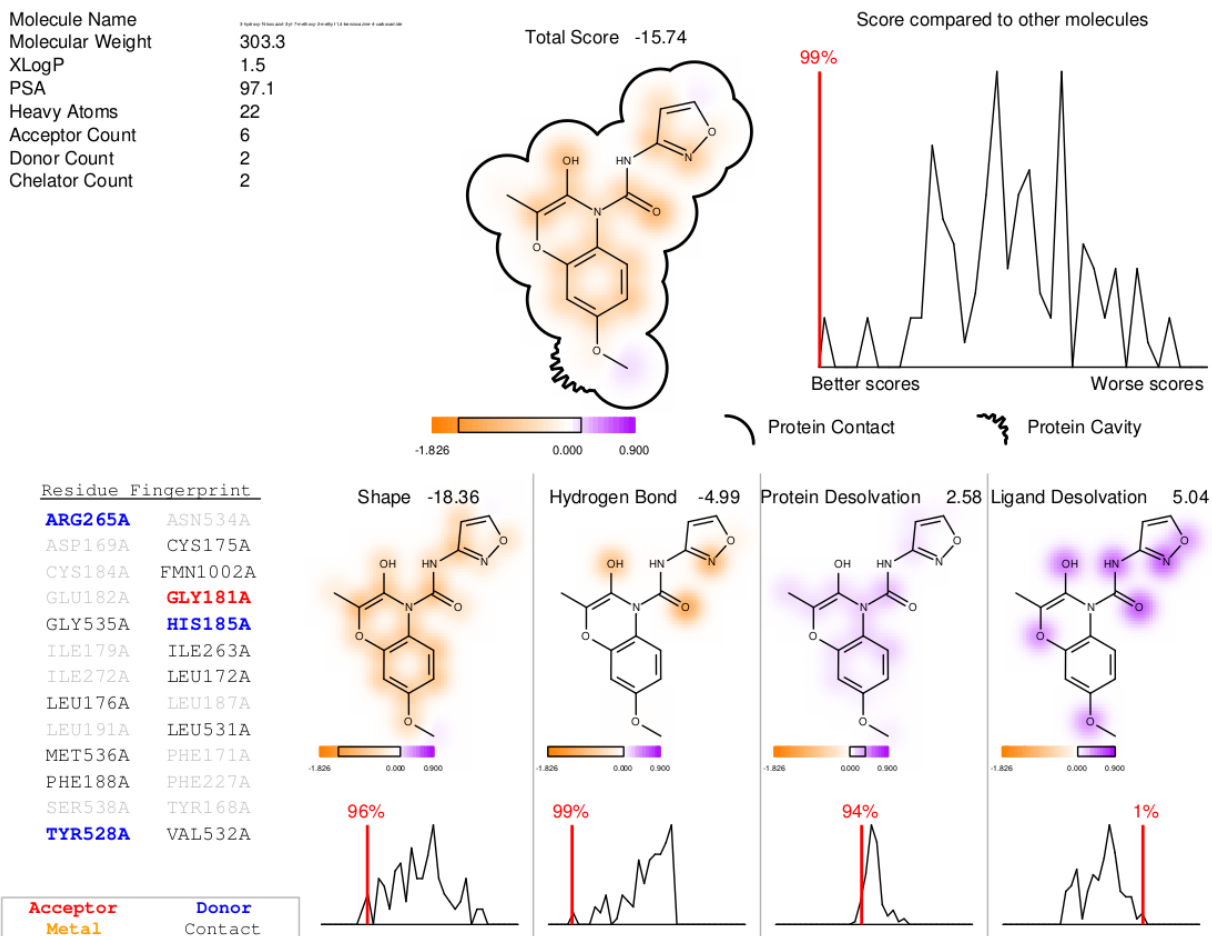
Figure 4.5: Binding fingerprint of 3-hydroxy-N-isoxazol-3-yl-7-methoxy-2-methyl-1,4-benzoxazine-4-carboxamide
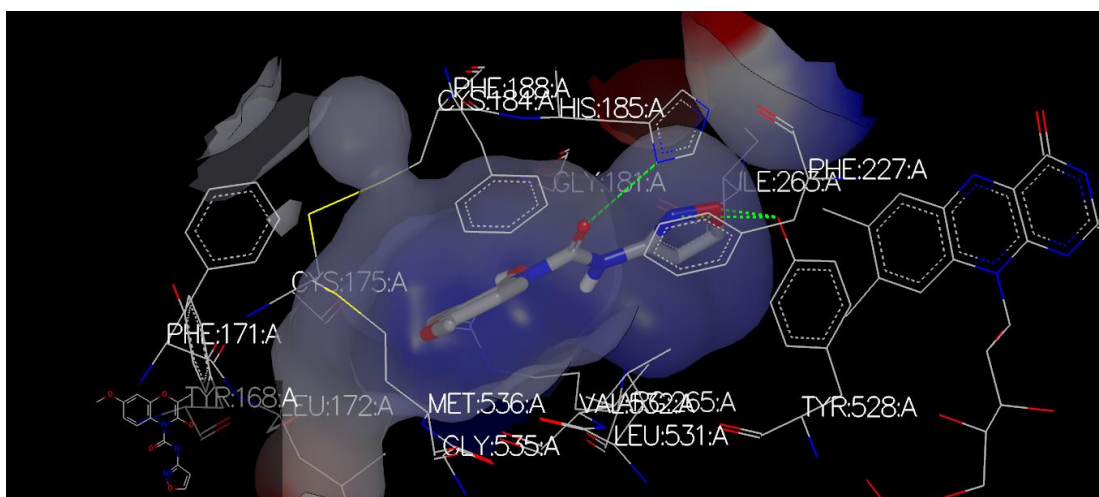

Figure 4.6: 3D binding view of 3-hydroxy-N-isoxazol-3-yl-7-methoxy-2-methyl-1,4-benzoxazine-4-carboxamide

In addition to its binding to three amino acid residues, this compound showed an extra interaction with **Gly181A**. **Gly181A** being an acceptor, it is likely that the interaction would be occurring with an atom donor of the molecule. This is a new interaction that would possibly increase the binding strength of the proposed new inhibitors. The fate of the binding molecules in respect to the **Gly181A** acceptor is unclear. However it seems that it has a positive outcome since adverse effects would have led to the molecule being ranked lower.

A look at the color (i.e. hydrogen donor and acceptor) characteristics of the top molecule shows that indeed its acceptor characteristics enhance its ability to bind to the residues as shown in Figure 4.7. It has three acceptors (a carbonyl of the amide and the oxygen and nitrogen of the isoxazole moiety) which bind to the donors **His185A**, **Arg265A**, and **Tyr528,** respectively. It is probable that **Gly181A** binds to the oxygen atom in the isoxazole ring. The 3D binding view of the molecule with the amino acid residues is shown in Figure 4.6.
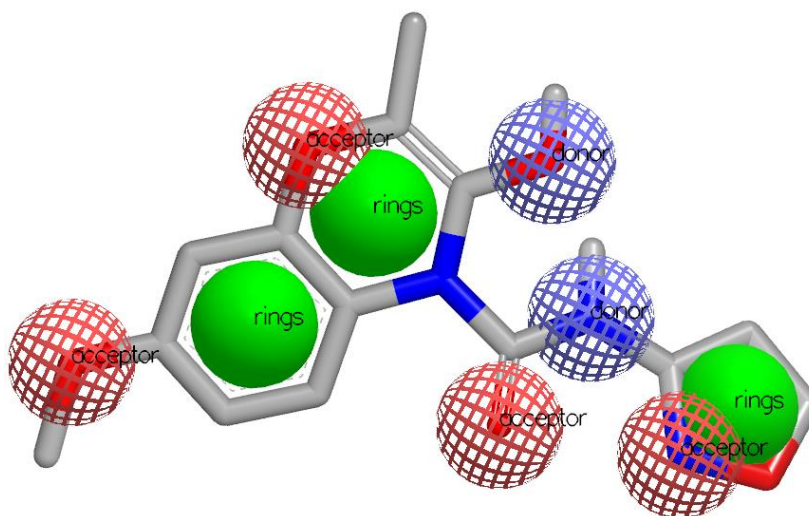
Figure 4.7: Chemical color of 3-hydroxy-N-isoxazol-3-yl-7-methoxy-2-methyl-1,4-benzoxazine-4-carboxamide

It is important to note that there are non-conserved residues (**Cys184A** and **Cys175A**) in the waist region of *Pf*DHODH which are unique to *Plasmodium* species and may also influence the binding towards the enzyme (Hurt *et al*., 2006). In this study, the unique residues were found to only have contact with most molecules but did not participate in binding. Another important point to note is that the decreased volume of *Pf*DHODH at the end of the binding-tunnel and the steric hindrance of **Phe188A** hinders binding and such should be considered as a factor (Hurt *et al*., 2006).

Surprisingly, most of the analogs including the top binding molecule made contact with **Phe188A**. The extent of the contact is not clear at the moment and would need further investigations. Furthermore there was a peculiar contact of most analogs with the cofactor **FMN1002A**. This suggests that there could be auxiliary interactions of the benzoxazine scaffolds with the FMN cofactor which is important in the biosynthesis of pyrimidines for *Pf*DHODH.

It is however difficult to conclude that these molecules would indeed be better inhibitors to the enzyme without doing further studies on the dataset. As a result, further shape comparison and electrostatics studies were carried out using the 108 molecules.

4.6   Docking of Known Inhibitors of *Pf*DHODH

In order to establish if there exist a relationship between z-score and IC_{50}, 172 known inhibitors of *Pf*DHODH obtained from http://bindingdb.org were docked and their scores normalized. A summary of the results for top 10 ranking molecules that were used to establish this relationship is shown in **Table *4.2***.

Table 4.2: Table of known *Pf*DHODH inhibitors docked against 1tv5 enzyme

No.	Name	Chemgauss4 score (Kcalmol^{-1})	z-score	PIC50
1	CHEMBL2431498	-14.0593	3	7.1
2	Triazolopyrimidine-based Cpd, 11	-12.8962	2	5.5
3	CHEMBL1784568	-12.8306	2	5.3
4	CHEMBL2431502	-12.7853	2	6.8
5	ChemBridge cpd no. 3	-12.7636	2	6.5
6	CHEMBL1784559	-12.7332	2	4.6
7	CHEMBL2431509	-12.4955	2	5.9
8	CHEMBL2431514	-12.4638	2	6.5
9	CHEMBL1784717	-12.4449	2	5.9
10	Triazolopyrimidine-based cpd, DSM69	-12.0969	1	5.3

The purpose of generating this data was to study whether there is a high probability of choosing an active molecule from the top ranked molecules based on their z-scores. The fundamental question being, can the z-score guide us in identifying an active molecule? To establish this relationship, the PIC$_{50}$ values of the 172 inhibitors were plotted against their respective z-scores as illustrated in **Graph *4.1***.
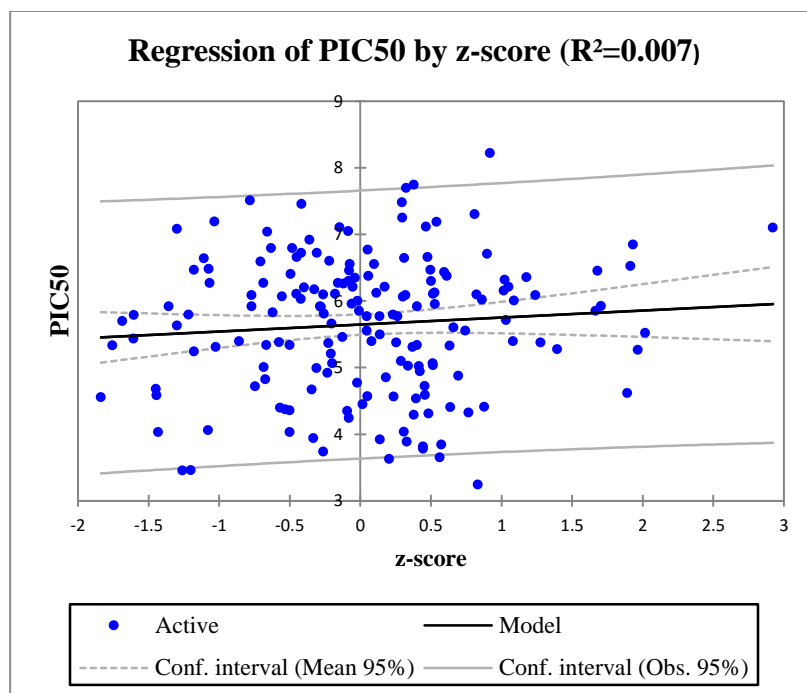
Graph 4.1: Correlation of z-score and PIC50 of 172 known *Pf*DHODH

There is low correlation on the entire dataset with a value of $R^2=0.007$. This means that the probability of picking an active molecule from an entire database of docked molecules is very low. However, considering only top 10 ranking molecules improves the correlation to 0.172 as shown in **Graph *4.2***. This translates to a 1% probability of picking an active molecule amongst the top 10 molecules. The data is in agreement with the suggestion that molecules with a z-score of 3 have a 1% probability of being active (Swann *et al*., 2011).
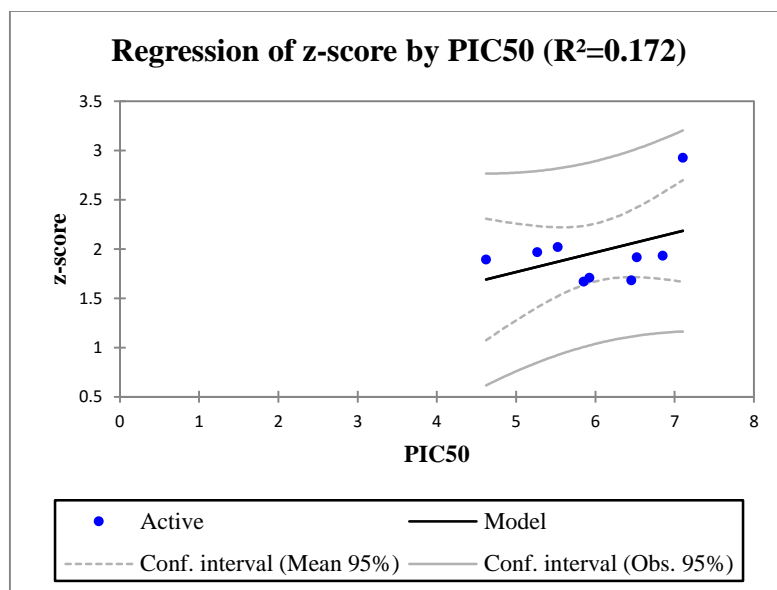
Graph 4.2: Correlation of z-score and PIC50 of top 10 known *Pf*DHODH inhibitors

To investigate how the binding of the 172 docked inhibitors was distributed, a distribution fitting of the z-scores was computed. *Graph 4.3* shows the histogram of the distribution of the z-scores.
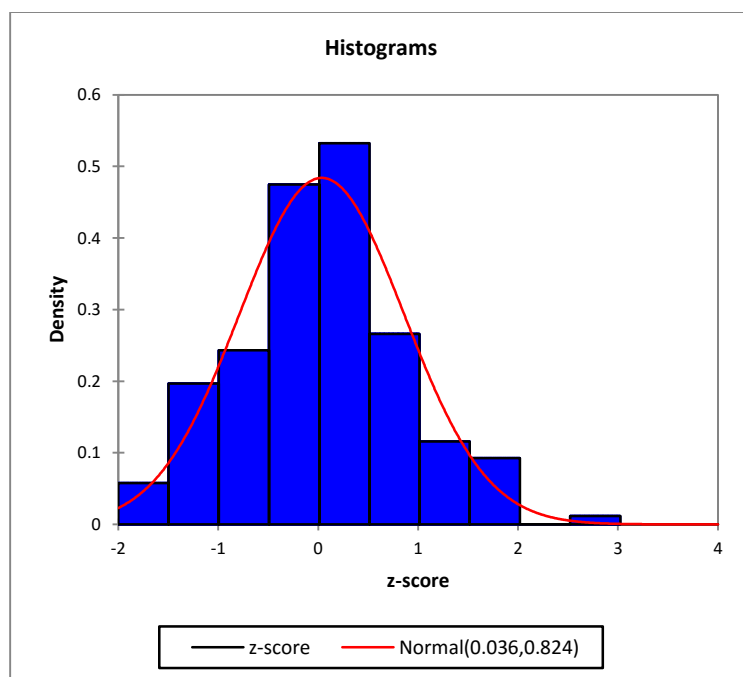
Graph 4.3: Graph of normal distribution of known *Pf*DHODH inhibitors

Table *4.3*, show the statistical results using the parameters of the normal distribution.

Table 4.3: Statistics computed using the parameters of the normal distribution

| Statistic	Data	Parameters
Mean	0.036	0.036
Variance	0.680	0.680
Skewness (Pearson)	0.266	0.000
Kurtosis (Pearson)	0.480	0.000
Kolmogorov-Smirnov test:		
D	0.061	
p-value	0.529	
alpha	0.05	

When the statistical data was subjected to the Kolmogorov-Smirnov test for equality of continuous, one-dimensional probability distributions, a p-value of 0.529 was obtained which translates to 52.87% confidence that the data is normally distributed. This lead us to a conclusion that the z-scores of the known inhibitors are normally distributed and therefore provide a good guide to the activity of the molecules.

4.7   Ligand Based Virtual Screening

The 108 molecules selected from structure based VS were subjected to shape similarities using a representative model ligand prepared from 10 inhibitors extracted from known *Pf*DHODH targets. Electrostatics similarity studies were consequently done using the *Pf*DHODH inhibitor (**6**).

4.7.1   Validating the Query

From *rocs* query builder, a model composed of two of the 10 ligands extracted from known *Pf*DHODH targets, (3I65.pdb and 3I6R.pdb) shown in Figure 4.8, was found to be the most representative of the dataset of the 10 *Pf*DHODH inhibitors.
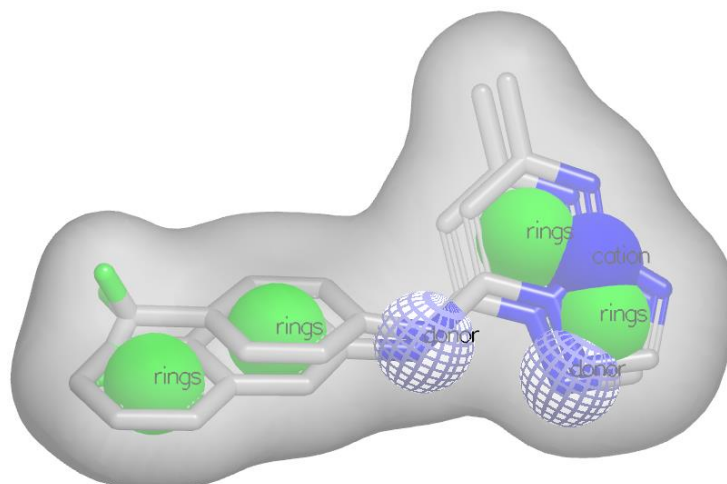
Figure 4.8: Model ligand query (3I65.pdb and 3I6R.pdb)

Validation of the query using a set of actives and decoys obtained from http://dude.docking.org gave ROC curves as shown in Figure 4.9 and Figure 4.10 for shape and *color_tanimoto* metrics, respectively.
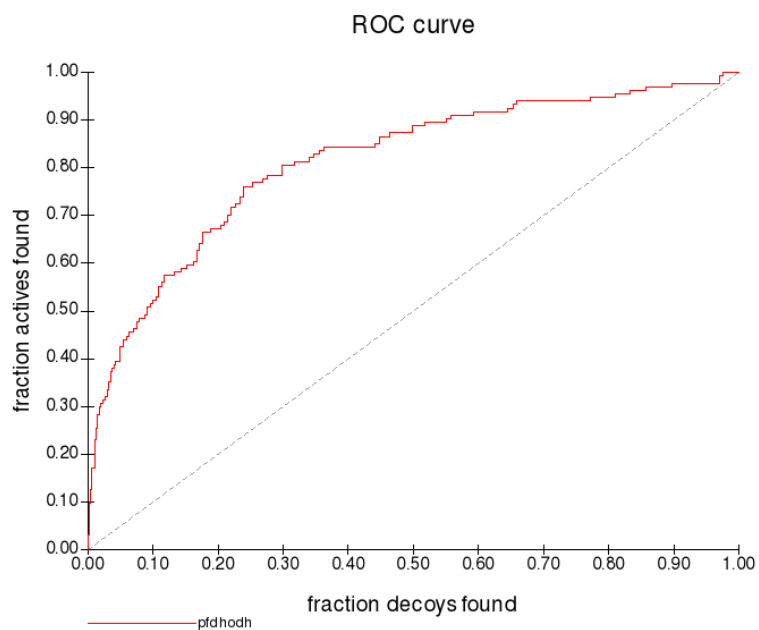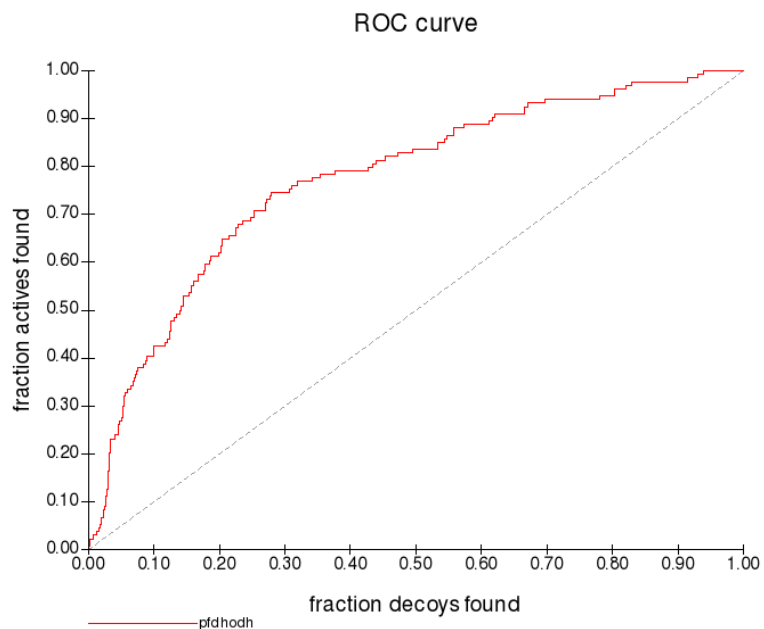
Figure 4.10*: ROC curve for color_tanimoto metric

The data for the ROC curves is summarized in Table 4.4 and Table 4.5 for shape and *color_tanimoto* metrics, respectively.

Table 4.4: AUC values of *Pf*DHODH query model run against a set of actives and decoys using shape metrics

Run Name	*Pf*DHODH shape	Lingos	p-Value
AUC	0.813328	0.764721	0.044
95% confidence min	0.771606	0.726836	
95% confidence max	0.854084	0.802999	
0.5% Enrichment	25.78617	6.005031	0.005
95% confidence min	13.33333	1.398601	
95% confidence max	40.94488	12.69841	
1.0% Enrichment	18.35000	6.533622	0.004
95% confidence min	11.64384	2.542373	
95% confidence max	26.81159	11.27820	
2.0% Enrichment	14.86040	5.638064	0
95% confidence min	11.02941	2.517986	
95% confidence max	19.06780	9.060403	

Table 4.5: AUC values of *Pf*DHODH query model run against a set of actives and decoys using Color_Tanimoto metrics

Run Name	*Pf*DHODH -*tanimoto*	Lingos	p-Value
AUC	0.774441	0.764721	0.370
95% confidence min	0.731000	0.726836	
95% confidence max	0.813954	0.802999	
0.5% Enrichment	4.530242	6.005031	0.644
95% confidence min	0	1.398601	
95% confidence max	10.43478	12.69841	
1.0% Enrichment	3.012252	6.533622	0.909
95% confidence min	0.714286	2.542373	
95% confidence max	6.164384	11.2782	
2.0% Enrichment	3.064989	5.638064	0.892
95% confidence min	1.102941	2.517986	
95% confidence max	5.442177	9.060403	

It is apparent from the tables that the query is more selective when shape metrics is used as opposed to *tanimoto* with an AUC (Area under the curve) value of 0.8133 and a p-value of 0.044 when compared with 2D similarity metrics (Lingos). This suggests that shape is more selective than *tanimoto* in identifying *Pf*DHODH actives from their respective decoys.

Statistically, the Gaussian underpinnings of AUC varies from 0.5 (no apparent accuracy) to 1.0 (perfect accuracy) as the ROC curve moves towards the left and top boundaries of the ROC graph (Hanley and McNeil, 1982). Using this index, the query has an AUC value 0.8133 close to 1.0 which validate it as discriminatory in the identification of actives from decoys in a given dataset. It therefore drives to the conclusion that when supplied with a dataset of actives and decoys, there is a high probability that the query can correctly identify true "actives" from "inactives".

In addition to the AUC values, enrichment which measures the ability of a tool to place a

large proportion of the active compounds at the top of the ranked list is given. The p-values for the shape metric comparisons are less than 0.05, suggesting that the 3D query is more superior to the 2D similarity one. Scientifically, *p*-values exceeding 0.05 (1 in 20) are not enough to be the sole evidence that two dataset being studied really differ (Stamatis, 2012). Ironically, the *p*-values of the results when *tanimoto* metric is used do not show any statistical evidence that the 3D and 2D comparisons are different. This gives confidence to the use of the shape metric as a method for the 3D comparison with the database molecules using the model query.

4.7.2 Shape Similarity Studies

The model query was used to carry out shape similarity studies against the 108 molecules selected from structure based VS. The results of the top 10 ranking molecules are summarized in Table 4.6.

Table 4.6: Table of top 10 ranking molecules compared to model ligand query

#	Smiles	Shape Tanimoto	Color Tanimoto	Tanimoto Combo	z-score
1	CC1C(=Nc2ccc(cc2O1)OC)CC3CCC(=C4C3C=CCC4)C	0.523	0.266	0.789	2
2	CC1C(=Nc2ccc(cc2O1)OC)CC3CCC(=C4C3C=CCC4)C	0.523	0.266	0.789	2
3	CC1=C(N(c2ccc(cc2O1)OC)C3CCC(CO3)OC)O	0.561	0.191	0.752	2
4	CC1=C(N(c2ccc(cc2O1)OC)C3CCC(CO3)OC)O	0.561	0.191	0.752	2
5	CC1C(=Nc2ccc(cc2O1)OC)Oc3cccc(c3)OC(=O)C	0.462	0.285	0.746	2
6	CC1C(=Nc2ccc(cc2O1)OC)Oc3cccc(c3)OC(=O)C	0.462	0.285	0.746	2
7	CC1C(=Nc2ccc(cc2O1)OC)Oc3cccc(c3)OC(=O)C	0.462	0.285	0.746	2

8	CC1C(=Nc2ccc(cc2O1)OC)Oc3cccc(c3)OC(=O)C	0.462	0.285	0.746	2
9	CC1C(=Nc2ccc(cc2O1)OC)Oc3cccc(c3)C[NH3+]	0.468	0.259	0.727	1
10	CC1C(=Nc2ccc(cc2O1)OC)Oc3cccc(c3)C[NH3+]	0.468	0.259	0.727	1

The results from **rocs** show very low color *tanimoto* (chemical complementary) scores of benzoxazine analogs to the model query. The shape similarity of the top ranking molecule is 0.523 which is average. The values decrease linearly down the table suggesting that there is a big variance in terms of shape between the query and the database molecules. Conversion of the molecules scores to their respective z-scores further confirms the low relationship. On average, the top molecule has a cumulative (color and shape) value of 0.789 with a bias on shape similarity only.

Eight out of the top 10 molecules had z-score of 2 with all molecules having higher shape similarity than color similarity. The dissimilarity in color is expected as it is brought about by the difference in frameworks and side chains of the benzoxazine molecules. Shape similarity is averagely satisfying because all of the top 10 molecules have values more than 0.5. Indeed it can be concluded that this query identified benzoxazines that are potential inhibitors from the **rocs** run based on the shape complementarity. A parallel **rocs** run using the *Pf*DHODH inhibitor (**6**) as a query gave the results shown in Table 4.7.

Table 4.7: Table of top 10 ranking molecules using A77 1726 query

#	Compound	Sh_*tani*	Col_ *Tani*	*Tani* combo	zscore
1	CC(O)C(C#N)C(=O)Nc1ccc(cc1)C(F)(F)F	1	1	2	6

2	CC(O)C(C#N)C(=Nc1ccc(cc1)C(F)(F)F)O	0.727	0.382	1.108	1.4
3	COc1ccc2N=C(Oc3ccccc3O)C(C)Oc2c1	0.672	0.298	0.97	0.8
4	COc1ccc2N=C(C(C)Oc2c1)C3C(O)C(C)OC(C)C3O	0.639	0.29	0.929	0.6
5	COc1ccc2N=C(C(C)Oc2c1)C34CCCC3C4	0.786	0.086	0.872	0.3
6	CN(CC(=O)N1C(=C(C)Oc2cc(OC)ccc12)O)C=O	0.618	0.253	0.87	0.3
7	CN(CC(=O)N1C(=C(C)Oc2cc(OC)ccc12)O)C=O	0.617	0.253	0.87	0.3
8	COc1ccc2N=C(C(C)Oc2c1)C34CCCC3C4	0.783	0.086	0.868	0.3
9	COc1ccc2N(C(=O)CC#N)C(=C(C)Oc2c1)O	0.596	0.264	0.861	0.3
10	COc1ccc2N=C(C(C)Oc2c1)C3(C)CC3C(=O)C	0.68	0.178	0.858	0.3

It also gave consistent results in that all of the database molecules showed a bias of shape similarity as opposed to color similarity. In the run however, the shape similarity values were higher than the representative model with the top molecule having a *Tanimoto* Combo value of 1.108.

The top ranking molecule is the *Pf*DHODH inhibitor (**6**), which produces a perfect match with itself. The results decrease linearly, but with improvements, in comparison with the model query used in Table 4.6. In terms of shape, the second entry in Table 4.7 almost matches *Pf*DHODH inhibitor (**6**). Color scores are relatively low and are in harmony from both tables suggesting that the chemical complementarity of benzoxazines is very different with most known inhibitors of *Pf*DHODH.

4.7.3   Electrostatics Similarity Studies

The *Pf*DHODH inhibitor (**6**) was used to carry out electrostatics similarity studies against

the 108 molecules selected from structure based VS. The molecule database was obtained

by preparing a pre aligned *rocs* output as an input for the *eon* program. The results from

the *eon* run are shown in Table 4.8.

Table 4.8: Electrostatics comparison between benzoxazine database and A177 1726

#	Smiles	ET_ pb	*EON* shape	ET_ combo	Z- score
1	CC(C(C#N)C(=O)Nc1ccc(cc1)C(F)(F)F)O	1	1	2	5
2	CC1=C(N(c2ccc(cc2O1)OC)C(=O)Nc3ccon3)O	0.606	0.59	1.196	2
3	CC1=C(N(c2ccc(cc2O1)OC)C(=O)Nc3ccon3)O	0.605	0.589	1.195	2
4	CC1=C(N(c2ccc(cc2O1)OC)C(=O)N(C)CC#N)O	0.546	0.608	1.154	2
5	CC1=C(N(c2ccc(cc2O1)OC)C(=O)N(C)CC#N)O	0.534	0.615	1.149	2
6	CCN(CC(=O)N1c2ccc(cc2OC(=C1O)C)OC)C=O	0.486	0.627	1.113	1
7	CCN(CC(=O)N1c2ccc(cc2OC(=C1O)C)OC)C=O	0.488	0.625	1.113	1
8	Cc1cc(c(cc1O)OC)C(=O)C2=Nc3ccc(cc3OC2C)OC	0.487	0.619	1.106	1
9	CC1=C(N(c2ccc(cc2O1)OC)C(=O)CC#N)O	0.484	0.620	1.104	1
10	CC1=C(N(c2ccc(cc2O1)OC)C(=O)CC#N)O	0.483	0.620	1.103	1

As was done with other ranking VS tools, the scores were normalized to their respective z-

scores. The top molecule *Pf*DHODH inhibitor (**6**), query shows scores of a perfectly

matched molecule. Since it is compared to its structure, it gives 100% expected results.

Entries two to five in Table 4.8 show relatively high electrostatic similarity with the query.

In general, the coulombic electrostatics (ET_coul) compare better than the Poisson

Boltzmann electrostatics (ET_pb). Most of the molecules show more than 50% similarity
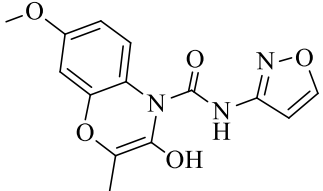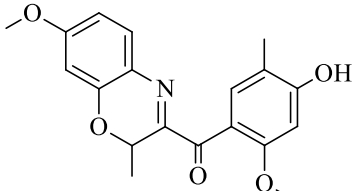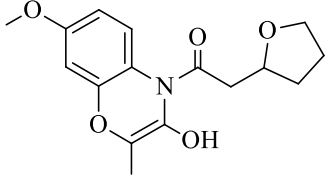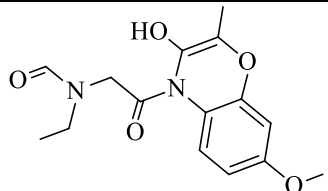
as compared to the PB metric.

Conventionally ET_pb uses an outer dielectric of 80, while ET_coul uses a value of 2.0

which makes ET_pb preferred to ET-coul. The hit list ranking from the dataset shows more

consistency in the ET_pb scores because the ranking is linear. Consequently,

characteristics of the dataset were defined based on the ET_pb scores. Four of the top 10
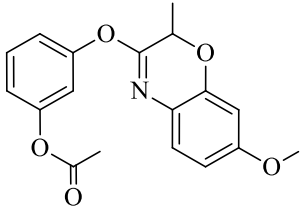
ranking molecules have more than 50% similarity to the query. As binding is dictated by electrostatics coupled with correct shape and pose, it is likely that these molecules would mimic the binding channel of the known inhibitor. However, it requires synthesis to verify biding potential of the top molecules.

4.8   Synthetic Targets

Data from *rocs* and *eon* comparisons for the 108 benzoxazine analogs were combined and ranked based on their cumulative scores. The scores of the top 5 molecules are shown in Table 4.9.

Table 4.9: Table of cumulative scores from *rocs* and *eon*
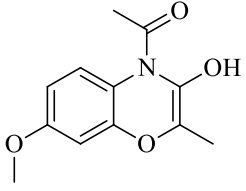
No	Structure	ET_Combo	*Tanimoto Combo*	Cum_score	z-score
1		1.196	0.691	1.887	2
2		1.106	0.706	1.812	2
3		1.068	0.72	1.788	2
4		1.113	0.648	1.761	1
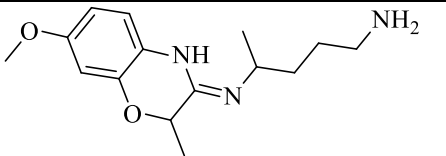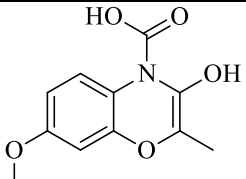
No	Structure	ET_Combo	*Tanimoto* Combo	Cum_score	z-score
5		1.006	0.747	1.753	1

Shape and electrostatics coupled with molecular pose play the most important role during the interaction of a ligand with the protein of interest. The molecules above meet the threshold of the three factors. The methods used above give convincing data that the molecules in Table 4.6 can inhibit the *Pf*DHODH enzyme and therefore qualify for synthesis and biological assays.

The structures presented in Table 4.6 would need rigorous planning and therefore not achievable during the time frame of this study. Simpler analogs were therefore targeted for synthesis in order to achieve the projects goals. These molecules were among the dataset used for both shape and electrostatics studies and also showed reasonable probability of being active as shown in Table 4.10.

Table 4.10*: Molecules targeted for synthesis

Entry	Structure	ET_Combo	*Tanimoto* Combo	Cum_score
1		0.955	0.593	1.548

| 2 | | 0.76 | 0.61 | 1.37 |
| 3 | | 0.733 | 0.563 | 1.296 |

4.9 Physicochemical Properties of the Molecules Targeted for Synthesis

There are several studies that have investigated the 'drug-likeness' of different compounds based on their physicochemical properties. For example, Lipinski's rule of five (Lipinski, 2004) defines four simple parameters for prediction that a compound would be orally active. i.e. ($MWT \leq 500$, $\log P \leq 5$, H-bond donors ≤ 5, H-bond acceptors ≤ 10). In addition, Veber *et al.* (2002) rules suggest 10 or fewer rotatable bonds and polar surface area equal to or less than 140 Å for a compound to be orally bioactive fit the chemical nature of these compounds. The compounds targeted for synthesis had physicochemical characteristics (Table 4.11) consistent with 'drug-like' requirements suggested by Lipinski and Veber.

Table 4.11*: Physicochemical properties of benzoxazines targeted for synthesis*

Entry	MW	Mmff Energy	LogP	PSA	Rotatable bonds	Lipinski Acceptors	Lipinski Donors
1	235	75.68	1.39	58	2	5	1
2	277	70.71	1.69	68	5	5	2
3	237	70.70	0.84	79	2	6	2

4.10 Synthesis of Benzoxazines

There are several strategies for the synthesis of 2H-1,4-benzoxazines (Ilaš *et al*., 2005). Most of the strategies in the synthesis involve alkylating an appropriate 2-aminophenol with acyl halides, commonly in the presence of a base and a reducing agent. In our synthesis, a similar approach was used as highlighted in the retrosynthetic Scheme 4.1.
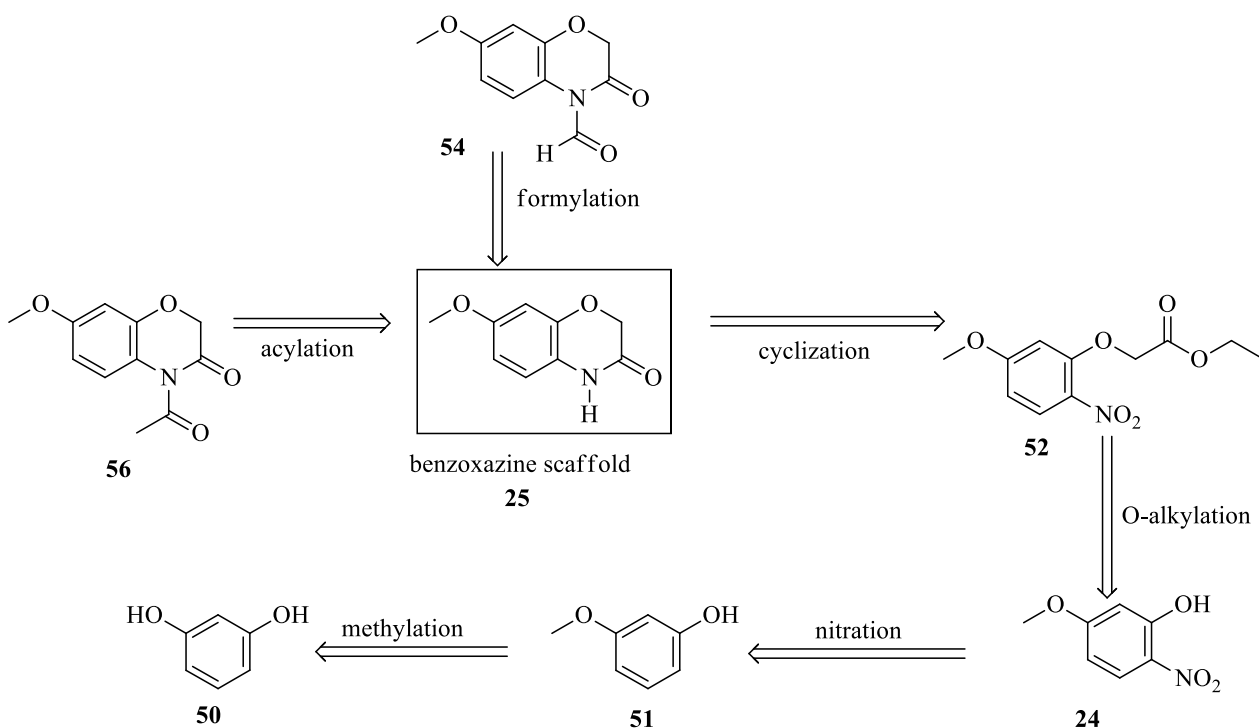

Scheme 4.1: Retrosynthetic scheme for synthesis of the target molecule

The strategy for the synthesis of the target benzoxazines began by mono methylating resorcinol followed by mono nitration. The nitrophenol was then *O*-alkylated and cyclized to access the benzoxazine scaffold. The scaffold was then acylated to the target benzoxazines of this study.

4.10.1 Synthesis of 3-Methoxyphenol (51)

3-Methoxyphenol was obtained by methylating resorcinol (**50**) with iodomethane as the alkylating agent owing to the good leaving nature of the bulky iodine in the presence of potassium carbonate as a base. Low equivalent (1.5 eq.) of the alkylating agent is used to prevent dimethylation.
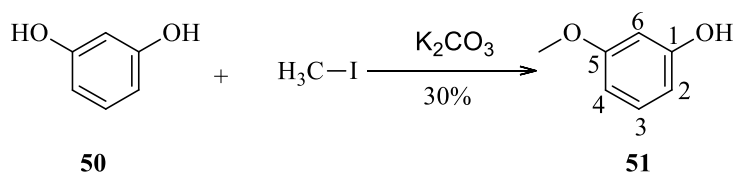

The low yield (30%) of the reaction can be attributed to the unreacted resorcinol which cannot be avoided because addition of extra alkylating agent would result in dimethylation (Plettner & Isman, 2013). The product is a yellow liquid with a characteristic ^{1}H and ^{13}C NMR peaks at the chemical shift δ 3.81 (*s*, 3H) and δ 55.2, respectively, confirming the presence of a methoxy in the compound. The expected four aromatic proton peaks are also present δ 7.17 (*t*, *J* = 8.1 Hz, 1H, H-3), 6.53 (*ddd*, *J* = 8.2, 2.4, 0.9 Hz, 1H, H-4), 6.46 (*ddd*, *J* = 8.1, 2.4, 0.9 Hz, 1H, H-2), 6.44 (*t*, *J* = 2.4 Hz, 1H, H-6).

4.10.2 Synthesis of 5-Methoxy-2-nitrophenol (24)

The 3-methoxyphenol (**51**) was mono nitrated through a two-step process using sodium nitrite in the presence of sulphuric acid and then nitric acid. The presence of methoxy and hydroxyl group, both electron donating groups would direct the nitroso group to either position 2 or 4 considering that both the hydroxyl and methoxy groups are ortho, para directors. However, the hydroxyl group is a stronger directing group than the methoxy, and can direct the NO group to either position 2 or 4, but based on steric considerations the NO

group is directed to position 2. Nitric acid is used to oxidize the NO into a nitro group.
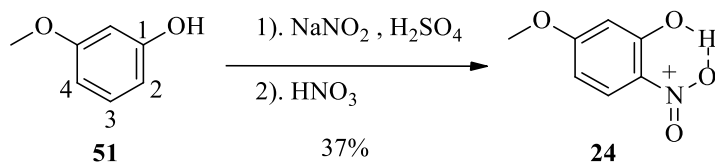
Analysis of the compound using NMR technique revealed three aromatic protons at a chemical shift of δ 6.59 (*m*, 2H), 8.07 (*d*, *J* = 9.1 Hz, 1H) as opposed to four in the starting material. Furthermore there is a unique peak at δ 11.04 (*s*, 1H) which is usually associated with a hydroxyl hydrogen involved in chelation. This is an indication that indeed there is a nitro group *ortho* to a hydroxyl group which contributes to hydrogen bonding seen in the structure as confirmed by NMR peaks. The ^{13}C NMR also show peaks at δ 167.2 and 157.9 which are shifts for the carbons attached to the methoxy and hydroxyl groups, respectively.

## 4.10.3 Synthesis of Ethyl-2-bromoacetate (38)

Ethyl-2-bromoacetate (**38**) for *O*-alkylation of 5-methoxy-2-nitrophenol (**24**) was synthesized by esterification of bromoacetic acid (**52**) with ethanol in the presence of concentrated sulphuric acid as a catalyst.
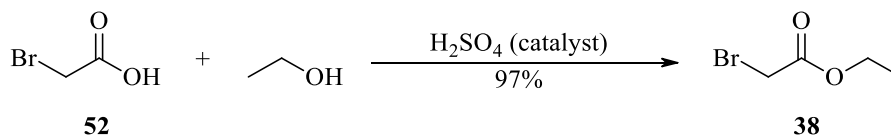
The reaction procedure was adopted from Han *et al*. (2008). A yellow liquid ester was obtained in 97% yield. The product was difficult to handle and caution had to be taken to avoid eye and throat irritation.

### 4.10.4 Synthesis of Ethyl 2-(5-methoxy-2-nitrophenoxy)acetate (52)

A similar procedure for *O*-alkylation used in Section 4.10.1 was employed in the synthesis of ethyl 2-(5-methox-2-nitrophenoxy)acetate.
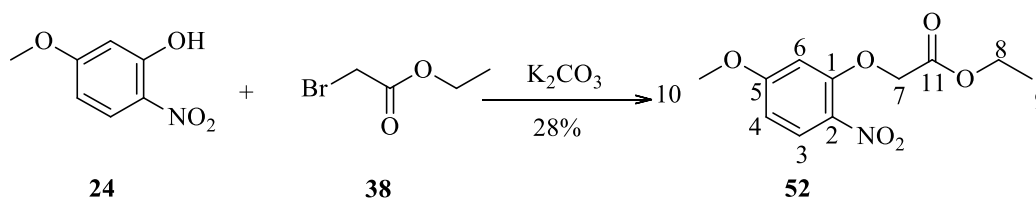
Yellow needle-like crystals of the product were obtained in 28% yield. The ^{1}H and ^{13}C NMR were similar except for the additional ethyl acetoxy peaks. The ^{1}H NMR shows two sets of oxymethylene peaks resonating at δ 4.17 (*q*, *J* = 7.14 Hz, 2H), 4.67 (*s*, 2H) and a methyl peak δ 1.20 (*t*, *J* = 7.16 Hz, 3H). The corresponding carbons of the ethyl acetoxy resonated at δ 164.5(ester carbonyl, C-11), 66.3(C-8), 61.6(C-7), 13.8(C-9).

4.10.5 Synthesis of 7-Methoxy-4H-1, 4-benzoxazin-3-one (25)

7-Methoxy-4H-1, 4-benzoxazin-3-one (**25**) was synthesized by reducing ethyl 2-(5-methoxy-2-nitrophenoxy)acetate (**52**) using sodium borohydride in the presence of palladium on charcoal as a catalyst.
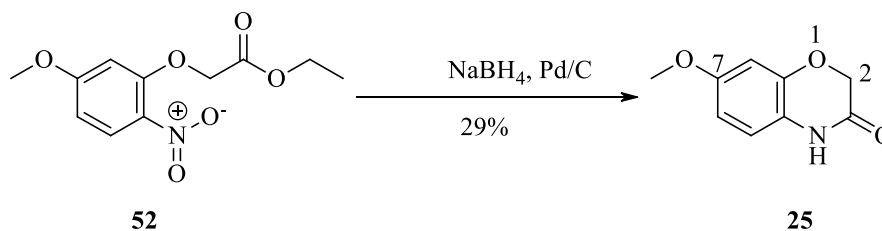

The reaction involved *in situ* reduction of the nitro group to an amine followed by intramolecular lactamization. A mixture of water and 1,4-dioxane is used as a solvent in

the reaction since sodium borohydride is almost insoluble in dioxane but very soluble in water. The reaction time for this method is significantly reduced as compared to other ring cyclizations as it took only 15-30 minutes for a product to be formed.

The ^{1}H and ^{13}C NMR peaks show transformation of the starting material. The number of ^{13}C peaks is reduced from eleven to nine suggesting that a group containing two carbons (possibly an alkoxy) has been eliminated from the starting material. As in the starting material, the product has a characteristic methoxy at δ_H 3.79 (*s*, 3H), three aromatic protons 6.59 (*d*, *J* = 2.64 Hz, 1H), 6.67 (*dd*, *J* = 8.78, 2.66 Hz, 1H), 7.25 (*d*, *J* = 8.80 Hz, 1H), but there was only one set of methylene proton at δ_H 4.71 (*s*, 2H) which is assigned to C-2.

4.10.6 Synthesis of 7-Methoxy-3-oxo-1,4-benzoxazine-4-carbaldehyde (54)

7-Methoxy-3-oxo-1,4-benzoxazine-4-carbaldehyde (**54**) was synthesized through formylation of 7-methoxy-4H-1, 4-benzoxazin-3-one (**54**) using formic acid.
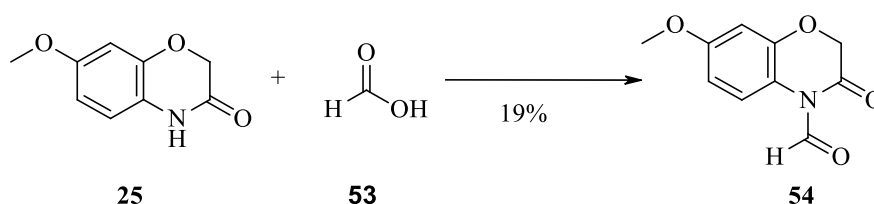
The product is a dark-brown solid whose ^{1}H NMR matches the proposed structure of the product. There is an additional hydrogen with a chemical shift of δ 8.74 (s, 1H) which is characteristic of an aldehyde proton. All the other protons in the starting material can be seen as before i.e. the three aromatic protons 6.78 (d, *J* = 8.6 Hz, 1H), 6.60 (d, *J* = 2.6 Hz, 1H), 6.56 (dd, *J* = 8.6, 2.7 Hz, 1H), a methoxy peak at 3.78 (s, 3H) and a methylene peak at 4.61 (s, 2H). The ^{13}C NMR also confirms the addition of an extra carbon at peak δ

219.54. The other peaks remain the same indicating an addition of only one carbon thereby confirming that indeed a formylation reaction has taken place.

The lone pair of electrons on the nitrogen attacks the acid at the polarized carbon. Consequently, the lone pair of electron electrons from the hydroxyl group picks the hydrogen attached on the nitrogen group. Water is then lost on formation of the carbonyl group. The proposed reaction mechanism for the product above is as shown in Scheme 4.2.
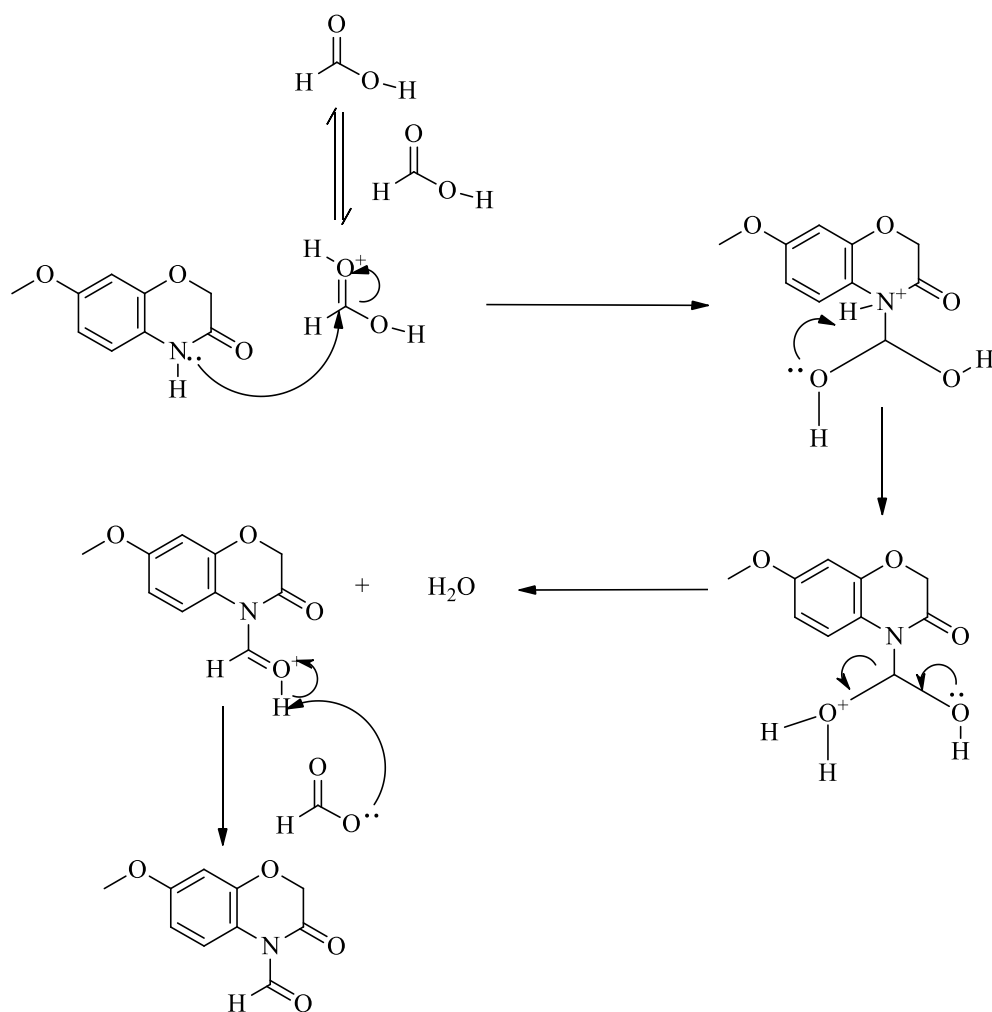
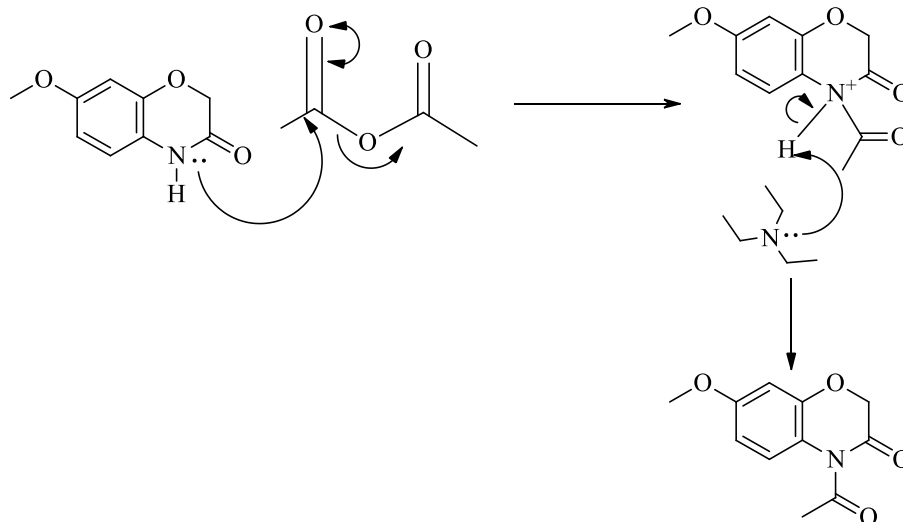**Scheme 4.2**: Proposed reaction mechanism for formylation of 7-methoxy-4H-1, 4-benzoxazin-3-one (**27**)

4.10.7 Synthesis of 4-Acetyl-7-methoxy-1,4-benzoxazin-3-one (56)

4-Acetyl-7-methoxy-1,4-benzoxazin-3-one (**56**) was synthesized via *N*-acetylation of 7-methoxy-4H-1, 4-benzoxazin-3-one (**25**) using acetic anhydride in the presence of triethylamine.
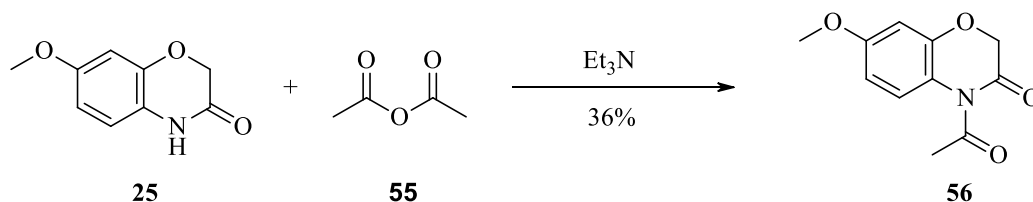
The product was isolated as yellow crystals in 36% yield. The reaction occurs at elevated temperatures and took a longer period to achieve the desired products as was observed by Bravo & Weiss-Lopez (1999). The NMR of the product indicates notable changes in the starting material. The product had an additional one peak in the ^{1}H NMR at δ 2.68 (*s*, 3H) attributed to the methyl group of the acetate. The corresponding carbons of the acetate resonated at δ 28.2 (CO$\underline{C}$H$_3$) and 170.8 (CO). All the other peaks of the starting material were the similar indicating that the acylation took place at the *N* position.

From a mechanistic point of view, the reaction proceeds by nucleophilic attack of the nitrogen of the benzoxazine on the electrophilic carbon of the acetic anhydride followed by the displacement of the ethanoate as illustrated in Scheme 4.3. Triethylamine acts as a base to pick the activated proton on the amide.

Scheme 4.3: Proposed reaction mechanism for synthesis of 4-acetyl-7-methoxy-1,4-benzoxazin-3-one

4.11 *In vitro* Antiplasmodial Activity

The virtual screening of benzoxazines against *Pf*DHODH identified potential inhibitors. These molecules were synthesized and there antiplasmodial activity were determined against chloroquine resistant K1 isolate and chloroquine sensitive 3D7. The results are as shown in Table 4.12.

Table 4.12: In vitro values of compounds synthesized from benzoxazine scaffold

Sample	IC$_{50}$ in µg/mL CQ K1	IC$_{50}$ in µg/mL CQ 3D7
7-Methoxy-4H-1, 4-benzoxazin-3-one (27)	4.00 ± 1.61	7.53 ± 1.91
7-Methoxy-3-oxo-1,4-benzoxazine-4-carbaldehyde (28)	11.03 ± 1.95	12.10 ± 0.17
4-Acetyl-7-methoxy-1,4-benzoxazin-3-one (29)	8.32	4.73 ± 0.64
Chloroquine*	0.46 ± 0.04	0.0063 ± 0.0022
Mefloquine*	1.15 ± 1.97	0.00084 ± 0.0004

* Standard reference drugs

Among the compounds assayed, compound **27** was found to be the most active against K1 isolate while compound **29** was the most active against **3D7** strain. Structure **27** and **29** falls within the WHO recommended scale of compounds which are active (i.e. compounds

with an activity of less than 10 µg/mL), while compound **28** is within the scale of moderately active (compounds with IC$_{50}$ between 10 and 50 µg/mL). The data from the assay is in line with the modeled data. However the structure needs to be optimized to achieve a desired activity comparable to existing drugs. Compound **29** was the most promising in terms of its *in silico* ability to bind to the *Pf*DHODH enzyme compared to compound **27** and **28**. This is in agreement with assay data; a proof that the methodology was a success. Compound **27** is the scaffold that was used to prepare both compound **28** and **29**. It is surprising that it has a higher activity towards **K1** strain as it showed a weaker *in silico* binding affinity towards the enzyme.

Generally, the results prove the success of the methodology in terms of identifying molecules that can be used in development of novel antimalarial compounds. It is a methodology that needs to be refined in order to improve its robustness.

CHAPTER FIVE

CONCLUSIONS AND RECOMMENDATIONS

The objectives of this study was to generate a database of natural products of Kenya for the design of antiplasmodial lead compounds guided by the following specific objectives: develop a web based database, model antiplasmodial benzoxazines using *in silico* techniques and synthesize and carry out *in vitro* evaluation of the promising analogs.

5.1   CONCLUSIONS

In this study:

I.   A searchable web-based *in silico* database of natural products of Kenya was created and is hosted online at http://mitishamba.uonbi.ac.ke domain.

II.   Structure based virtual screening identified 108 benzoxazine analogs as promising inhibitors of the *Pf*DHODH enzyme. Further ligand based 3D shape and electrostatic studies were carried out to yield three benzoxazine derivatives targeted for synthesis.

III.   Three benzoxazines (7-methoxy-4H-1, 4-benzoxazin-3-one (**27**), 7-methoxy-3-oxo-1,4-benzoxazine-4-carbaldehyde (**28**) and 4-acetyl-7-methoxy-1,4-benzoxazin-3-one (**29**)) were synthesized and evaluated in an *in vitro* antiplasmodial assay. The activity of the compounds range from 4 to 12 μg/mL.

5.2 RECOMMENDATIONS

The database of natural products of Kenya developed in this study is an essential tool that can spur research on the potential of natural products of Kenya in drug discovery. I therefore recommend that:

I. The database should be continually updated to increase the number of new structures which are constantly isolated. Older structures that were not previously captured in the database should also be updated.

II. More scaffolds should be identified from the database to explore the diverse skeletons existing among the natural products of Kenya and potential applications in drug design and discovery.

III. Further computational studies (possibly quantum calculations) need to be done on benzoxazine analogs in order to investigate their inhibition of *Pf*DHODH when electronic factors are considered.

IV. The benzoxazine scaffold needs to be modeled against other enzymes to investigate its therapeutic potential towards other diseases.

REFERENCES

Abdi, Y. A. (2003). *Handbook of drugs for tropical parasitic infections*. London; Bristol, PA: Taylor & Francis. Retrieved from http://site.ebrary.com/id/10070472

Achan, J., Talisuna, A. O., Erhart, A., Yeka, A., Tibenderana, J. K., Baliraine, F. N., D'Alessandro, U. (2011). Quinine, an old anti-malarial drug in a modern world: role in the treatment of malaria. *Malar J*, *10*(144), 1475–2875.

Allen, F. H. (2002). The Cambridge Structural Database: a quarter of a million crystal structures and rising. *Acta Crystallographica Section B: Structural Science*, *58*(3), 380–388.

Amzel, L. M. (1998). Structure-based drug design. *Current Opinion in Biotechnology*, *9*(4), 366–369. http://doi.org/10.1016/S0958-1669(98)80009-8

Andayi, A. W., Yenesew, A., Derese, S., Midiwo, J. O., Gitu, P. M., Jondiko, O. J., Peter, M. G. (2006). Antiplasmodial Flavonoids from *Erythrina sacleuxii*. *Planta Medica*, *72*(2), 187–189. http://doi.org/10.1055/s-2005-873200

Anderluh, M., Cesar, J., Štefanič, P., Kikelj, D., Janeš, D., Murn, J., Dolenc, M. S. (2005). Design and synthesis of novel platelet fibrinogen receptor antagonists with 2H-1,4-benzoxazine-3(4H)-one scaffold. A systematic study. *European Journal of Medicinal Chemistry*, *40*(1), 25–49. http://doi.org/10.1016/j.ejmech.2004.09.004

Anderson, A. C. (2003). The process of structure-based drug design. *Chemistry & Biology*, *10*(9), 787–797.

Azam, S. S., & Abbasi, S. W. (2013). Molecular docking studies for the identification of novel melatoninergic inhibitors for acetylserotonin-O-methyltransferase using different docking routines. *Theoretical Biology & Medical Modelling*, *10*, 63.

http://doi.org/10.1186/1742-4682-10-63

Balint, G. A. (2001). Artemisinin and its derivatives: an important new class of antimalarial agents. *Pharmacology & Therapeutics*, *90*(2), 261–265.

Bemis, G. W., & Murcko, M. A. (1999). Properties of Known Drugs. 2. Side Chains. *Journal of Medicinal Chemistry*, *42*(25), 5095–5099. http://doi.org/10.1021/jm9903996

Berman, H. M., Kleywegt, G. J., Nakamura, H., & Markley, J. L. (2013). How Community Has Shaped the Protein Data Bank. *Structure*, *21*(9), 1485–1491. http://doi.org/10.1016/j.str.2013.07.010

Bienfait, B., & Ertl, P. (2013). JSME: a free molecule editor in JavaScript. *Journal of Cheminformatics*, *5*(1), 24. http://doi.org/10.1186/1758-2946-5-24

Bird, T. G. C. (2004, June 24). Benzoxazinone derivatives for use in the treatment of angiogenesis. Retrieved from http://worldwide.espacenet.com/publicationDetails/biblio?FT=D&date=20040624 &DB=worldwide.espacenet.com&locale=en_EP&CC=US&NR=2004122006A1 &KC=A1&ND=4

Bloland, P. B., & Organization, W. H. (2001). *Drug resistance in malaria*. World Health Organization Geneva. Retrieved from http://www.who.int/entity/csr/resources/publications/drugresist/malaria.pdf

Booker, M. L., Bastos, C. M., Kramer, M. L., Barker, R. H., Skerlj, R., Sidhu, A. B., … Sybertz, E. (2010). Novel Inhibitors of Plasmodium falciparum Dihydroorotate Dehydrogenase with Anti-malarial Activity in the Mouse Model. *Journal of Biological Chemistry*, *285*(43), 33054–33064.

http://doi.org/10.1074/jbc.M110.162081

Bravo, H. R., & Weiss-Lopez, B. E. (1999). N-ACYLATION OF LACTAMS DERIVED FROM NATURAL 2- BENZOXAZOLINONES AND 1,4-BENZOXAZIN-3-ONES. *Boletín de La Sociedad Chilena de Química*, *44*(4), 443–450. http://doi.org/10.4067/S0366-16441999000400007

Breman, J. G., Alilio, M. S., White, N. J., Nosten, F., & White, N. J. (2007). Artemisinin-based combination treatment of falciparum malaria. Retrieved from http://www.ncbi.nlm.nih.gov/books/NBK1713/

Caliendo, G., Perissutti, E., Santagada, V., Fiorino, F., Severino, B., Cirillo, D., Sorrentino, R. (2004). Synthesis by microwave irradiation of a substituted benzoxazine parallel library with preferential relaxant activity for guinea pig trachealis. *European Journal of Medicinal Chemistry*, *39*(10), 815–826. http://doi.org/10.1016/j.ejmech.2004.05.003

Cereto-Massagué, A., Ojeda, M. J., Valls, C., Mulero, M., Garcia-Vallvé, S., & Pujadas, G. (2015). Molecular fingerprint similarity search in virtual screening. *Methods*, *71*, 58–63. http://doi.org/10.1016/j.ymeth.2014.08.005

Cheeseman, I. H., Miller, B. A., Nair, S., Nkhoma, S., Tan, A., Tan, J. C., Anderson, T. J. C. (2012). A Major Genome Region Underlying Artemisinin Resistance in Malaria. *Science*, *336*(6077), 79–82. http://doi.org/10.1126/science.1215966

Chen, C. Y.-C. (2011). TCM Database@Taiwan: The World's Largest Traditional Chinese Medicine Database for Drug Screening In Silico. *PLoS ONE*, *6*(1), e15939. http://doi.org/10.1371/journal.pone.0015939

Cohen, N. C., Blaney, J. M., Humblet, C., Gund, P., & Barry, D. C. (1990). Molecular

modeling software and methods for medicinal chemistry. *Journal of Medicinal Chemistry*, *33*(3), 883–894. http://doi.org/10.1021/jm00165a001

Cragg, G. M., & Newman, D. J. (2013). Natural products: A continuing source of novel drug leads. *Biochimica et Biophysica Acta (BBA) - General Subjects*, *1830*(6), 3670–3695. http://doi.org/10.1016/j.bbagen.2013.02.008

Cramer, C. J. (2004). *Essentials of computational chemistry: theories and models*. Chichester, West Sussex, England; Hoboken, NJ: Wiley.

Cui, L., & Su, X. (2009). Discovery, mechanisms of action and combination therapy of artemisinin. *Expert Review of Anti-Infective Therapy*, *7*(8), 999–1013. http://doi.org/10.1586/eri.09.68

Dean, P. M. (2012). *Molecular Similarity in Drug Design*. Springer Science & Business Media.

Duffy, B. C., Zhu, L., Decornez, H., & Kitchen, D. B. (2012). Early phase drug discovery: Cheminformatics and computational techniques in identifying lead series. *Bioorganic & Medicinal Chemistry*, *20*(18), 5324–5342. http://doi.org/10.1016/j.bmc.2012.04.062

Ebalunode, J. O., Ouyang, Z., Liang, J., & Zheng, W. (2008). Novel Approach to Structure-Based Pharmacophore Search Using Computational Geometry and Shape Matching Techniques. *Journal of Chemical Information and Modeling*, *48*(4), 889–901. http://doi.org/10.1021/ci700368p

Egan, W. J., Merz, K. M., & Baldwin, J. J. (2000). Prediction of Drug Absorption Using Multivariate Statistics. *Journal of Medicinal Chemistry*, *43*(21), 3867–3877. http://doi.org/10.1021/jm000292e

Fernando, D., Rodrigo, C., & Rajapakse, S. (2011). Primaquine in vivax malaria: an update and review on management issues. *Malaria Journal*, *10*(1), 351. http://doi.org/10.1186/1475-2875-10-351

Fidock, D. A., Rosenthal, P. J., Croft, S. L., Brun, R., & Nwaka, S. (2004). Antimalarial drug discovery: efficacy models for compound screening. *Nature Reviews Drug Discovery*, *3*(6), 509–520. http://doi.org/10.1038/nrd1416

Fleury, M., Largeron, M., Lestage, P., & Lockhart, B. (1999, December 9). Novel 8-Amino-1,4-Benzoxazine Compounds, Preparation Method and Pharmaceutical Compositions Containing Them. Retrieved from http://worldwide.espacenet.com/publicationDetails/biblio?FT=D&date=19991209&DB=worldwide.espacenet.com&locale=en_EP&CC=WO&NR=9962889A1&KC=A1&ND=4

Frechette, R., & Beach, M. (1997, August 7). 2-Substituted Amino and Thio Alkyl Benzoxazine Antimicrobial Agents. Retrieved from http://worldwide.espacenet.com/publicationDetails/biblio?FT=D&date=19970807&DB=worldwide.espacenet.com&locale=en_EP&CC=WO&NR=9728167A1&KC=A1&ND=4

Frosch, A. E., Venkatesan, M., & Laufer, M. K. (2011). Patterns of chloroquine use and resistance in sub-Saharan Africa: a systematic review of household survey and molecular data. *Malar J*, *10*(1), 116.

Ghose, A. K., Herbertz, T., Salvino, J. M., & Mallamo, J. P. (2006). Knowledge-based chemoinformatic approaches to drug discovery. *Drug Discovery Today*, *11*(23–24), 1107–1114. http://doi.org/10.1016/j.drudis.2006.10.012

Haider, N. (2010). Functionality Pattern Matching as an Efficient Complementary Structure/Reaction Search Tool: an Open-Source Approach, 5079–5092. http://doi.org/10.3390/molecules15085079

Han, Y., Alexander, T. E., & Tochtrop, G. P. (2008). Design, synthesis, and evaluation of an isotopic labeling strategy for studying fatty acid–protein binding by NMR. *Molecular BioSystems*, *4*(6), 551–557. http://doi.org/10.1039/B800471D

Hanley, J. A., & McNeil, B. J. (1982). The meaning and use of the area under a receiver operating characteristic (ROC) curve. *Radiology*, *143*(1), 29–36. http://doi.org/10.1148/radiology.143.1.7063747

Hartenstein, H., & Sicker, D. (2010). An Efficient Synthesis of 5-Methoxy-2-nitrophenol. *ChemInform*, *25*(3), no-no. http://doi.org/10.1002/chin.199403125

Hawkins, P. C. D., Warren, G. L., Skillman, A. G., & Nicholls, A. (2008). How to do an evaluation: pitfalls and traps. *Journal of Computer-Aided Molecular Design*, *22*(3–4), 179–190. http://doi.org/10.1007/s10822-007-9166-3

Heydenreich, M., Muiva, L. M., Eyase, F. L., Akala, H. M., Wanyama, P. J., Yenesew, A., others. (2011). Terpurinflavone: An antiplasmodial flavone from the stem of Tephrosia Purpurea.

Hinchliffe, A. (2003). *Molecular modelling for beginners*. Chichester, West Sussex, England; Hoboken, NJ: Wiley.

Huang, H.-J., Lee, K.-J., Yu, H. W., Chen, C.-Y., Hsu, C.-H., Chen, H.-Y.,Chen, C. Y.-C. (2010). Structure-Based and Ligand-Based Drug Design for HER 2 Receptor. *Journal of Biomolecular Structure and Dynamics*, *28*(1), 23–37. http://doi.org/10.1080/07391102.2010.10507341

Huang, N., Shoichet, B. K., & Irwin, J. J. (2006). Benchmarking Sets for Molecular Docking. *Journal of Medicinal Chemistry*, *49*(23), 6789–6801. http://doi.org/10.1021/jm0608356

Huang, W., Zhang, P., Zuckett, J. F., Wang, L., Woolfrey, J., Song, Y., … Zhu, B.-Y. (2003). Design, synthesis and structure–Activity relationships of benzoxazinone-Based factor Xa inhibitors. *Bioorganic & Medicinal Chemistry Letters*, *13*(3), 561–566. http://doi.org/10.1016/S0960-894X(02)00927-7

Hurt, D. E., Widom, J., & Clardy, J. (2006). Structure of *Plasmodium falciparum* dihydroorotate dehydrogenase with a bound inhibitor. *Acta Crystallographica Section D Biological Crystallography*, *62*(3), 312–323. http://doi.org/10.1107/S0907444905042642

Ilaš, J., Anderluh, P. Š., Dolenc, M. S., & Kikelj, D. (2005). Recent advances in the synthesis of 2H-1,4-benzoxazin-3-(4H)-ones and 3,4-dihydro-2H-1,4-benzoxazines. *Tetrahedron*, *61*(31), 7325–7348. http://doi.org/10.1016/j.tet.2005.05.037

Jones, G., & Willett, P. (1995). Docking small-molecule ligands into active sites. *Current Opinion in Biotechnology*, *6*(6), 652–656. http://doi.org/10.1016/0958-1669(95)80107-3

Kokwaro, J. O. (2009). *Medicinal Plants of East Africa*. University of Nairobi Press.

Lee, C.-H., Huang, H.-C., & Juan, H.-F. (2011). Reviewing Ligand-Based Rational Drug Design: The Search for an ATP Synthase Inhibitor. *International Journal of Molecular Sciences*, *12*(12), 5304–5318. http://doi.org/10.3390/ijms12085304

Lipinski, C. A. (2004). Lead- and drug-like compounds: the rule-of-five revolution. *Drug*

Discovery Today: Technologies, *1*(4), 337–341. http://doi.org/10.1016/j.ddtec.2004.11.007

Lipinski, C. A., Lombardo, F., Dominy, B. W., & Feeney, P. J. (1997). Experimental and computational approaches to estimate solubility and permeability in drug discovery and development settings. *Advanced Drug Delivery Reviews*, *23*, 3–25.

Lipinski, C. A., Lombardo, F., Dominy, B. W., & Feeney, P. J. (2012). Experimental and computational approaches to estimate solubility and permeability in drug discovery and development settings. *Advanced Drug Delivery Reviews*, *64*, 4–17.

Liu, T., Lin, Y., Wen, X., Jorissen, R. N., & Gilson, M. K. (2007). BindingDB: a web-accessible database of experimentally determined protein-ligand binding affinities. *Nucleic Acids Research*, *35*(Database), D198–D201. http://doi.org/10.1093/nar/gkl999

Lohray, B., Lohray, V., Ashok, C., Kalchar, S., Gurram, R., Rajagopalan, R., & Ranjan, C. (2000, November 9). Substituted Bicyclic Heterocycles, Process for Their Preparation and Their Use as Antiobesity and Hypocholesterolemic Agents. Retrieved from http://worldwide.espacenet.com/publicationDetails/biblio?FT=D&date=20001109&DB=&locale=&CC=WO&NR=0066572A1&KC=A1&ND=1

Maag, H., Sui, M., & Zhao, S.-H. (2004, May 21). Substituted benzoxazinones and uses thereof. Retrieved from http://www.google.com/patents/WO2004041792A1

Manabu, H., Ikuo, W., Hiroshi, O., Kengo, H., & Joji, M. (1996, March 7). 1,4-Benzoxazine derivative, pharmaceutical composition containing the same and use thereof.

Merz, K. M. (Ed.). (2010). *Drug Design structure and ligand-based approaches*. Cambridge [u.a.]: Cambridge Univ. Press.

Midiwo, J. O., Yenesew, A., Juma, B. F., Omosa, K. L., Omosa, I. L., & Mutisya, D. (2001). Phytochemical Evaluation of Some Kenyan Medicinal Plants. In *11th NAPRECA Symposium Book of Proceedings, Antananarivo, Madagascar* (pp. 9–19). Retrieved from http://www.napreca.net/publications/11symposium/pdf/B-9-19-Midiwo.pdf

Morris, C. A., Duparc, S., Borghini-Fuhrer, I., Jung, D., Shin, C.-S., & Fleckenstein, L. (2011). Review of the clinical pharmacokinetics of artesunate and its active metabolite dihydroartemisinin following intravenous, intramuscular, oral or rectal administration. *Malar J*, *10*, 263.

Muiva, L. M., Yenesew, A., Derese, S., Heydenreich, M., Peter, M. G., Akala, H. M., … Walsh, D. (2009). Antiplasmodial β-hydroxydihydrochalcone from seedpods of Tephrosia elata. *Phytochemistry Letters*, *2*(3), 99–102. http://doi.org/10.1016/j.phytol.2009.01.002

Mysinger, M. M., Carchia, M., Irwin, J. J., & Shoichet, B. K. (2012). Directory of Useful Decoys, Enhanced (DUD-E): Better Ligands and Decoys for Better Benchmarking. *Journal of Medicinal Chemistry*, *55*(14), 6582–6594. http://doi.org/10.1021/jm300687e

Nguta, J. M., Mbaria, J. M., Gakuya, D. W., Gathumbi, P. K., Kabasa, J. D., & Kiama, S. G. (2012). Evaluation of Acute Toxicity of Crude Plant Extracts from Kenyan Biodi-versity using Brine Shrimp, Artemia salina L.(Artemiidae). Retrieved from http://erepository.uonbi.ac.ke/handle/11295/9796

Ntie-Kang, F., Mbah, J. A., Mbaze, L. M., Lifongo, L. L., Scharfe, M., Hanna, J. N., … others. (2013). CamMedNP: Building the Cameroonian 3D structural natural products database for virtual screening. *BMC Complementary and Alternative Medicine*, *13*(1), 88.

Ochieng', C. O., Owuor, P. O., Mang'uro, L. A. O., Akala, H., & Ishola, I. O. (2012). Antinociceptive and antiplasmodial activities of cassane furanoditerpenes from Caesalpinia volkensii H. root bark. *Fitoterapia*, *83*(1), 74–80. http://doi.org/10.1016/j.fitote.2011.09.015

O'Donnell, T. J. (2008). *Design and Use of Relational Databases in Chemistry* (1 edition). Boca Raton: CRC Press.

OpenEye Scientific. (2015). Similarity Measures — Toolkits -- Python. Retrieved October 2, 2015, from https://docs.eyesopen.com/toolkits/python/graphsimtk/measure.html

Patel, V., Booker, M., Kramer, M., Ross, L., Celatka, C. A., Kennedy, L. M., … Clardy, J. (2008). Identification and Characterization of Small Molecule Inhibitors of Plasmodium falciparum Dihydroorotate Dehydrogenase. *Journal of Biological Chemistry*, *283*(50), 35078–35085. http://doi.org/10.1074/jbc.M804990200

Patrick, G. L., & Spencer, J. (2009). *An introduction to medicinal chemistry*. New York: Oxford University Press.

Phillips, M. A., & Rathod, P. K. (2010). Plasmodium dihydroorotate dehydrogenase: a promising target for novel anti-malarial chemotherapy. *Infectious Disorders Drug Targets*, *10*(3), 226.

Plettner, E., & Isman, M. B. (2013, May 23). Methods and Compositions for Control of Cabbage Looper, Trichoplusia ni. Retrieved from

http://www.google.com/patents/US20130131185

Ramesh, C., Raju, B. R., Kavala, V., Kuo, C.-W., & Yao, C.-F. (2011). A simple and facile route for the synthesis of 2H-1,4-benzoxazin-3-(4H)-ones via reductive cyclization of 2-(2-nitrophenoxy)acetonitrile adducts in the presence of Fe/acetic acid. *Tetrahedron*, *67*(6), 1187–1192. http://doi.org/10.1016/j.tet.2010.11.095

Rückemann, K., Fairbanks, L. D., Carrey, E. A., Hawrylowicz, C. M., Richards, D. F., Kirschbaum, B., & Simmonds, H. A. (1998). Leflunomide Inhibits Pyrimidine de Novo Synthesis in Mitogen-stimulated T-lymphocytes from Healthy Humans. *Journal of Biological Chemistry*, *273*(34), 21682–21691. http://doi.org/10.1074/jbc.273.34.21682

Rukunga, G. M., Muregi, F. W., Omar, S. A., Gathirwa, J. W., Muthaura, C. N., Peter, M. G., … Mungai, G. M. (2008). Anti-plasmodial activity of the extracts and two sesquiterpenes from Cyperus articulatus. *Fitoterapia*, *79*(3), 188–190. http://doi.org/10.1016/j.fitote.2007.11.010

Rukunga, G. M., Muregi, F. W., Tolo, F. M., Omar, S. A., Mwitari, P., Muthaura, C. N., … Kofi-Tsekpo, W. M. (2007). The antiplasmodial activity of spermine alkaloids isolated from Albizia gummifera. *Fitoterapia*, *78*(7–8), 455–459. http://doi.org/10.1016/j.fitote.2007.02.012

Rutar, A., & Kikelj, D. (1998). Selective Alkylation of 3-Oxo-3,4-Dihydro-2 *H* -1,4-Benzoxazine-2-Carboxylates. *Synthetic Communications*, *28*(15), 2737–2749. http://doi.org/10.1080/00397919808004847

Schlitzer, M. (2008). Antimalarial Drugs – What is in Use and What is in the Pipeline. *Archiv Der Pharmazie*, *341*(3), 149–163. http://doi.org/10.1002/ardp.200700184

Sharifi, A., Barazandeh, M., Saeed Abaee, M., & Mirzaei, M. (2010). [Omim][BF4], a green and recyclable ionic liquid medium for the one-pot chemoselective synthesis of benzoxazinones. *Tetrahedron Letters*, *51*(14), 1852–1855. http://doi.org/10.1016/j.tetlet.2010.01.122

Stamatis, D. H. (2012). *Essential statistical concepts for the quality professional*. CRC Press. Retrieved from http://books.google.com/books?hl=en&lr=&id=XhjSBQAAQBAJ&oi=fnd&pg=PP1&dq=%22hypothesis+is+true.+In+many+applications,+the+test+statistic+is+defined+so+that+its%22+%22or+out+in+a+tail+of+the+distribution+(making+the+alternative+hypothesis+seem%22+&ots=sortFtbgyB&sig=CM6ywVka4ate83YTA0kr-gGs7Fo

Swann, S. L., Brown, S. P., Muchmore, S. W., Patel, H., Merta, P., Locklear, J., & Hajduk, P. J. (2011). A Unified, Probabilistic Framework for Structure- and Ligand-Based Virtual Screening. *Journal of Medicinal Chemistry*, *54*(5), 1223–1232. http://doi.org/10.1021/jm1013677

Sykes, M. J., McKinnon, R. A., & Miners, J. O. (2008). Prediction of Metabolism by Cytochrome P450 2C9: Alignment and Docking Studies of a Validated Database of Substrates. *Journal of Medicinal Chemistry*, *51*(4), 780–791. http://doi.org/10.1021/jm7009793

Valli, M., dos Santos, R. N., Figueira, L. D., Nakajima, C. H., Castro-Gamboa, I., Andricopulo, A. D., & Bolzani, V. S. (2013). Development of a Natural Products Database from the Biodiversity of Brazil. *Journal of Natural Products*, *76*(3), 439–444. http://doi.org/10.1021/np3006875

van Agtmael, M. A., Eggelte, T. A., & van Boxtel, C. J. (1999). Artemisinin drugs in the treatment of malaria: from medicinal herb to registered medication. *Trends in Pharmacological Sciences*, *20*(5), 199–205. http://doi.org/10.1016/S0165-6147(99)01302-4

Veber, D. F., Johnson, S. R., Cheng, H.-Y., Smith, B. R., Ward, K. W., & Kopple, K. D. (2002). Molecular Properties That Influence the Oral Bioavailability of Drug Candidates. *Journal of Medicinal Chemistry*, *45*(12), 2615–2623. http://doi.org/10.1021/jm020017n

Vianello, P., & Bandiera, T. (2004, June 15). Substituted benzoxazines as integrin antagonists.

Wells, T. N. (2011). Natural products as starting points for future anti-malarial therapies: going back to our roots. *Malar J*, *10*(Suppl 1), S3.

World Health Organization. (2014). *World malaria report 2013.* [S.l.]: World Health Organization.

World Health Organization, & Global Malaria Programme. (2012). *World malaria report 2012*. Geneva: World Health Organization. Retrieved from http://www.who.int/malaria/publications/world_malaria_report_2012/wmr2012_full_report.pdf

Wu, J.-H., Chang, F.-R., Hayashi, K., Shiraki, H., Liaw, C.-C., Nakanishi, Y., … Lee, K.-H. (2003). Antitumor agents. Part 218: Cappamensin A, a new In vitro anticancer principle, from Capparis sikkimensis. *Bioorganic & Medicinal Chemistry Letters*, *13*(13), 2223–2225. http://doi.org/10.1016/S0960-894X(03)00379-2

Xu, J., & Hagler, A. (2002). Chemoinformatics and drug discovery. *Molecules*, *7*(8), 566–

600.

Yenesew, A., Derese, S., Midiwo, J. O., Bii, C. C., Heydenreich, M., & Peter, M. G. (2005). Antimicrobial flavonoids from the stem bark of Erythrina burttii. *Fitoterapia*, *76*(5), 469–472. http://doi.org/10.1016/j.fitote.2005.04.006

Yenesew, A., Induli, M., Derese, S., Midiwo, J. O., Heydenreich, M., Peter, M. G., … Waters, N. C. (2004). Anti-plasmodial flavonoids from the stem bark of Erythrina abyssinica. *Phytochemistry*, *65*(22), 3029–3032. http://doi.org/10.1016/j.phytochem.2004.08.050

Yenesew, A., Twinomuhwezi, H., Kabaru, J. M., Akala, H. M., Kiremire, B. T., Heydenreich, M., … Walsh, D. S. (2009). Antiplasmodial and larvicidal flavonoids from Derris trifoliata. *Bulletin of the Chemical Society of Ethiopia*, *23*(3). Retrieved from http://www.ajol.info/index.php/bcse/article/view/47665

APPENDICES

Appendix A: NMR Spectra for 3-Methoxyphenol (**22**)
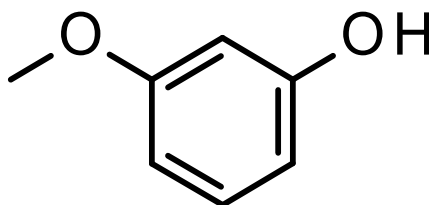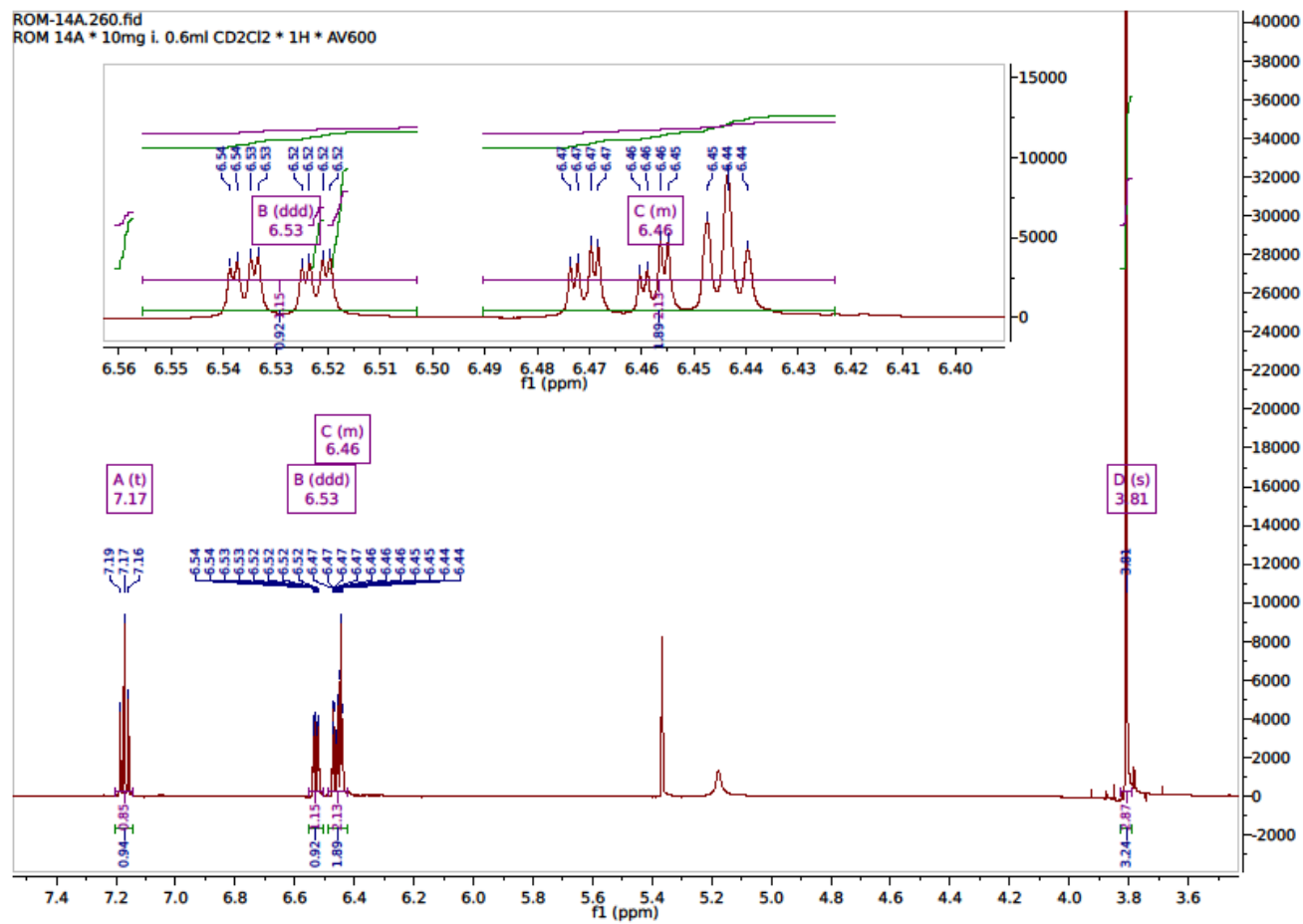
^{1}HNMR for 3- methoxyphenol

^{13}C NMR (151 MHz, CD$_2$Cl2) δ 161.041, 156.890, 130.098, 107.580, 106.242, 101.322, 55.229.

ROM-14A.264.fid
ROM 14A * 10mg i. 0.6ml CD2Cl2 * 13C * AV600
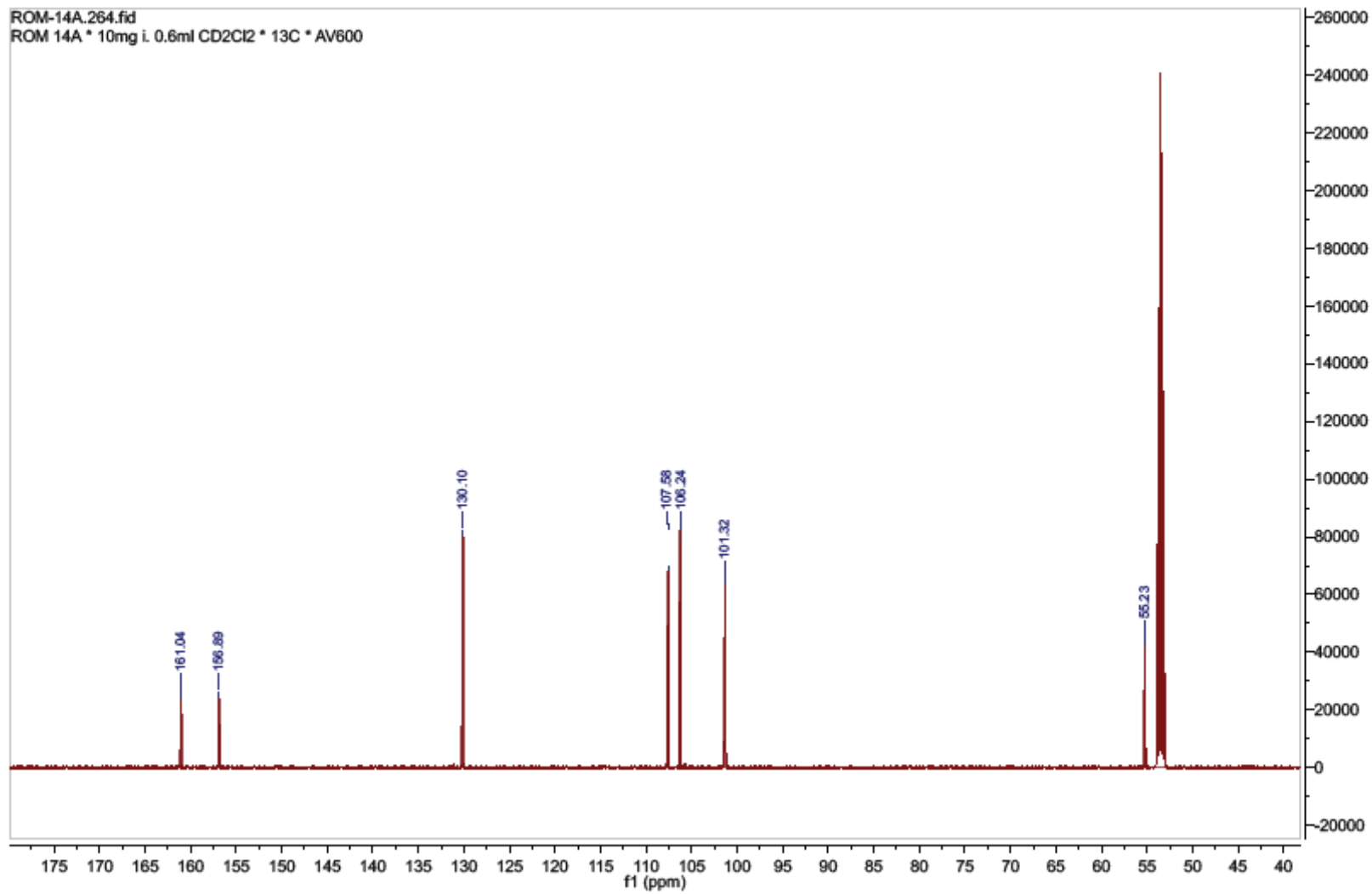
^{13}C NMR for 3- methoxyphenol
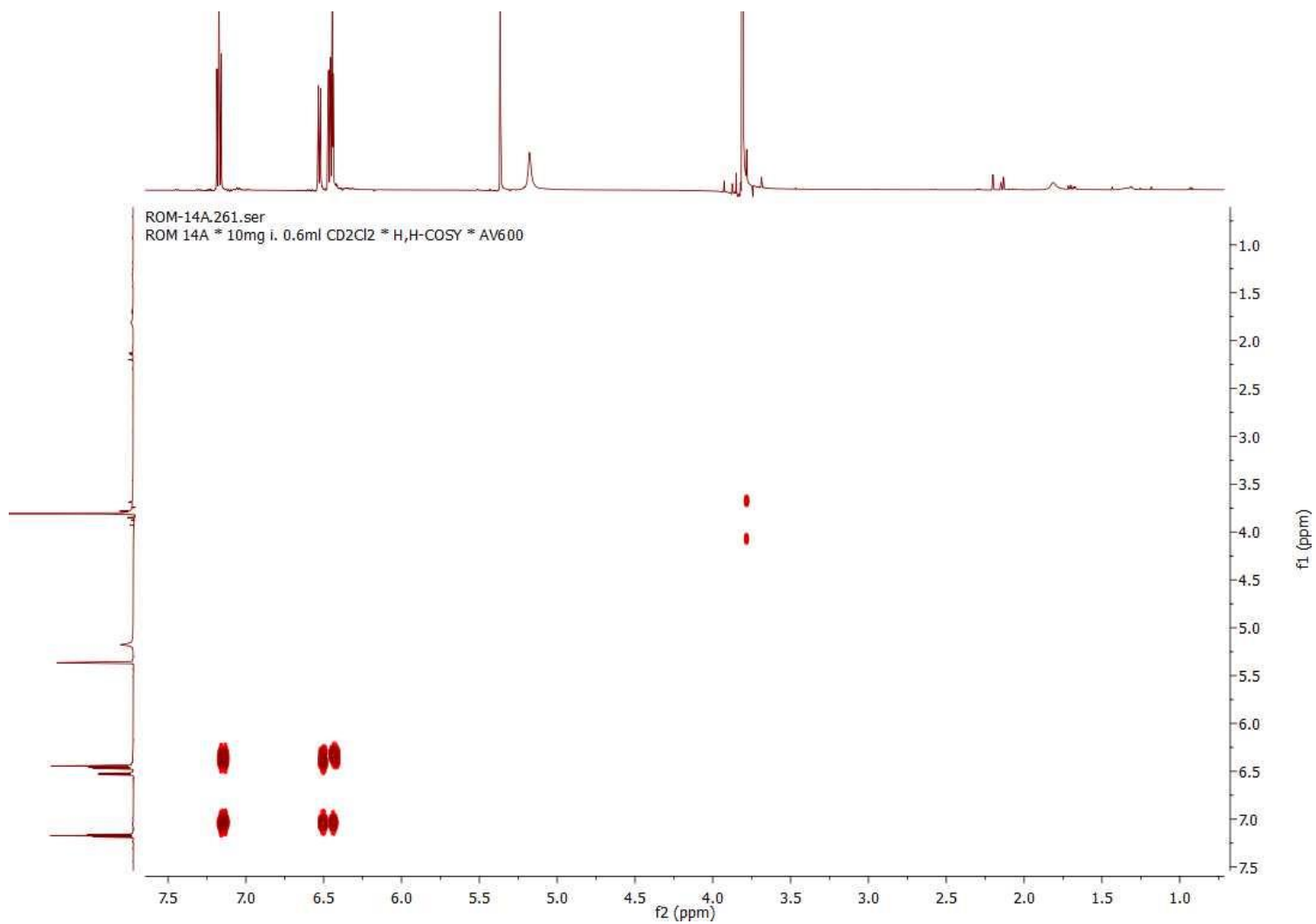
H,H-COSY NMR for 3- methoxyphenol
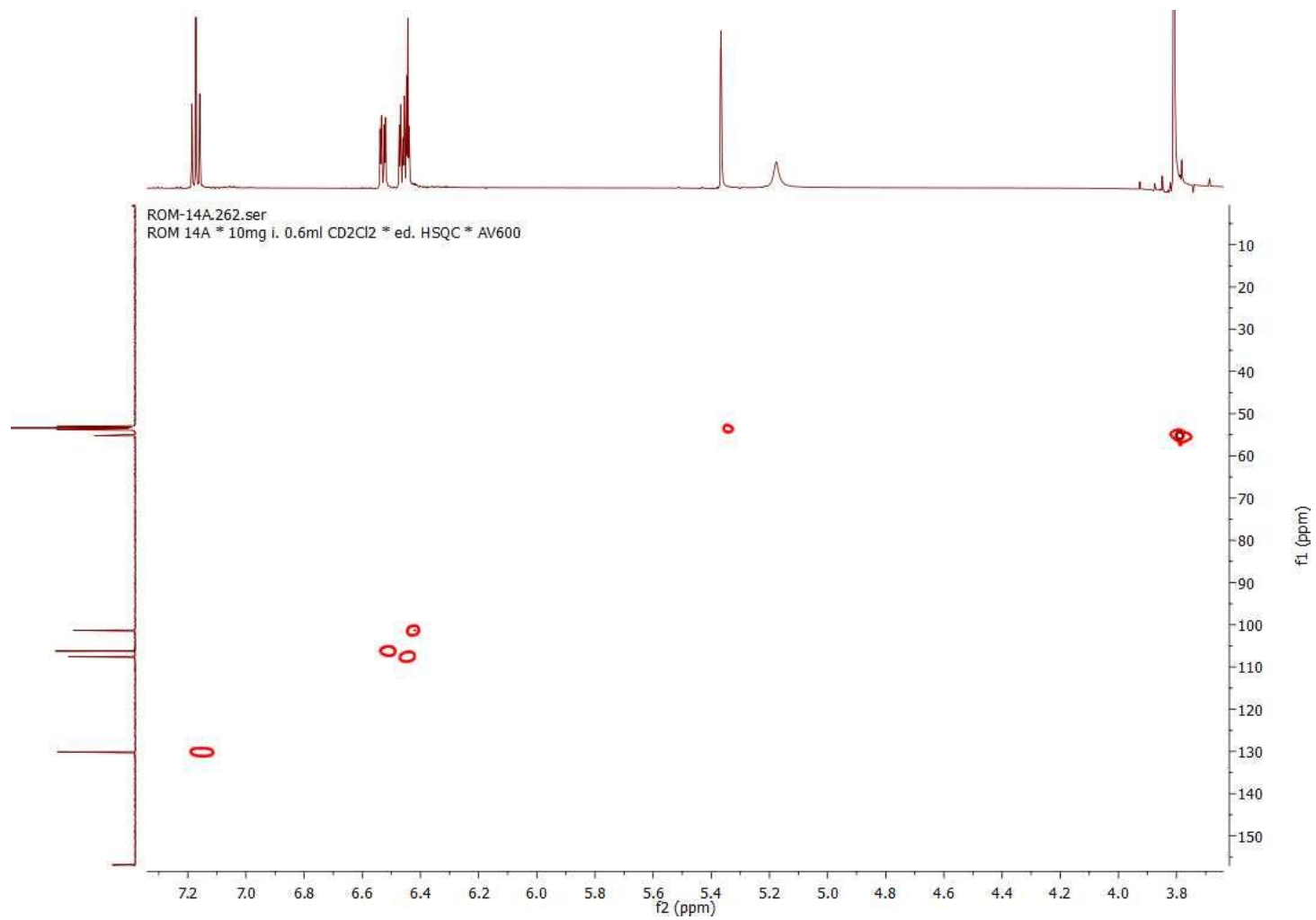
HSQC NMR for 3- methoxyphenol

Appendix B: NMR Spectra for 5-Methoxy-2-nitrophenol (**23**)
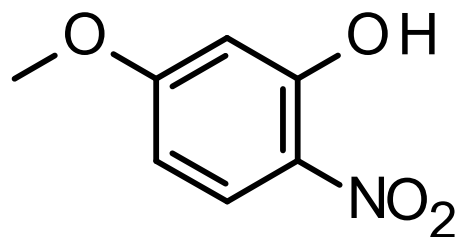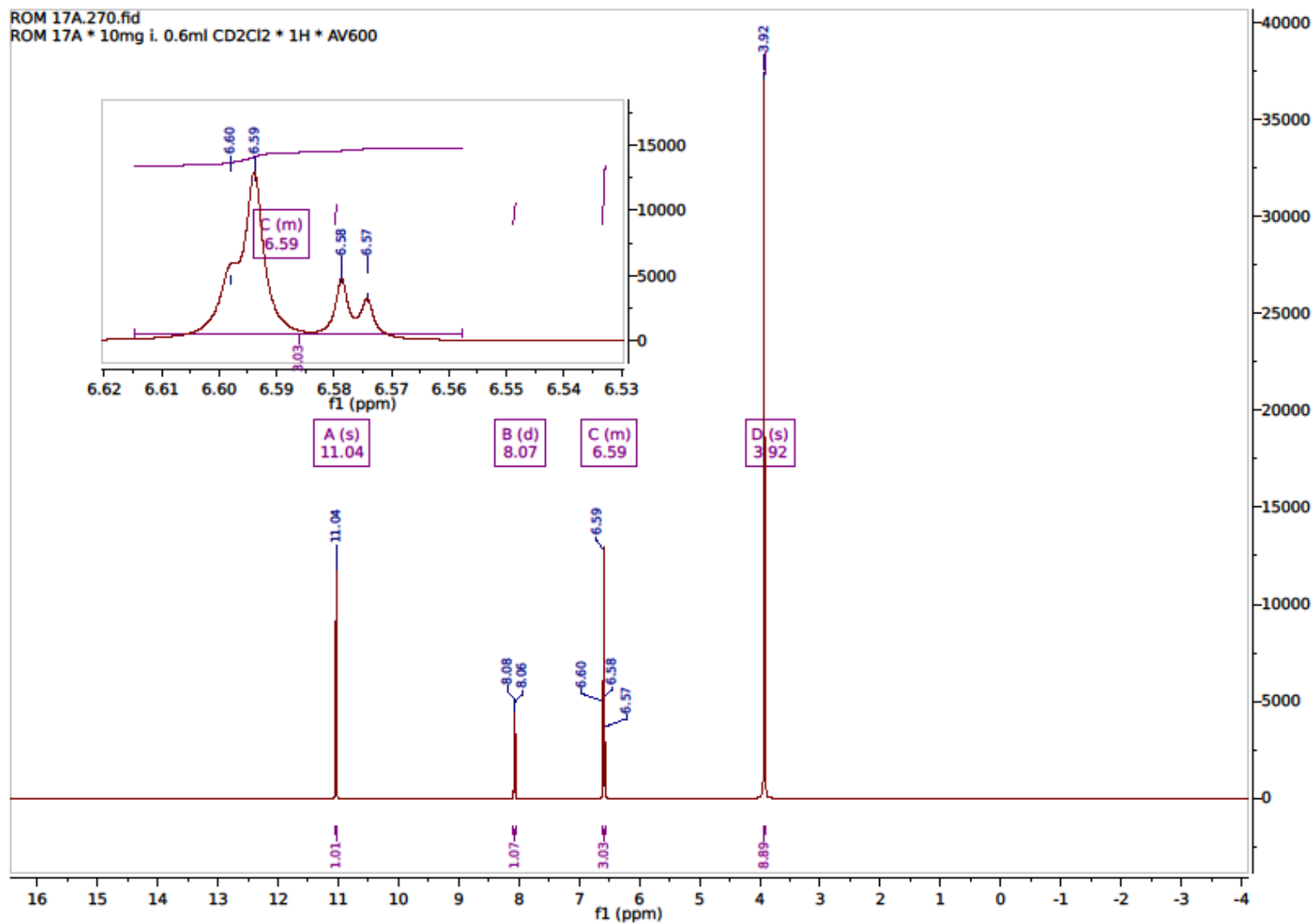
^{1}HNMR for 5-methoxy-2-nitrophenol

^{13}C NMR (151 MHz, CD$_2$Cl2) δ 167.2, 157.9, 126.9, 109.4, 101.4, 56.3, 53.6.

ROM 17A.274.fid
ROM 17A * 10mg i. 0.6ml CD2Cl2 * 13C * AV600
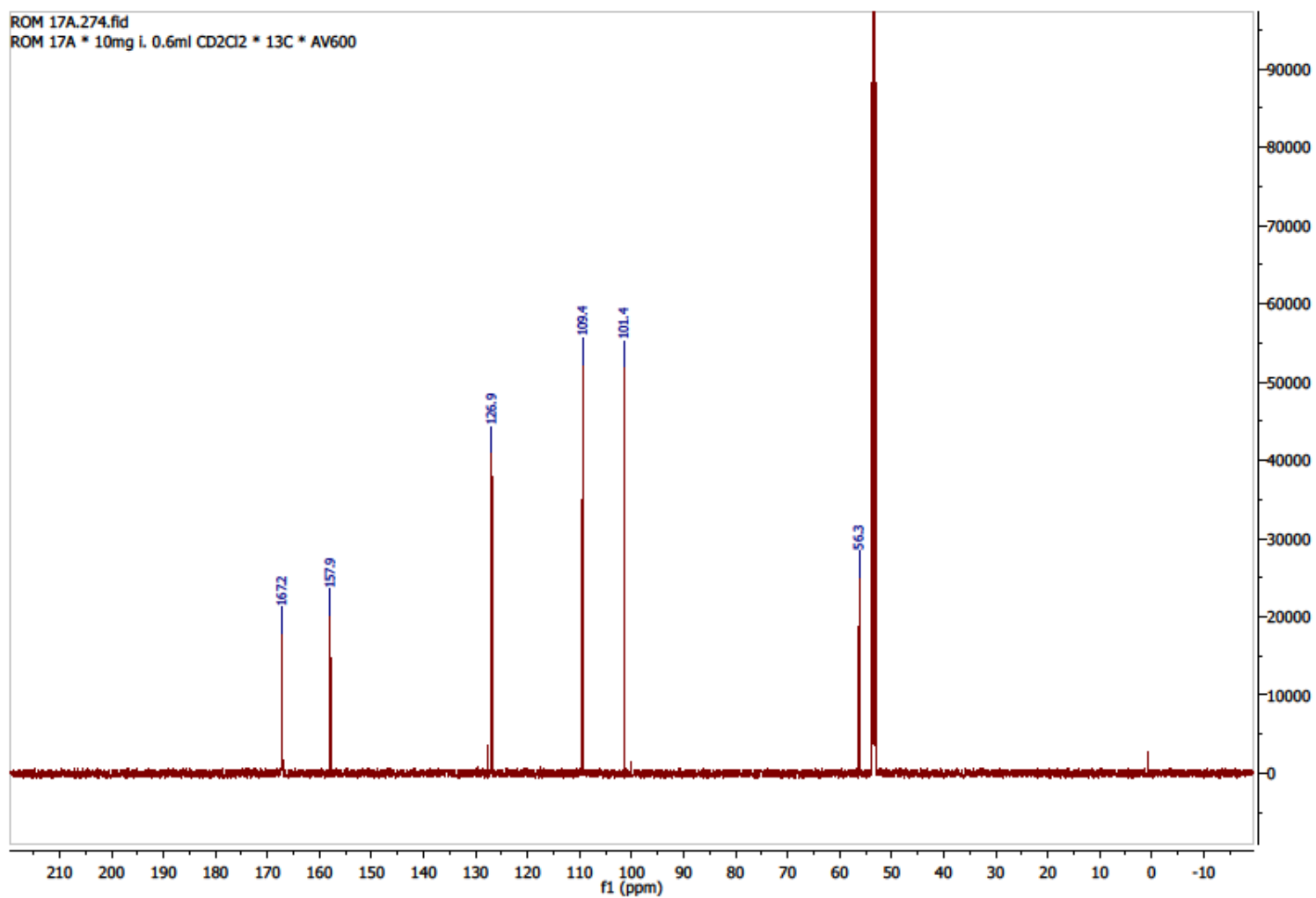
^{13}C NMR for 5-methoxy-2-nitrophenol
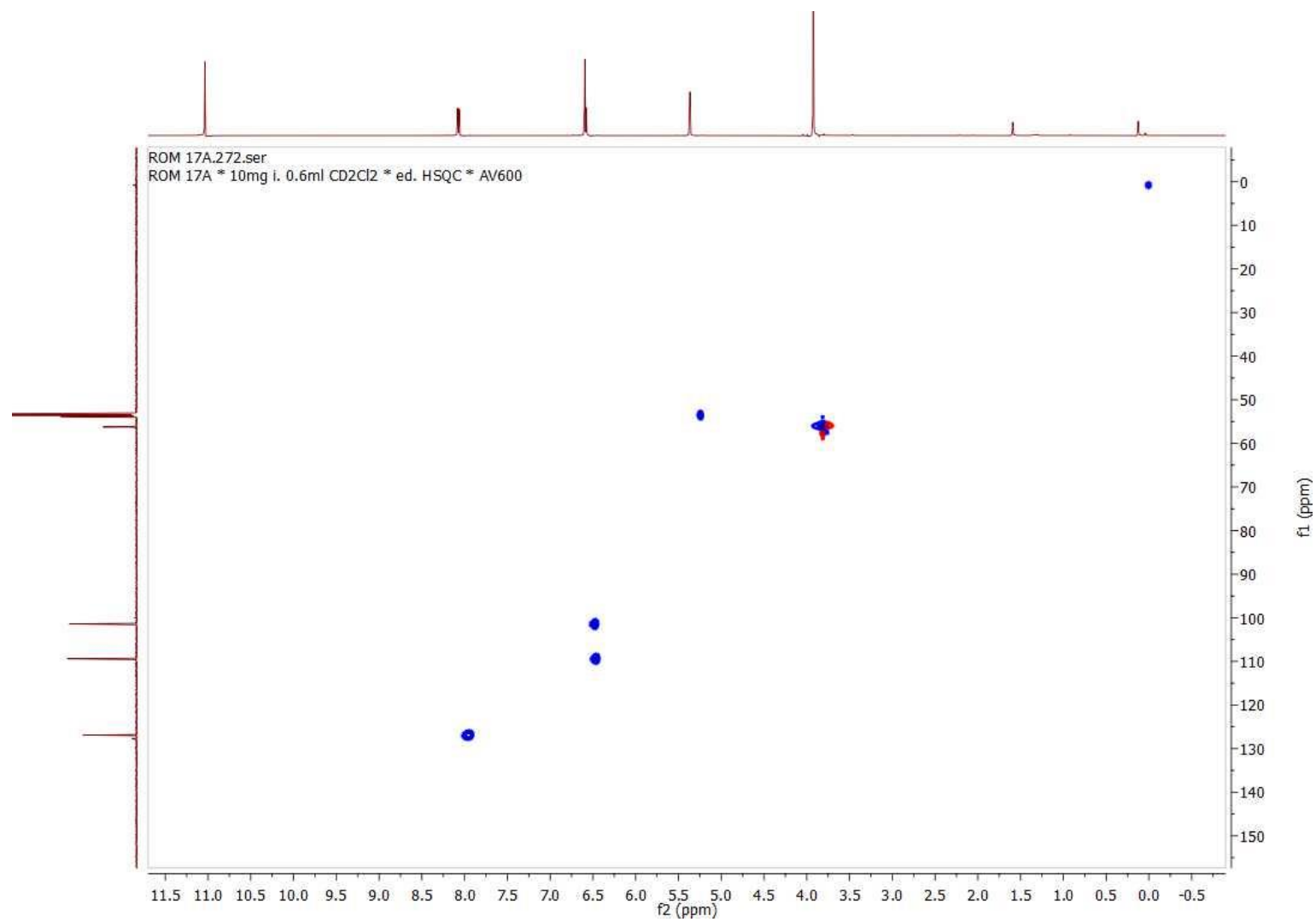
HSQC NMR for 5-methoxy-2-nitrophenol
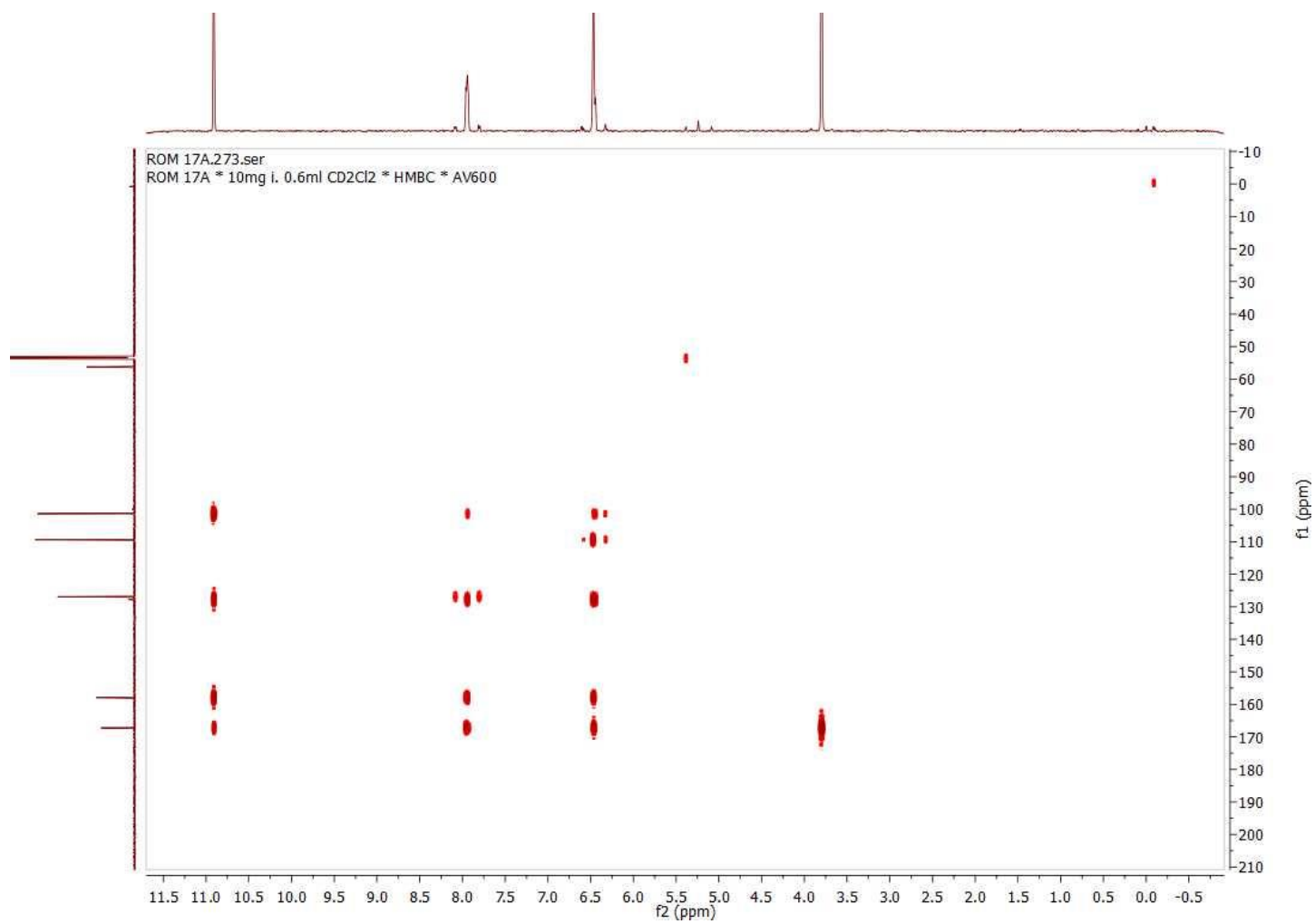
HMBC NMR for 5-methoxy-2-nitrophenol
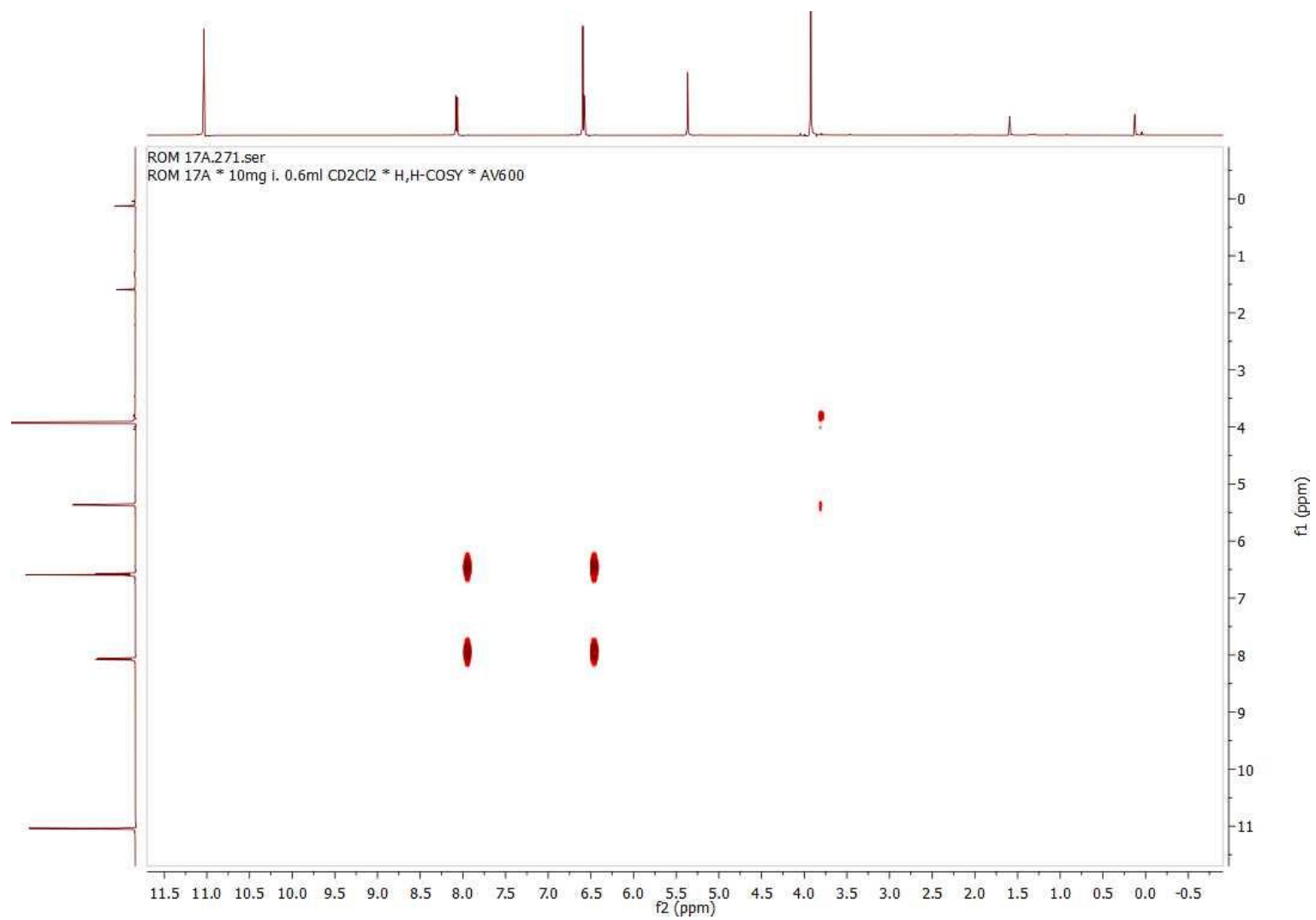
H,H-COSY NMR for 5-methoxy-2-nitrophenol

Appendix C: NMR Spectra for Ethyl 2-(5-methoxy-2-nitrophenoxy) acetate (**26**)

^{1}H NMR for ethyl 2-(5-methoxy-2-nitrophenoxy) acetate

ROM 18A.284.fid
ROM 18A * 20mg i. 0.6ml CD2Cl2 * 13C * AV600
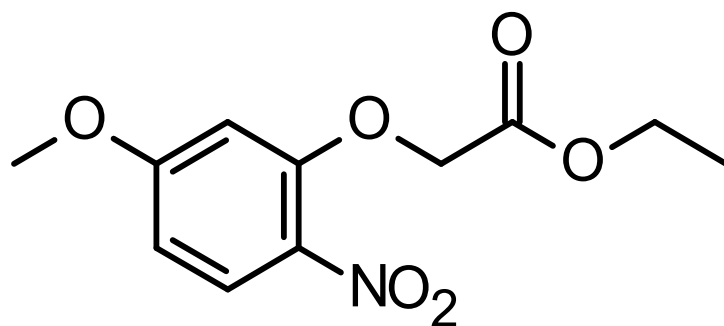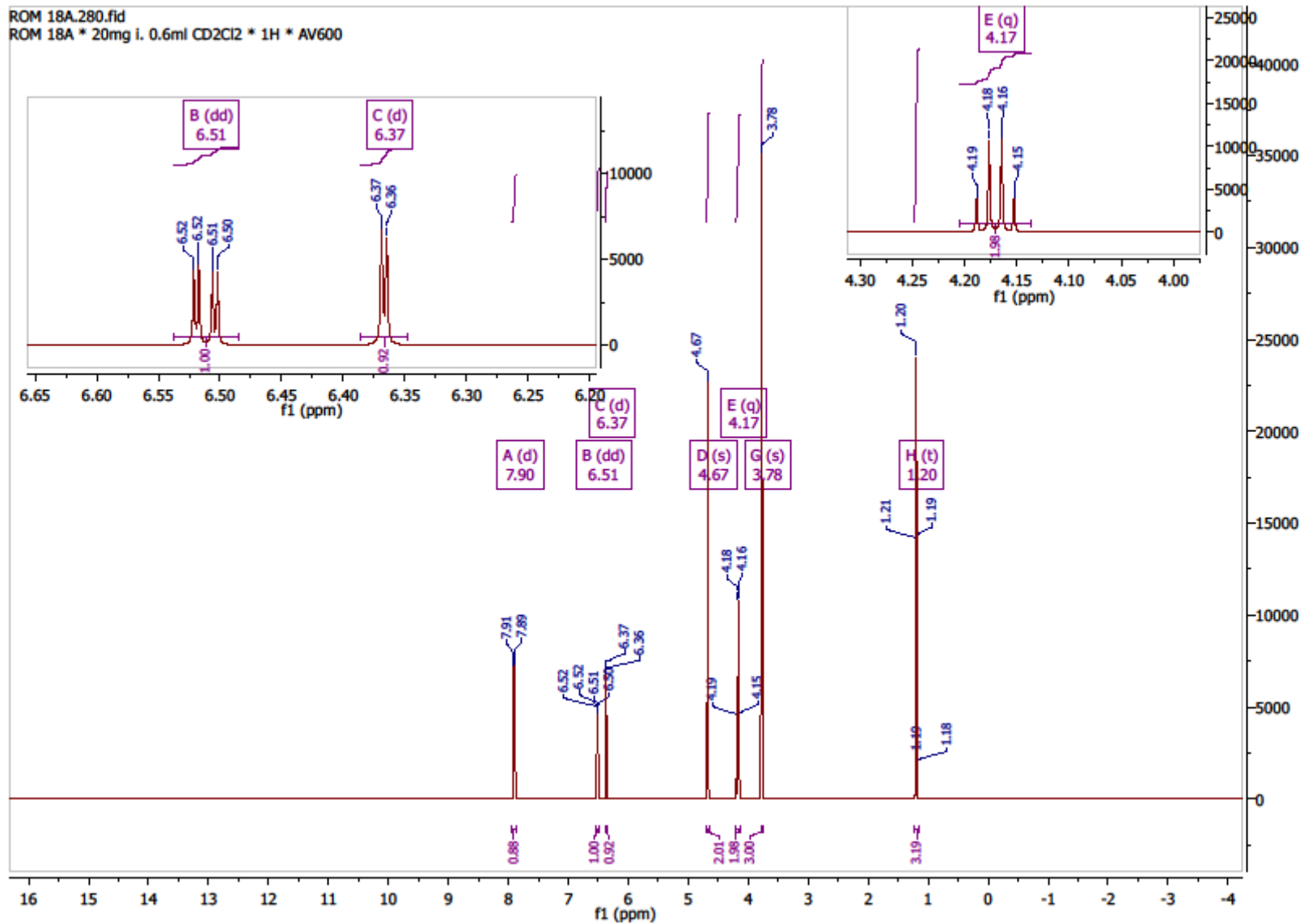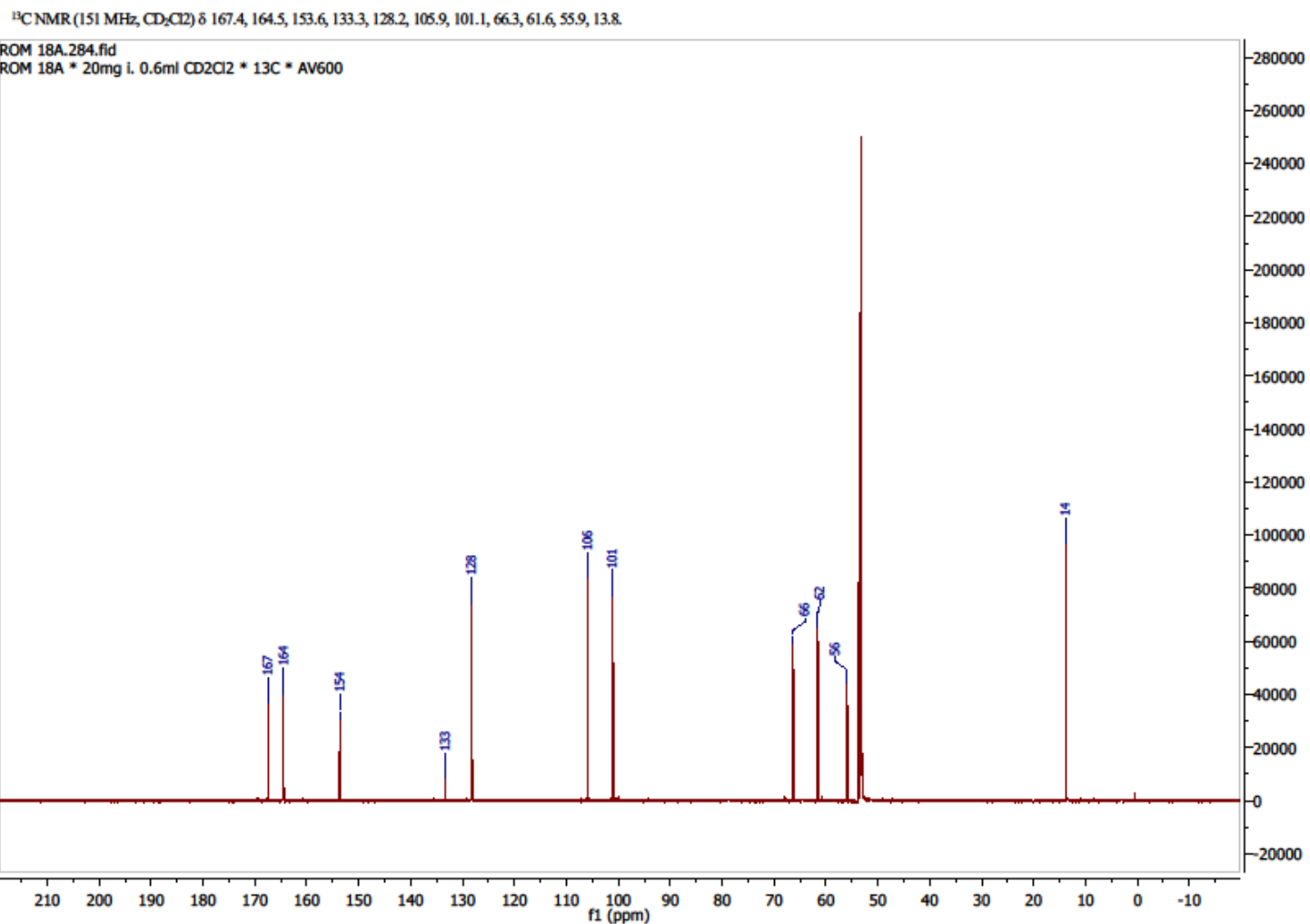
^{13}C NMR for ethyl 2-(5-methoxy-2-nitrophenoxy) acetate
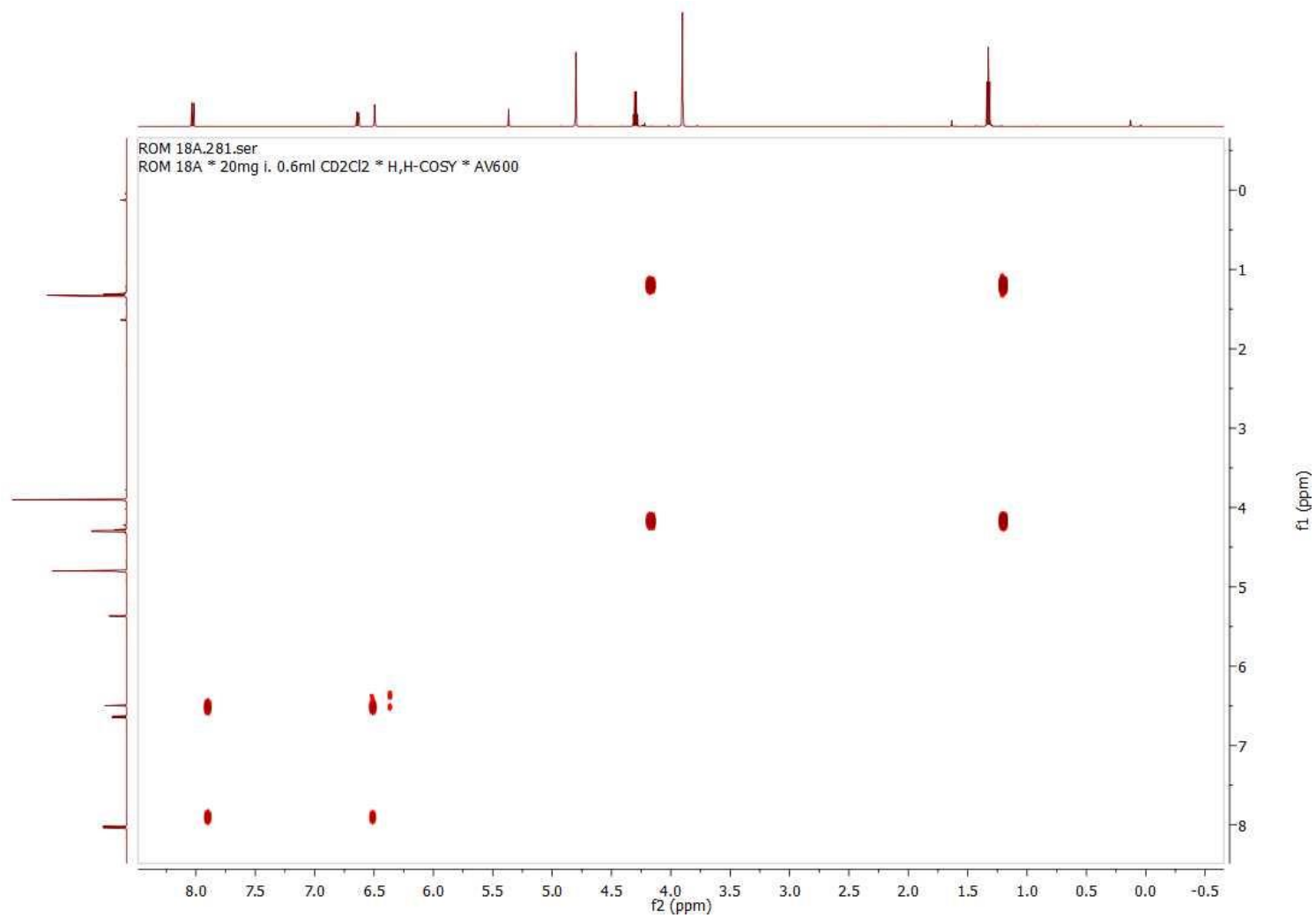
H,H-COSY NMR for ethyl 2-(5-methoxy-2-nitrophenoxy) acetate
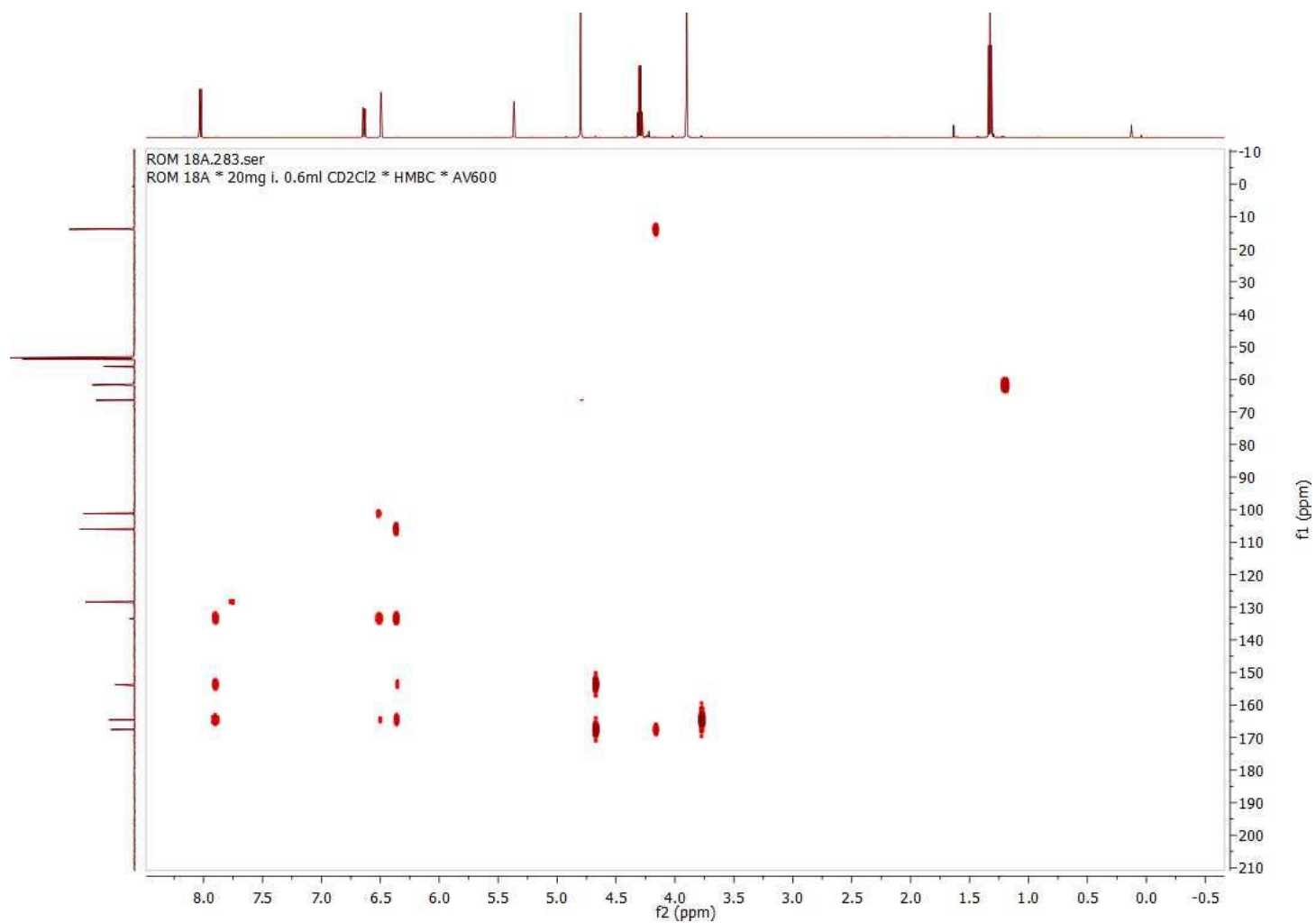
HMBC NMR for ethyl 2-(5-methoxy-2-nitrophenoxy) acetate
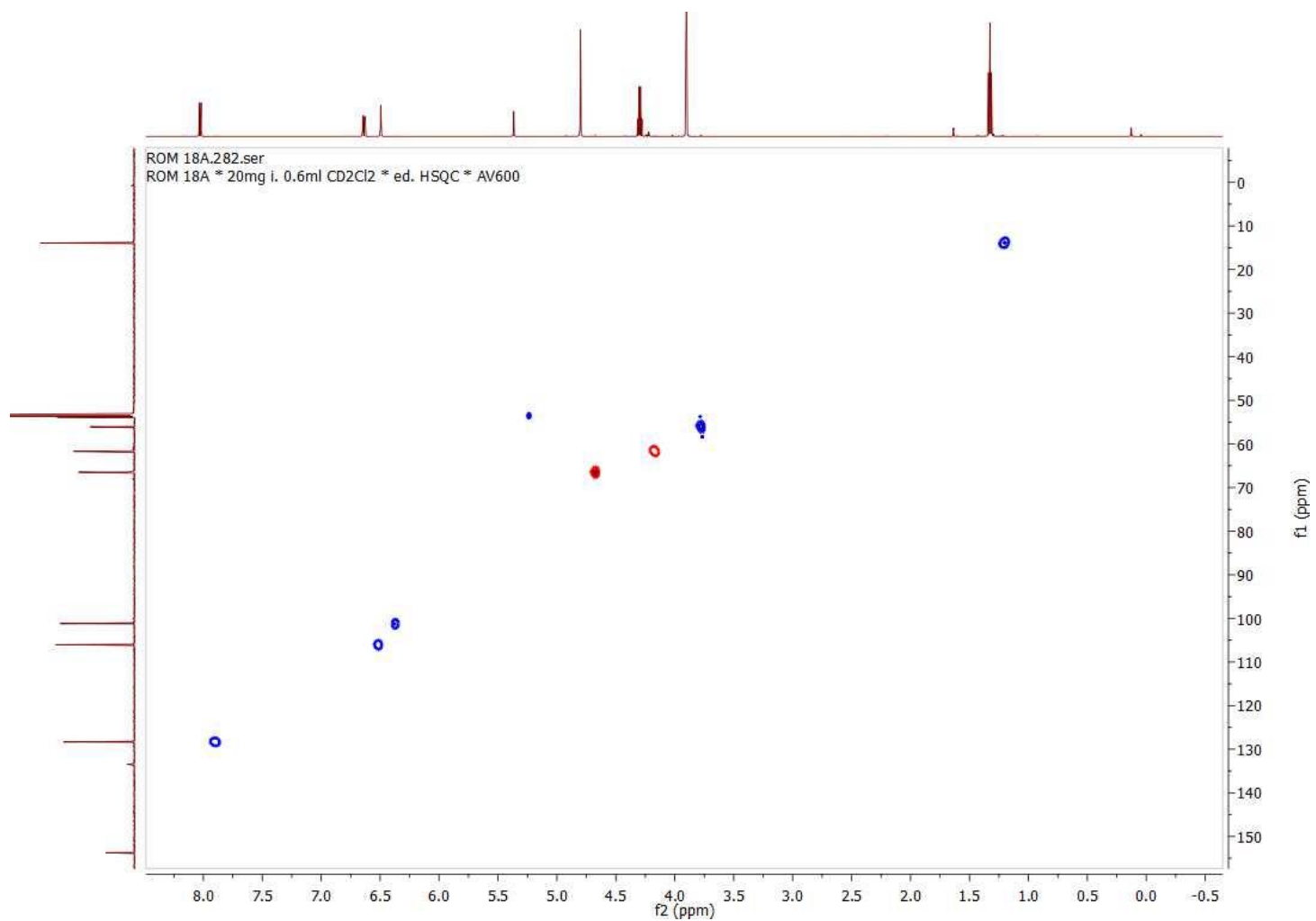
HSQC NMR for ethyl 2-(5-methoxy-2-nitrophenoxy) acetate

Appendix D: NMR Spectra for 7-Methoxy-4H-1, 4-benzoxazin-3-one (**27**)
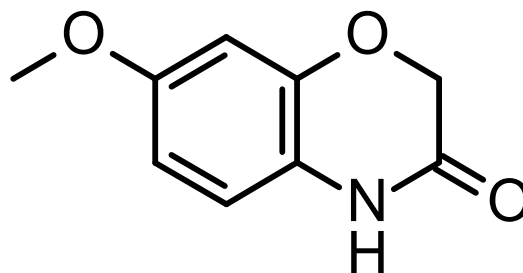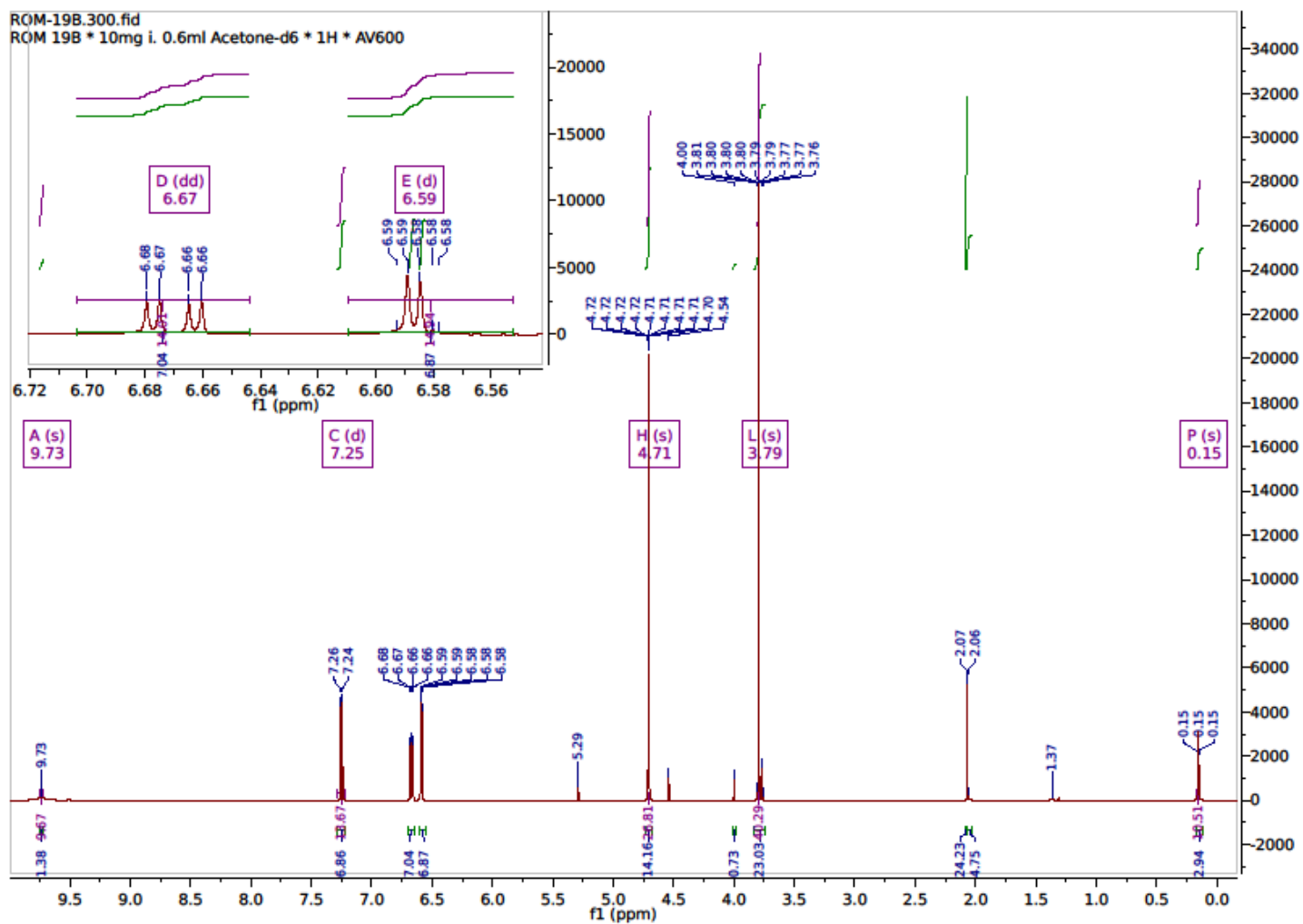
^{1}H NMR for 7-Methoxy-4H-1, 4-benzoxazin-3-one
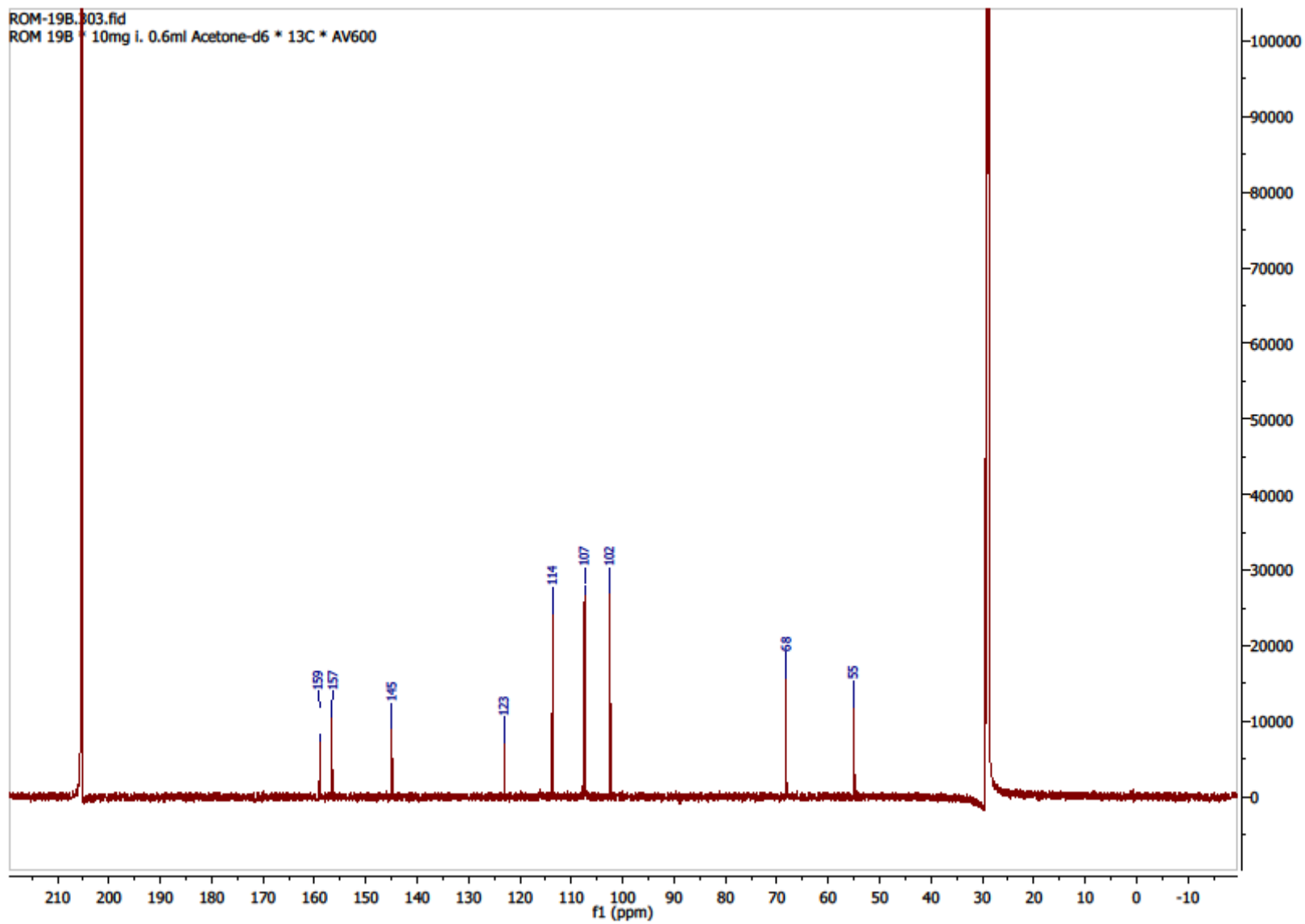
^{13}C NMR for 7-Methoxy-4H-1, 4-benzoxazin-3-one
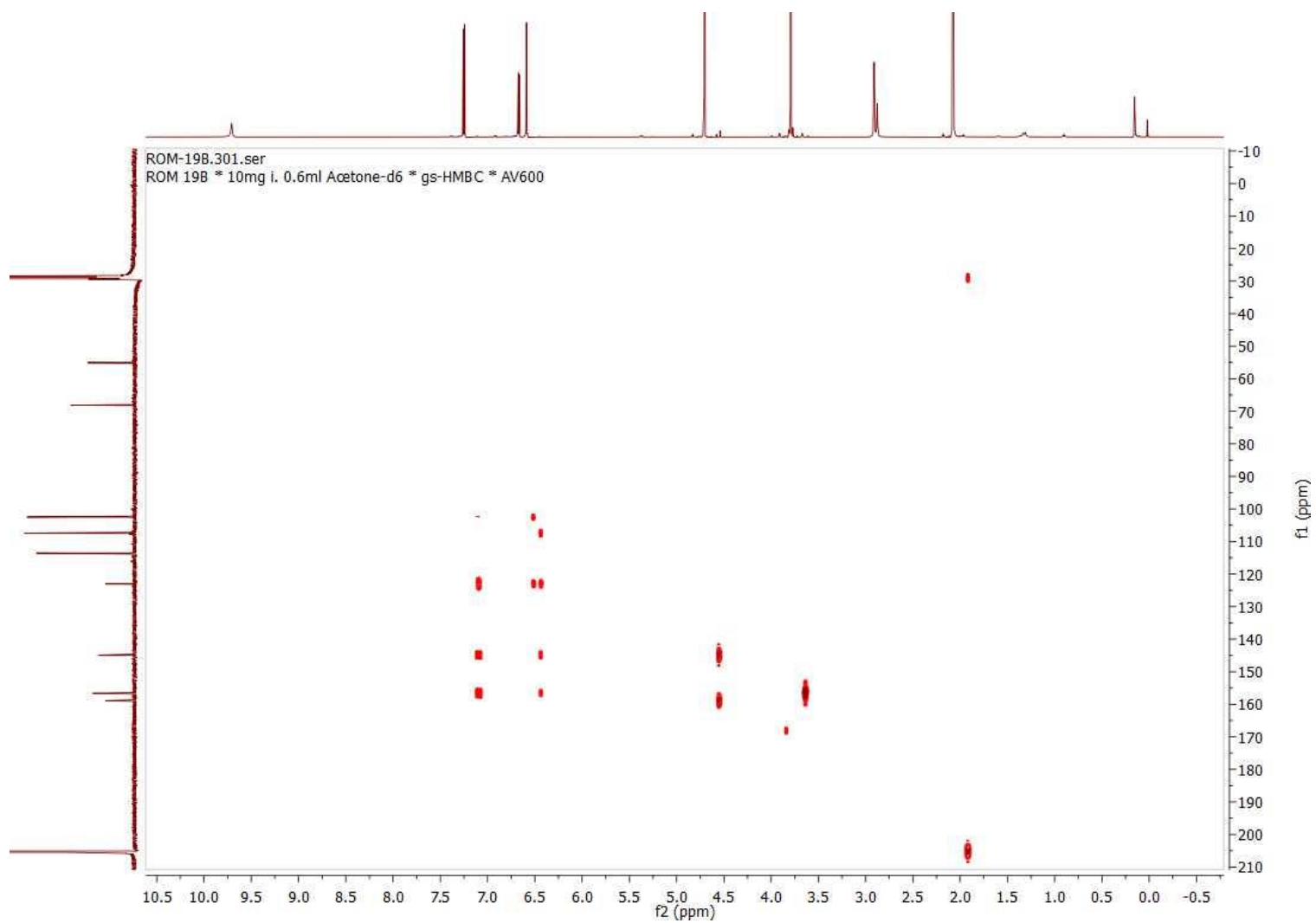
HMBC NMR for 7-Methoxy-4H-1, 4-benzoxazin-3-one
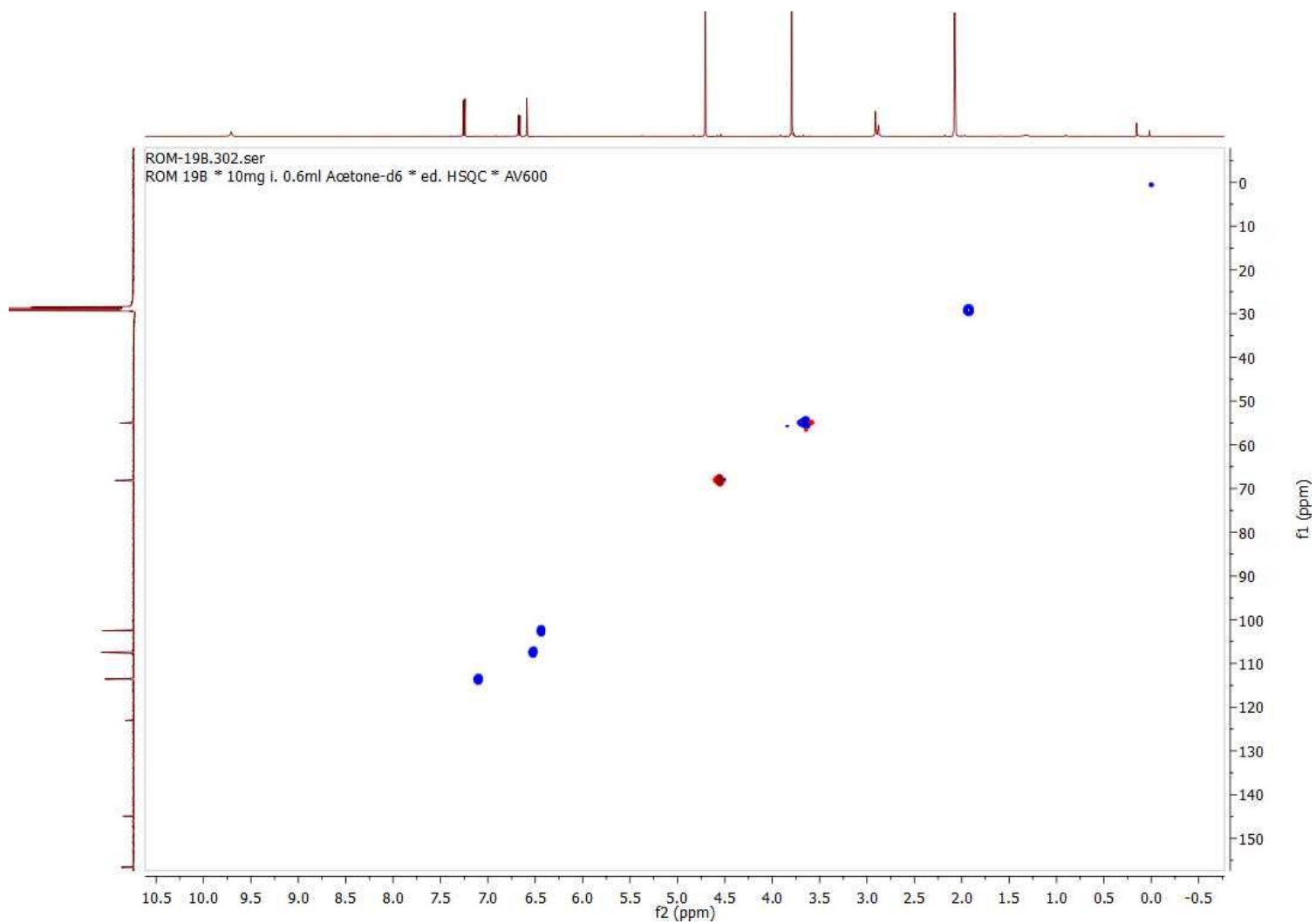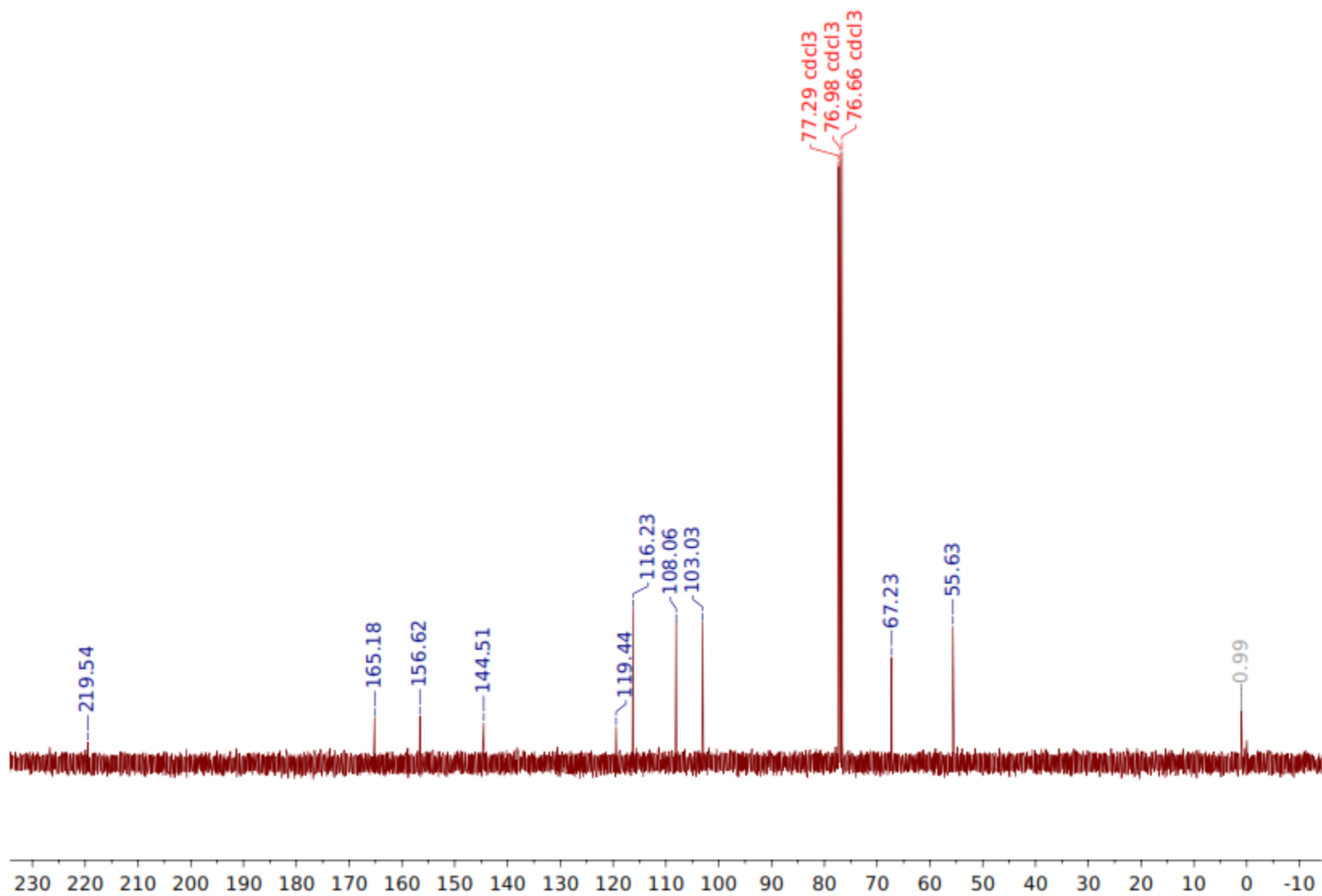
HSQC NMR for 7-Methoxy-4H-1, 4-benzoxazin-3-one

Appendix E: NMR Spectra for 7-Methoxy-3-oxo-1,4-benzoxazine-4-carbaldehyde (**28**)
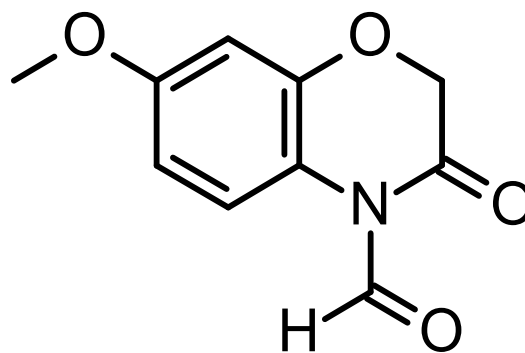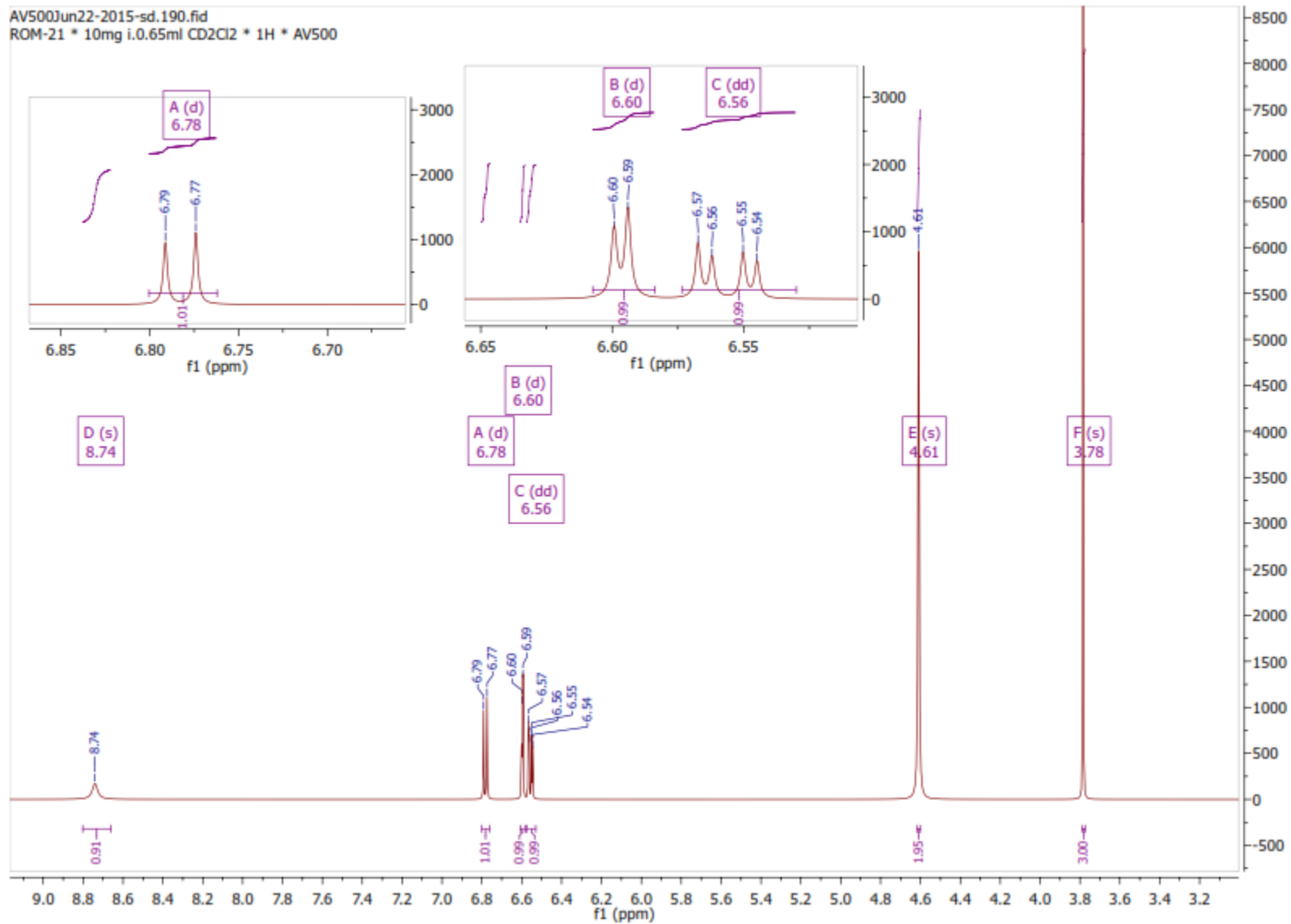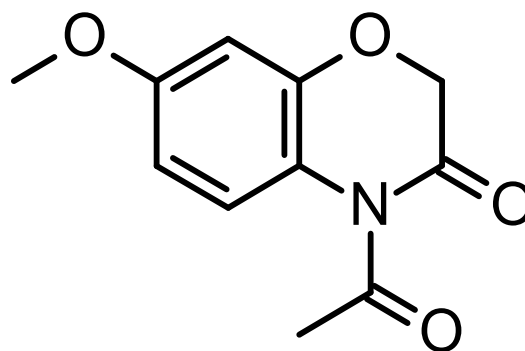
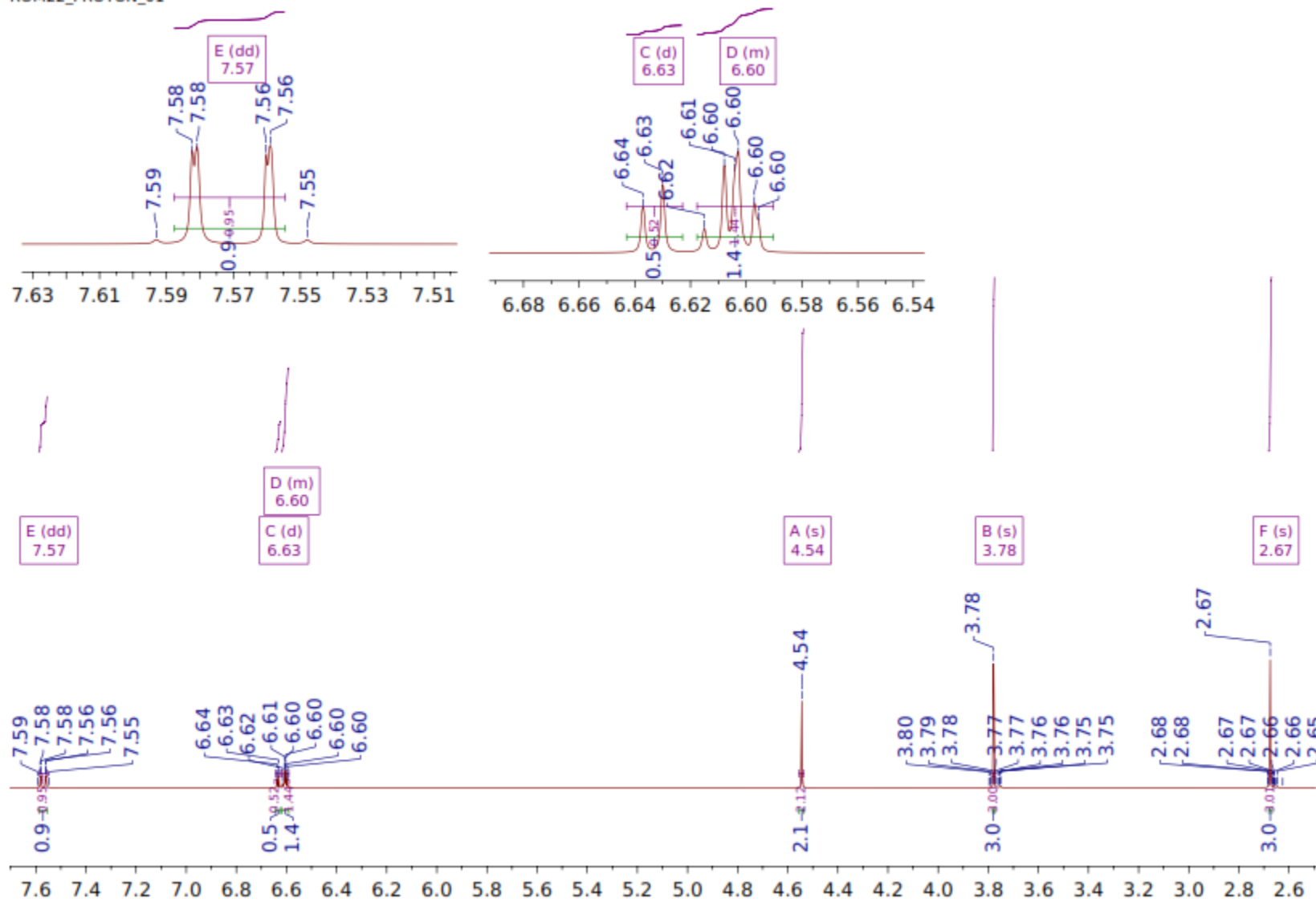^{1}H NMR for 7-Methoxy-3-oxo-1,4-benzoxazine-4-carbaldehyde

^{13}C NMR for 7-Methoxy-3-oxo-1,4-benzoxazine-4-carbaldehyde

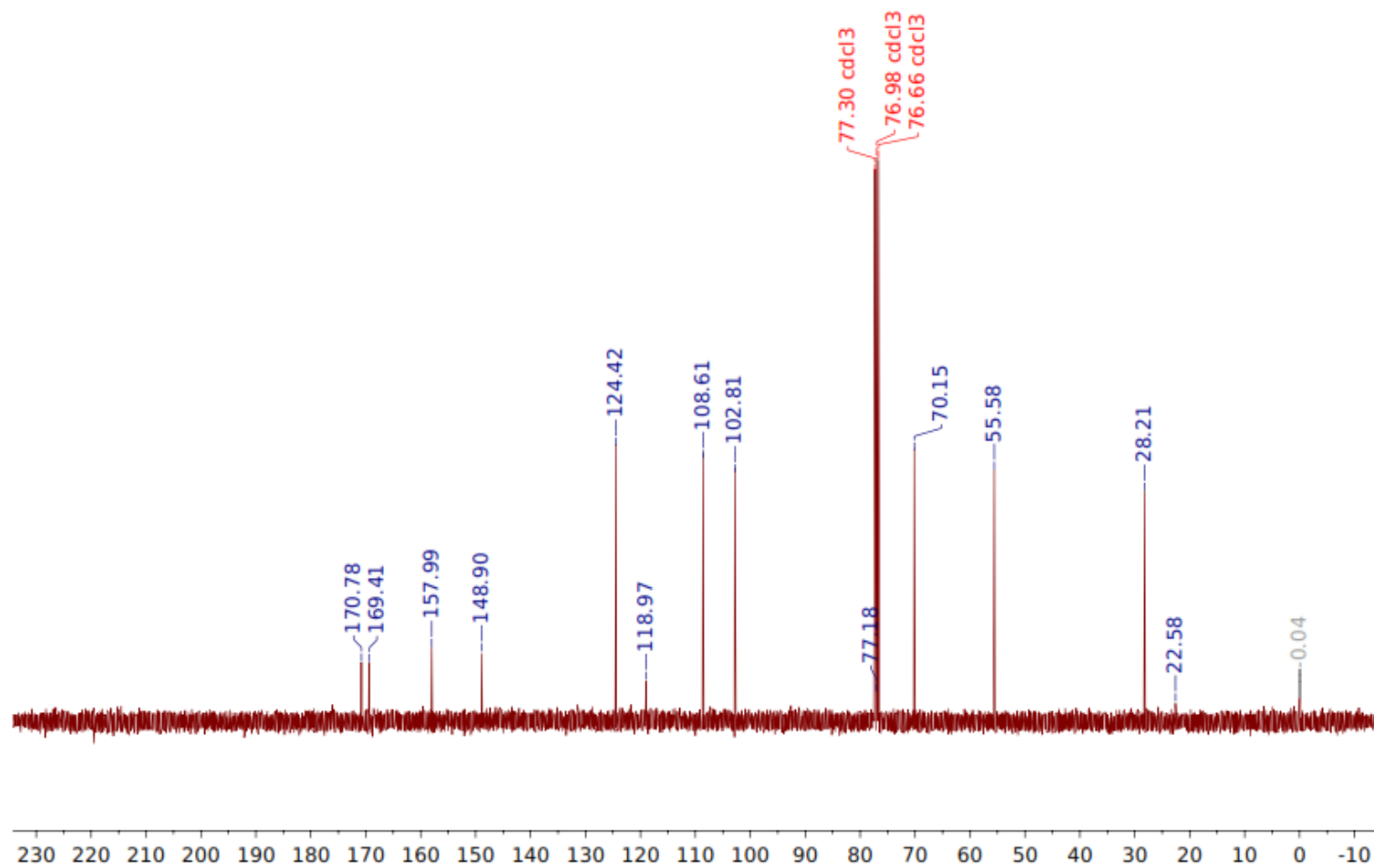Appendix F: NMR Spectra for 4-Acetyl-7-methoxy-1,4-benzoxazin-3-one (**29**)

E (dd)
7.57

C (d)
6.63

D (m)
6.60

A (s)
4.54

B (s)
3.78

F (s)
2.67

^{1}H NMR for 4-Acetyl-7-methoxy-1,4-benzoxazin-3-one

^{13}C NMR for 4-Acetyl-7-methoxy-1,4-benzoxazin-3-one